

# Crustal breakup and continent-ocean transition at South Atlantic conjugate margins

Olav A. Blaich,<sup>1,2</sup> Jan Inge Faleide,<sup>1</sup> and Filippou Tsikalas<sup>1,3</sup>

Received 6 May 2010; revised 16 October 2010; accepted 22 October 2010; published 7 January 2011.

[1] Seismic reflection and refraction profiles, and potential field data, complemented by crustal-scale gravity modeling and plate reconstructions are used to study the evolution of the central and south segments of the South Atlantic conjugate margins. The central segment is characterized by a hyperextended continent-ocean transitional domain that shows evidence of rotated fault blocks and a detachment surface active during rifting. A polyphase rifting evolution mode, associated with a complex time-dependent thermal structure of the lithosphere, is substantiated for the central segment that is not a “magma-poor” end-member. Increase of volcanic activity during the late stages of rifting may have “interrupted” the extensional system implying a failed exhumation phase that was replaced instead by continental breakup and emplacement of fully igneous crust. The continent-ocean transitional domain along the “magma-dominated” south segment is characterized by a large volume of flood basalts and high-velocity/high-density lower crust. The northern province of the south segment is characterized by symmetrical seaward-dipping reflections and symmetrical continent-ocean transitional domain. The influence of the Tristan da Cunha plume on this province is very likely. The central province of the south segment is characterized by along-strike tectonomagmatic asymmetry, which can be caused by the initial continental stretching and accompanying magmatism rather than by the subsequent seafloor spreading. The Tristan da Cunha plume on the central province may have influenced the volume of magmatism but did not necessarily alter the process of rifted margin formation, implying that the central province of the south segment may have much in common with “magma-poor” margins.

**Citation:** Blaich, O. A., J. I. Faleide, and F. Tsikalas (2011), Crustal breakup and continent-ocean transition at South Atlantic conjugate margins, *J. Geophys. Res.*, 116, B01402, doi:10.1029/2010JB007686.

## 1. Introduction

[2] The extensional margin evolution from rift through breakup rupture of the continental lithosphere to progressive oceanic crust formation remains controversial [e.g., Rosendahl *et al.*, 2005; Sawyer *et al.*, 2007; Reston and Pérez-Gussinyé, 2007; Rosenbaum *et al.*, 2008]. Complicating the issue, the deep crustal structures along several margins are partially or totally masked by evaporite deposits and/or by magmatic materials which deteriorate the seismic reflection resolution at depth. Furthermore, the complex interaction of structural and magmatic relationships during continental rifting and breakup results in a wide variety of margin styles, ranging from narrow to wide, and from “magma-dominated” to “magma-poor” conjugate margin pair rift systems. A typical rifted “magma-dominated” margin is characterized by large

volume of flood basalts which flow across the continental hinterlands during continental breakup [Eldholm *et al.*, 1989; Hopper *et al.*, 2003; Eldholm *et al.*, 2000; Mjelde *et al.*, 2005; Gernigon *et al.*, 2006; White and Smith, 2009]. Underlying the extrusive lavas at the continent-ocean transition zone, these margins exhibit high seismic velocities in the lower crust, which are associated with voluminous igneous rocks intruded into the lower crust [e.g., Eldholm *et al.*, 2000; Mjelde *et al.*, 2005; White *et al.*, 2008]. On the other hand, rifted “magma-poor” margins can be defined as those that are controlled by tectonic rather than magmatic processes [Reston, 2009a]. These margins show evidence of polyphase rift evolution which is associated with a complex time-dependent thermal structure of the lithosphere [Lavier and Manatschal, 2006; Péron-Pinvidic *et al.*, 2007; Péron-Pinvidic and Manatschal, 2009]. “Magma-poor” margins are characterized by hyperextended crust accompanied by normal faulting; a broad zone of exhumed continental mantle between oceanic and continental crust, accompanied by the development of detachment faults; and serpentinization of the mantle beneath the extremely thin crust [e.g., Whitmarsh *et al.*, 2001; Lavier and Manatschal, 2006; Péron-Pinvidic *et al.*, 2007; Reston and Pérez-Gussinyé, 2007; Reston, 2009a].

<sup>1</sup>Department of Geosciences, University of Oslo, Oslo, Norway.

<sup>2</sup>Now at Fugro Multi Client Services, Oslo, Norway.

<sup>3</sup>Now at Eni E&P, GEOLAB, Milan, Italy.

[3] The South Atlantic passive margins formed during Mesozoic time as a result of lithospheric extension followed by breakup of the Paleozoic Gondwana supercontinent [e.g., Rabinowitz and LaBrecque, 1979; Austin and Uchupi, 1982; Nürnberg and Müller, 1991; Chang *et al.*, 1992]. The opening of the South Atlantic, which started in the southern portion and propagated toward the north, resulted in considerable diachronic deformation [Matos,

2000]. The South Atlantic Ocean can therefore be divided into four segments (Figure 1), from north to south: equatorial segment, central segment, south segment, and Falkland segment; in this study we focus on the conjugate evolution of selected provinces along the central and south segments.

[4] The central segment is confined between the Rio Grande Fracture Zone to the south and the Ascension Fracture Zone to the north. This segment is characterized by the presence of

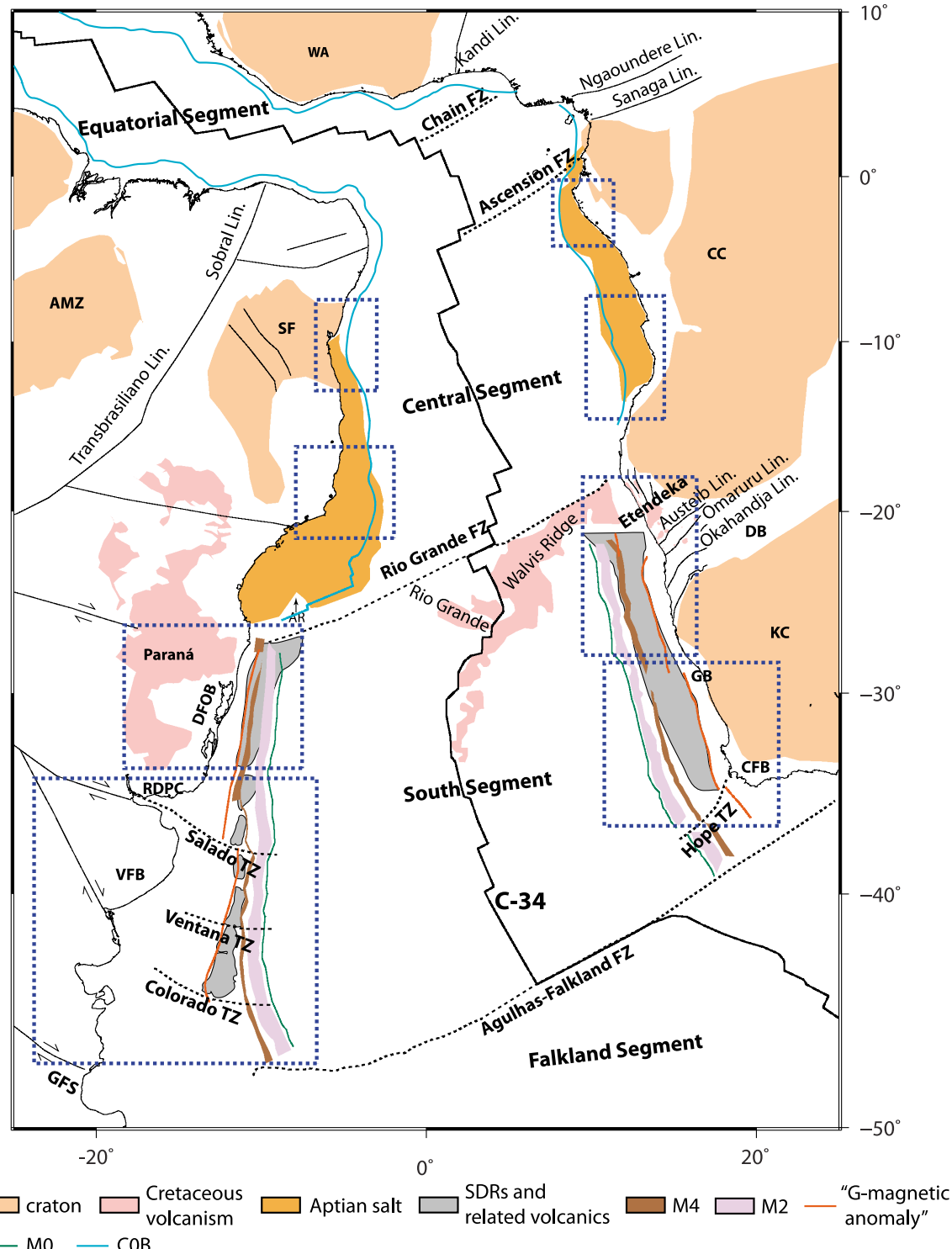


Figure 1

a large evaporitic basin, developed during Aptian time [e.g., *Asmus and Ponte*, 1973; *Mohriak and Rosendahl*, 2003; *Mohriak et al.*, 2008]. Seafloor spreading in this segment occurred at the Aptian-Albian transition, around 112 Ma, corresponding to the last salt deposition [*Moulin et al.*, 2005, 2010; *Mohriak et al.*, 2008; *Torsvik et al.*, 2009]. Although the central segment was earlier considered to be associated with well-defined seaward-dipping reflections (SDRs) [*Mohriak et al.*, 1995, 1998; *Jackson et al.*, 2000], recent high-resolution sub-salt seismic images from this margin segment [*Blaich et al.*, 2010] are very different from the images obtained on well-studied volcanic margins worldwide [e.g., *Eldholm et al.*, 1989; *Gladzenko et al.*, 1998; *Hinz et al.*, 1999; *Hopper et al.*, 2003]. This implies that although the central segment experienced volcanism during breakup magmatic products were not sufficiently voluminous to form SDRs [*Sawyer et al.*, 2007], and thus the central segment conjugate margins exhibit “magma-poor” affinity.

[5] The south segment is limited between the Falkland-Agulhas Fracture Zone to the south and the Rio Grande Fracture Zone to the north. The first oceanic crust in this segment was formed in Hauterivian time, between 134 and 132 Ma in the south and 132–130 Ma toward the north [*Austin and Uchupi*, 1982; *Moulin et al.*, 2010]. Furthermore, this segment is characterized by SDRs and high-velocity/high-density lower crust, which are associated with voluminous igneous activity during continental breakup, implying “magma-dominated” conjugate margins [*Gladzenko et al.*, 1998; *Hinz et al.*, 1999; *Talwani and Abreu*, 2000; *Franke et al.*, 2007; *Schnabel et al.*, 2008; *Blaich et al.*, 2009; *Hirsch et al.*, 2009].

[6] In this study of the South Atlantic margins, we investigate four representative conjugate provinces: the northeastern Brazil-Gabon and the southeastern Brazil-Angola margins located on the central segment; the southeastern Brazil-Namibia and the Argentine-South Africa margins located on the south segment (Figure 1). We analyze an available grid of regional multichannel seismic (MCS) reflection profiles together with published seismic reflection/refraction profiles across the four provinces. In the conjugate margin context, the integration of seismic and potential field data, and conducted 2-D gravity modeling, together with potential field plate reconstructions provide adequate means to study and understand the evolution of the South Atlantic margins, to elucidate structural elements and features that reflect the processes that lead to the rupture of the continental

crust, as well as to refine and constrain the structural architecture and nature of the continent-ocean transitional domain. Note that the term continent-ocean transitional domain is adopted in the current study and defined as the part of the lithosphere which is located between the clearly identifiable stretched continental crystalline crust domain, and the first appearance of fully oceanic (i.e., fully igneous) crust formed by seafloor spreading.

[7] We are aware of the 2-D gravity modeling methodology limitations, especially concerning the nonunique interpretation of gravity anomalies, and the effect of 3-D lateral density variations on the 2-D gravity model. In the absence of detailed seismic velocity constraints (e.g., seismic refraction data) along each transect, the use of uniform density crystalline crust and mantle is justified, as the first-order density contrasts in the gravity modeling exist at the top of crystalline basement and Moho levels. Application of both inverse gravity modeling for the initial Moho relief estimates and detailed 2-D forward gravity modeling provided insights into the density contrast at the crust-mantle interface, and essentially led to a rather similar geometry of the Moho discontinuity based on the two approaches. This convergence of results suggests that, despite the uncertainties regarding absolute petrophysical constraints for the crystalline crust and mantle, we were able to come up with reliable crustal structure configurations for the modeled transects.

## 2. Data Analysis

[8] The data utilized in this study comprise a compilation of large amount of integrated industrial seismic reflection profiles, published seismic reflection and wide-angle refraction profiles, and potential field data along the conjugate margin provinces. In particular, along the northeastern Brazil-Gabon conjugate margin, the data set was provided courtesy to Statoil and comprises seismic reflection profiles acquired by TGS-NOPEC (Camamu/Almada basins) and ION-GXT (South Gabon Basin). Published seismic reflection [*Rosendahl et al.*, 1991; *Meyers et al.*, 1996a, 1996b; *Rosendahl and Groschel-Becker*, 1999; *Rosendahl et al.*, 2005] and wide-angle refraction profiles [*Wannesson et al.*, 1991] along the Gabon margin have also been analyzed, revised and incorporated into our interpretations. Farther south, along the conjugate southeastern Brazil-Angola margin, industrial reflection seismic profiles acquired by Fugro Multi Client Services (Espírito Santo Basin) were at our disposal. In addition,

**Figure 1.** General tectonostructural plate reconstruction map of the South Atlantic at Chron 34 (~83 Ma). For this well-constrained reconstruction, we use rotation poles of *Nürnberg and Müller* [1991] and PLATES software (Institute for Geophysics, University of Texas at Austin). The blue dashed rectangles indicate the studied provinces along the South Atlantic conjugate margins. Cratons, Aptian salt extension, M sequences magnetic anomalies, C-34 magnetic anomaly, and main structural constraints are after *Moulin et al.* [2010, and references therein]. Cretaceous volcanism is after *Gladzenko et al.* [1998] and *Moulin et al.* [2010]. The location of the Abimael Ridge (AR) is based on the interpretation of *Mohriak* [2001]. The continent-ocean boundary (COB) location along the equatorial segment [*Moulin et al.*, 2010] and along the central segment (this study) is indicated. Structures located in onshore Namibia are after *Gladzenko et al.* [1998]. Seaward-dipping reflections (SDRs) and related volcanics are from *Moulin et al.* [2005] and *Franke et al.* [2007, 2010] for South America and *Bauer et al.* [2000] for Africa. “G magnetic anomaly” after *Rabinowitz and LaBrecque* [1979]; Lin, lineament; WA, West Africa Craton; CC, Congo Craton, DB, Damara Belt; GB, Gariep Belt; KC, Kalahari Craton; CFB, Cape Fold Belt; AMZ, Amazonia Craton; SF, São Francisco Craton; DFOB, Dom Feliciano Orogenic Belt; RDPC, Rio de La Plata Craton; VFB, Ventana Fold Belt; GFS, Gastre Fault System; TZ, transfer zone; FZ, fracture zone.

published seismic reflection profiles along both southeastern Brazil–Angola conjugate margins [Marton *et al.*, 2000; Hudec and Jackson, 2002, 2004; Mohriak *et al.*, 2008] have been analyzed and incorporated into our interpretations. Along the conjugate southeastern Brazil–Namibia margin, published seismic reflection profiles in Pelotas Basin [Abreu, 1998] and published deep seismic reflection/refraction profiles in the conjugate Walvis Basin [Gladchenko *et al.*, 1998; Bauer *et al.*, 2000] have been revised and incorporated into our interpretations. Furthermore, industrial reflection seismic profiles acquired by TGS-NOPEC (Namibia) were at our disposal. Finally, along the conjugate Argentine–South Africa margin, seismic reflection profiles acquired by BGR (Argentine margin) were at our disposal. Line drawings from Hinz *et al.* [1999] and Franke *et al.* [2007, 2010] together with two sets of wide-angle seismic refraction data [Franke *et al.*, 2006; Schnabel *et al.*, 2008] on the Argentine margin and published seismic reflection/refraction profiles on the conjugate South Africa margin [Emery *et al.*, 1979; Brown *et al.*, 1995; Séranne and Anka, 2005; Paton *et al.*, 2008; de Vera *et al.*, 2010; Hirsch *et al.*, 2009] have also been incorporated into our interpretations for this margin.

[9] Potential field data used in this study consist of  $1 \times 1'$  elevation grid [British Oceanographic Data Centre, 2003],  $1 \times 1'$  satellite radar altimeter gravity grid ([Sandwell and Smith, 1997]; version 16.1),  $3 \times 3'$  aeromagnetic anomaly grid [International Association of Geomagnetism and Aeronomy (IAGA), 2007], as well as publicly available shipborne bathymetry and potential field anomaly data (LDEO, Lamont-Doherty Earth Observatory) [Wessel and Watts, 1988; Smith, 1993]. A Bouguer-corrected gravity anomaly grid has also been constructed by utilizing the detailed bathymetry and free air gravity anomalies and a density of  $2670 \text{ kg/m}^3$  as infill to the bathymetric relief. A low-pass filter, suppressing wavelengths  $>200 \text{ km}$ , has been applied to the Bouguer gravity grid to better image the large-scale basement and Moho geometries as clearly demonstrated by several studies [e.g., Agarwal *et al.*, 1995; Das *et al.*, 1996; Lefort and Agarwal, 2000].

[10] Potential field plate reconstructions were performed using the PLATES software (Institute for Geophysics, University of Texas at Austin [e.g., Lawver *et al.*, 1999]) and published rotation poles [Nürnberg and Müller, 1991; Moulin *et al.*, 2010; Torsvik *et al.*, 2009]. Intraplate deformation in both South America and Africa is well accepted and constitutes an essential requirement in order to solve the kinematic problems during continental breakup and the subsequent formation of the South Atlantic Ocean [e.g., Moulin *et al.*, 2010; Torsvik *et al.*, 2009]. As the studied conjugate provinces are located between major zones of intraplate deformation, plate reconstructions were performed assuming rigid plates (Figure 1). Furthermore, plate reconstructions were used in this study in order to select conjugate profiles and to evaluate the tectonic evolution of the four segments expressed on potential field data.

[11] The MCS profiles within the study area were compiled and extended to the ultra deep water oceanic province, in order to construct representative regional conjugate transects used in crustal-scale gravity modeling. The regional transects are based on the interpreted seismic reflection profiles, extracted bathymetry and gravity anomaly data, and on initial estimates of the Moho relief using both isostatic balancing

and inverse gravity modeling; the latter method is described in detail by Blaich *et al.* [2008, 2009]. The conjugate crustal transects presented in this study comprise both new transects along the southeastern Brazil–Angola and southeastern Brazil–Namibia conjugate margins, and updated ones presented earlier (along northeastern Brazil–Gabon [Blaich *et al.*, 2010] and along Argentine–South Africa [Blaich *et al.*, 2009]). In this setting, two sets of representative crustal transects were compiled for each conjugate province along the central and south segments.

### 3. Central Segment

#### 3.1. Margin Setting

[12] The potential field plate reconstructions at “forced breakup” ( $\sim 112 \text{ Ma}$ ; Figure 2) were performed using rotation poles of Torsvik *et al.* [2009]. In these reconstructions, the continent-ocean boundary (COB) location along the conjugate margin off northeastern Brazil–Gabon is based on Blaich *et al.* [2010], while farther south along the conjugate margin off southeastern Brazil–Angola, the COB location is modified from Mohriak *et al.* [2008] and is consistent with observations made in this study. Physiographically, the central segment is characterized by a continental shelf and slope that vary considerably in width and steepness, respectively, along the margin (Figure 2a). In this setting, the continental shelf is narrow along the northeastern Brazilian margin and considerable wider along the conjugate margin off Gabon, indicating a narrow/wide margin configuration (Figure 2a). Farther south, a wide shelf along the Brazilian margin is characterizing the Abrolhos volcanic complex and is conjugate to a wide shelf that is affected by the Congo Fan. Along the Espírito Santo–Kwanza conjugate basins a narrow/narrow margin configuration is observed (Figure 2a). Farther south, the conjugate continental shelf along the Santos/Campos–Benquela basins indicates a wide/narrow margin configuration.

[13] As the central segment was formed during the Cretaceous magnetically quiet superchron, there is absence of clearly orientation-defined magnetic anomalies, and broad zones of magnetic quiescence with some chaotic patterns of magnetic anomalies are observed (Figure 2b). The gravity grid reveals a continuous, prominent and elongated gravity anomaly high close to the shelf edge that trends subparallel to both conjugate coastlines (Figure 2c). Such elongate “edge effect” positive gravity anomalies are considered commonly observed features at passive continental margins [Rabinowitz and LaBrecque, 1979; Watts and Fairhead, 1999]; however, due to the inherent ambiguity in potential field interpretations, the genetic cause of these anomalies is not always clear. In particular, their cause has been ascribed in many margins to the difference in depth to major lateral, near-seafloor density contrasts and the equivalent depth difference of base crust compensation [e.g., Talwani and Eldholm, 1972; Tsikalas *et al.*, 2005]. These “edge effect” positive gravity anomalies have also been interpreted as caused by the juxtaposition of continental and oceanic crust [Rabinowitz and LaBrecque, 1979; Bauer *et al.*, 2000], as well as due to magmatic underplating [e.g., Watts, 2001]. The gravity anomaly low that flanks the “edge effect” anomaly high along the northeastern Brazilian margin is abruptly terminated by a belt of positive anomalies to the northeast, along the equivalent offshore

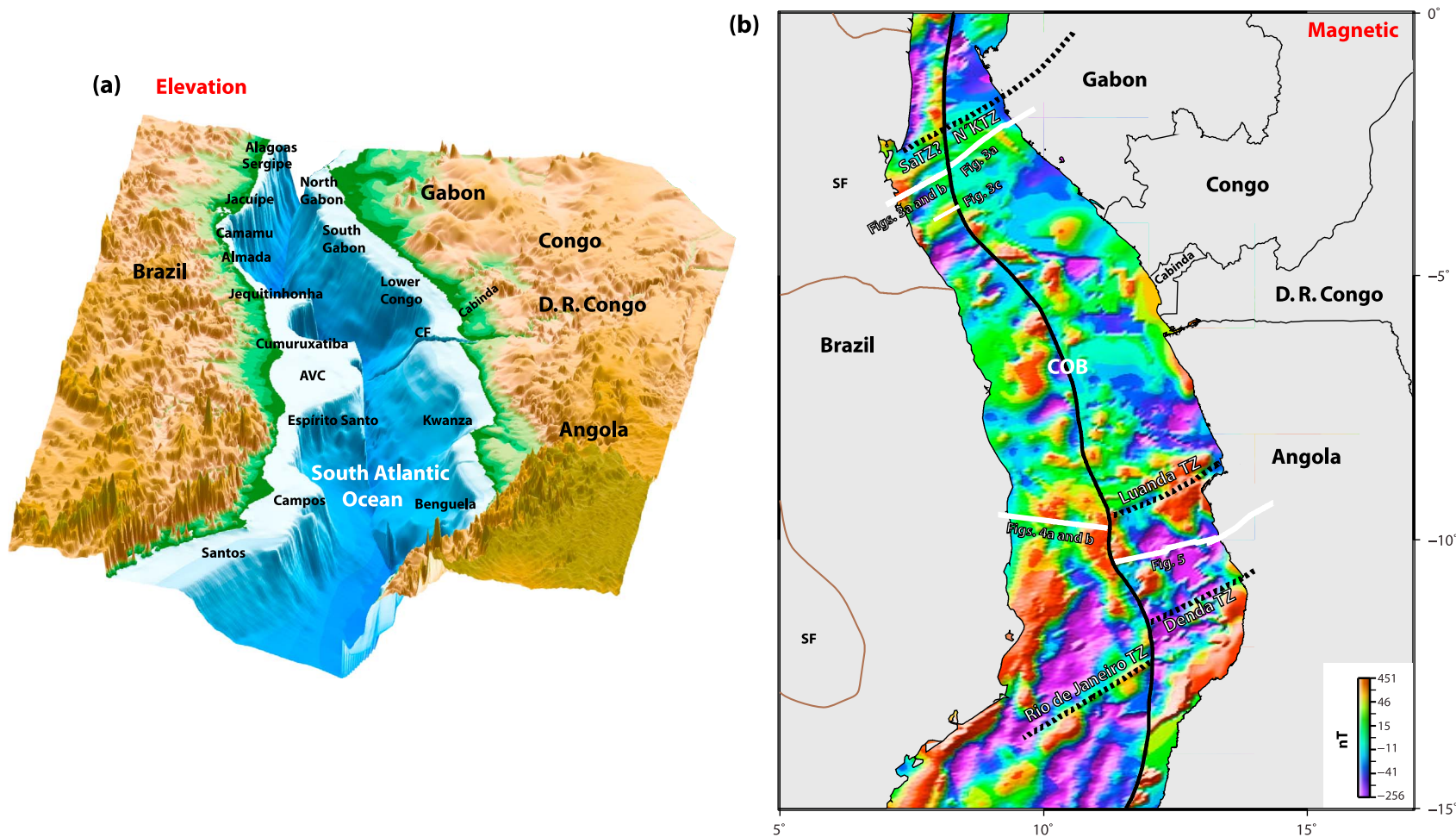


**Figure 2.** Plate reconstructions at forced breakup ( $\sim 112$  Ma) utilizing the rotation poles of Torsvik *et al.* [2009]; the continent-ocean boundary (COB) location along the conjugate margin off northeastern Brazil-Gabon is based on Blaich *et al.* [2010]. Farther south, along the conjugate margin off southeastern Brazil-Angola the COB location is modified from Mohriak *et al.* [2008] and is consistent with observations made in this study. (a) A  $1 \times 1'$  elevation grid [British Oceanographic Data Centre, 2003]. Offshore sedimentary basins are indicated. (b) A  $3 \times 3'$  gridded aeromagnetic anomaly field [IAGA, 2007]. (c) A  $1 \times 1'$  satellite radar free air gravity anomaly field ([Sandwell and Smith, 1997]; version 16.1). (d) Low-pass-filtered ( $>200$  km) Bouguer-corrected gravity anomaly field (utilizing a density of  $2670 \text{ kg/m}^3$  as infill to the bathymetric relief). The locations of conjugate transects are indicated. AVC, Abrolhos volcanic complex; CF, Congo Fan; N'KTZ, N'Komi Transfer Zone; SaTZ, Salvador Transfer Zone; SF, São Francisco; TZ, transfer zone.

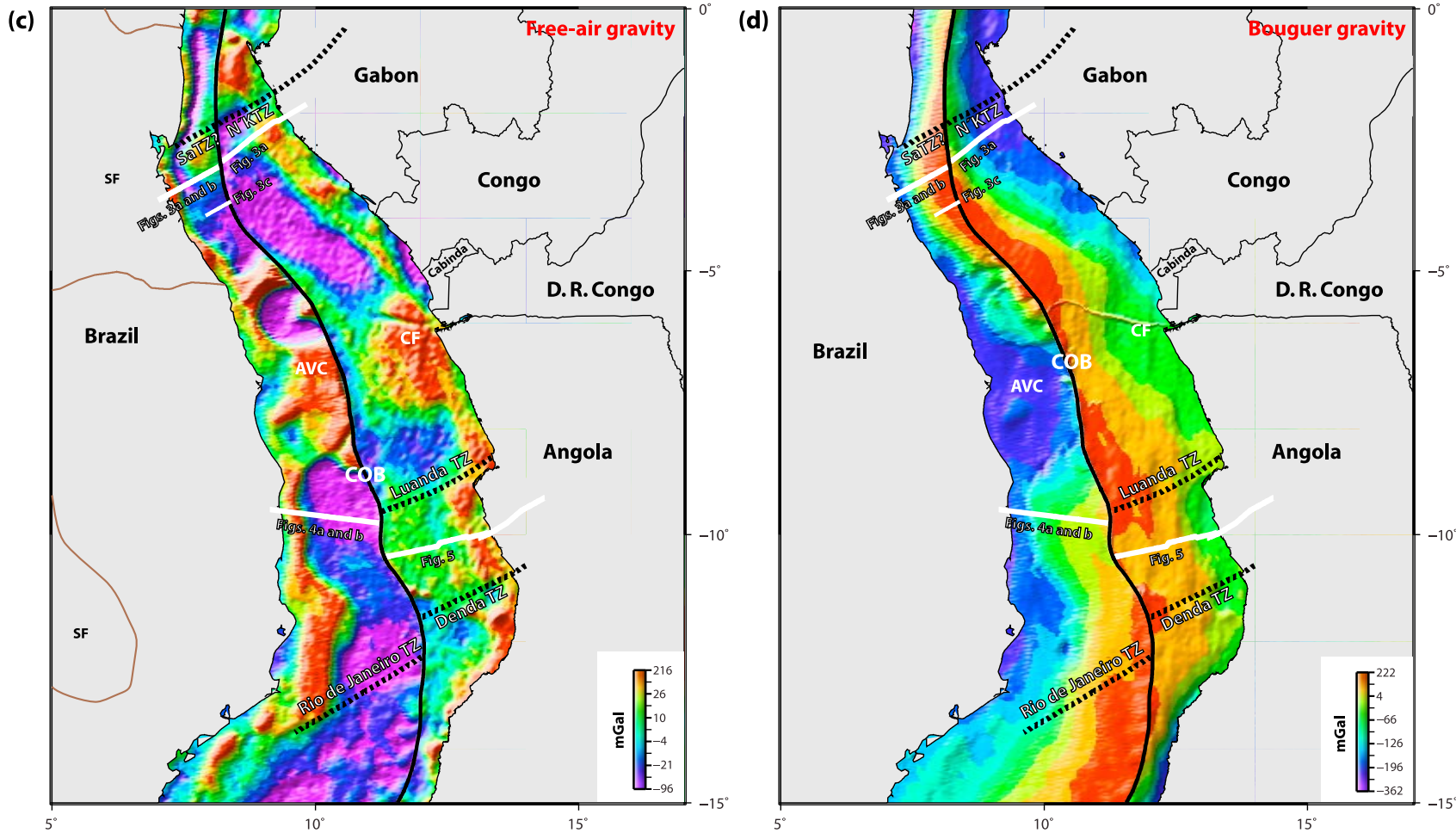


Figure 2. (continued)

extent of the northern boundary of the São Francisco craton (Figure 2c) [Blaich *et al.*, 2010]. Along the conjugate margin off Gabon, a prominent gravity anomaly low that flanks the “edge effect” gravity anomaly high abruptly terminates to the north at the N’Komi Transfer Zone (Figure 2c). These observations suggest a segmented along-margin character which may be attributed to a distinct and probably inherited segmentation of this part of the South Atlantic margins, where Archean-Paleoproterozoic structures probably exerted a strong control on the patterns of rifting and breakup and where major changes in lithospheric strength may have occurred [e.g., Watts and Stewart, 1998; Rosendahl *et al.*, 2005]. Farther south, the continuous, prominent and elongated gravity anomaly high along both conjugate margins is interrupted by a broad gravity high characterized by the Abrolhos volcanic complex and by the Congo Fan. Furthermore, the “edge effect” gravity anomaly high is clearly segmented by the Luanda Transfer Zone (Figure 2c).

[14] The low-pass-filtered Bouguer-corrected gravity field (Figure 2d) indicates a narrow zone of low values along the northeastern Brazilian margin that is conjugate to a considerably wider zone of low values along the Gabon margin. These observations may suggest dissimilar gradient of crustal thinning for the conjugate margins and therefore may indicate a sharp crustal taper along the northeastern Brazilian margin that is conjugate to a gentle crustal taper along the Gabon margin (Figure 2d). Farther south, along the conjugate Espírito Santo–Kwanza basins, the Bouguer-corrected gravity field reveals an overall symmetrical character that is replaced by a striking asymmetry farther south (Figure 2d). The Bouguer-corrected gravity field also reveals a prominent negative-positive gradient character (Figure 2d). This has previously been interpreted as the COB location [Karner and Driscoll, 1999; Blaich *et al.*, 2008]; however, in a recent study Blaich *et al.* [2010] clearly indicated that this is not necessarily the case.

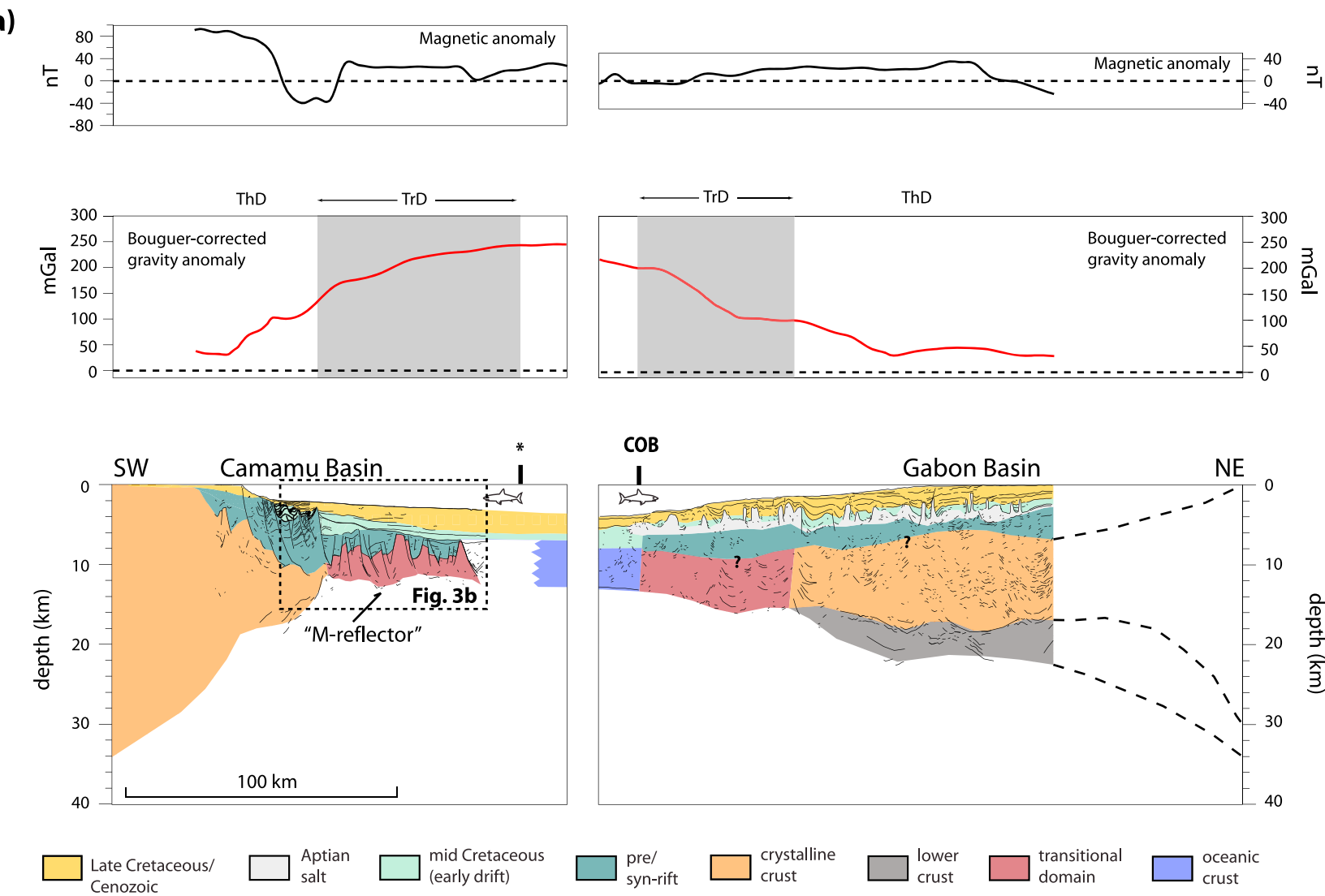
### 3.2. Crustal Architecture

[15] The representative conjugate crustal transects obtained through 2-D gravity modeling (Figure 3a) outline the crustal structure of the northeastern Brazil–Gabon conjugate margins. Explicit modeling details of the transects in Figure 3a are presented by Blaich *et al.* [2010], while in this study we discuss particular issues on the two transects that elucidate the central segment margin evolution. In this setting, the representative transect along the Camamu Basin (northeastern Brazil) does not suggest a typical rifted continental crust with progressive crustal thinning over an extensive distance toward oceanic crust formed due to breakup and seafloor spreading (Figure 3a). On the contrary, although seismic interpretation combined with gravity modeling suggests extreme crustal thinning, the thick synrift sedimentary basins overlying the thinned crystalline continental crust domain appear not to be the result of intense upper crust brittle deformation [Blaich *et al.*, 2010]. For instance, the data show that the continental crystalline crust along the northeastern Brazilian margin thins abruptly, from ~30 km to ~4 km over a distance of only ~80 km indicating a sharp crustal taper without prominent brittle deformation of the upper crust (Figure 3a). Along-margin variations of the thickness of the pre/synrift sedimentary package is observed on the MCS profiles, and correspond to prominent along-margin changes

in the potential field data [Blaich *et al.*, 2010]. In particular, a thick pre/synrift sedimentary package is characterized by a prominent and elongated gravity anomaly low (Figures 2c and 3a).

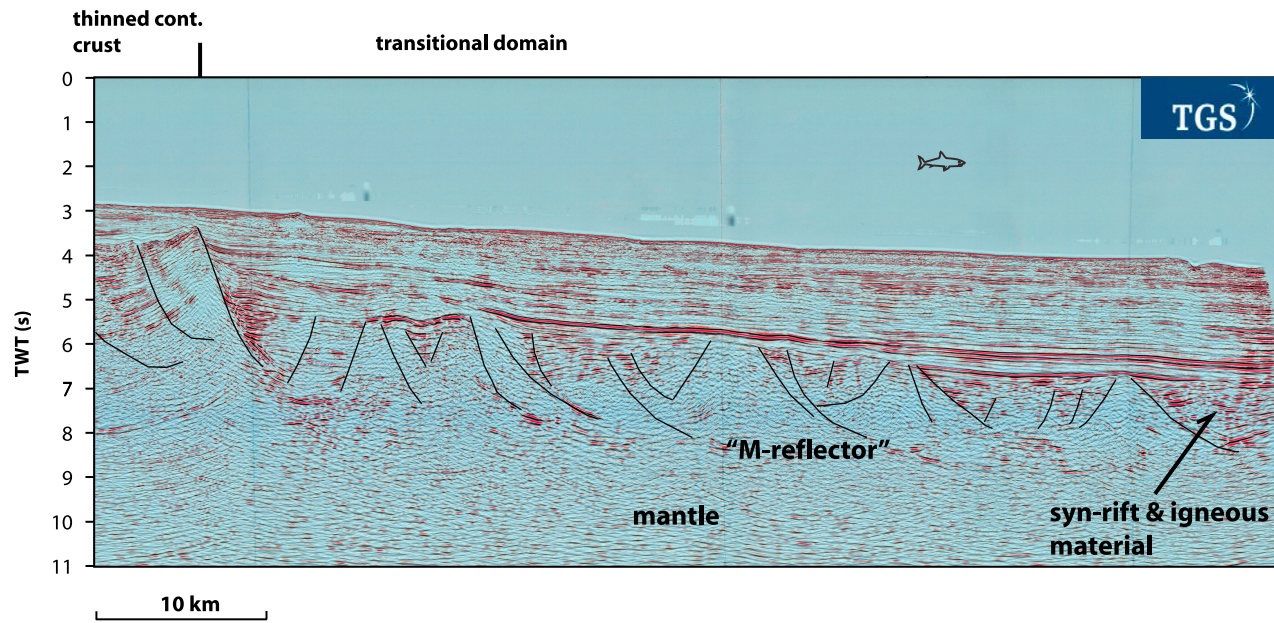
[16] Interpretation of the MCS profiles along the Camamu Basin [Blaich *et al.*, 2010] indicates that prominent salt tectonism is not present (Figures 3a and 3b), however, previous studies have identified salt deposits along the Camamu [Karner and Gambôa, 2007; Menezes and Milhomem, 2008], Jacuípe [Davison, 2007], and Sergipe-Alagoas basins [Castro, 1988; Mohriak *et al.*, 1995; Mohriak, 2003, 2004; Davison, 2007; Souza-Lima, 2008]. On the other hand, the MCS profile along the Gabon margin (Figure 3a) is characterized by a wide salt basin that considerably masks the underlying geology, implying that interpretation of the top basement horizon and rift structures are disputed and not easily recognized. Even though the Moho discontinuity is poorly constrained by seismic imaging along the Gabon margin, gravity modeling indicates a continental crust that thins gently toward the west, indicating a gentle crustal taper (Figure 3a). The high-amplitude and subhorizontal band of seismic reflections located at a depth of ~16–18 km (Figure 3a) exhibits the upper boundary of a velocity increase from 6.1 to 6.9 km/s [Wannesson *et al.*, 1991]. Furthermore in order to accomplish a reliable fit in the gravity modeling a high-density ( $3100 \text{ kg/m}^3$ ) is required for the lower crust [Blaich *et al.*, 2010]. Therefore, the high-amplitude and subhorizontal band of seismic reflections have been interpreted as the top of a high-density/high-velocity lower crustal body which is spatially related to a broad and prominent “edge effect” gravity anomaly high (Figure 2c). Similarly, an enigmatic high-velocity lower crustal body has also been documented farther south [Contrucci *et al.*, 2004; Moulin *et al.*, 2005]. Such a lower crustal body is not necessarily breakup related, but may be related to older tectonic episodes and, possibly, orogenies; e.g., inheritance from Transamazonian and Pan-African collision belts [e.g., Meyers *et al.*, 1996a].

[17] Farther south, the representative crustal transect obtained from 2-D gravity modeling in the current study (Figure 4a) outlines the crustal structure along the Espírito Santo Basin. The constructed transect extends ~400 km eastward, from the platform to the deep basin. Near the shelf edge, an abrupt shallowing of the Moho discontinuity is imaged in the seismic profile [Mohriak, 2003; Mohriak *et al.*, 2008] and observed on the gravity model (Figure 4a). The Moho shallowing is associated with crustal thinning from more than 30 km to less than 15 km over a distance of about 100 km. Furthermore, the continental crust is clearly deformed by synthetic listric faults (Figures 4a and 4b). A thick and broad presalt succession is characterized by a “sag” basin that does not seem to be affected by basement-involved faults [Mohriak *et al.*, 2008]. Along the conjugate margin off Angola, the representative crustal transect obtained from 2-D gravity modeling in the current study (Figure 5) outlines the crustal structure along the Kwanza Basin. The constructed transect extends for ~500 km westward, from the onshore part of the Kwanza Basin to the offshore part. Although the Moho discontinuity is poorly constrained by seismic reflection/refraction data along the Kwanza Basin, the analysis performed in this study indicates a gentle shallowing Moho discontinuity. In this setting, the crust thins

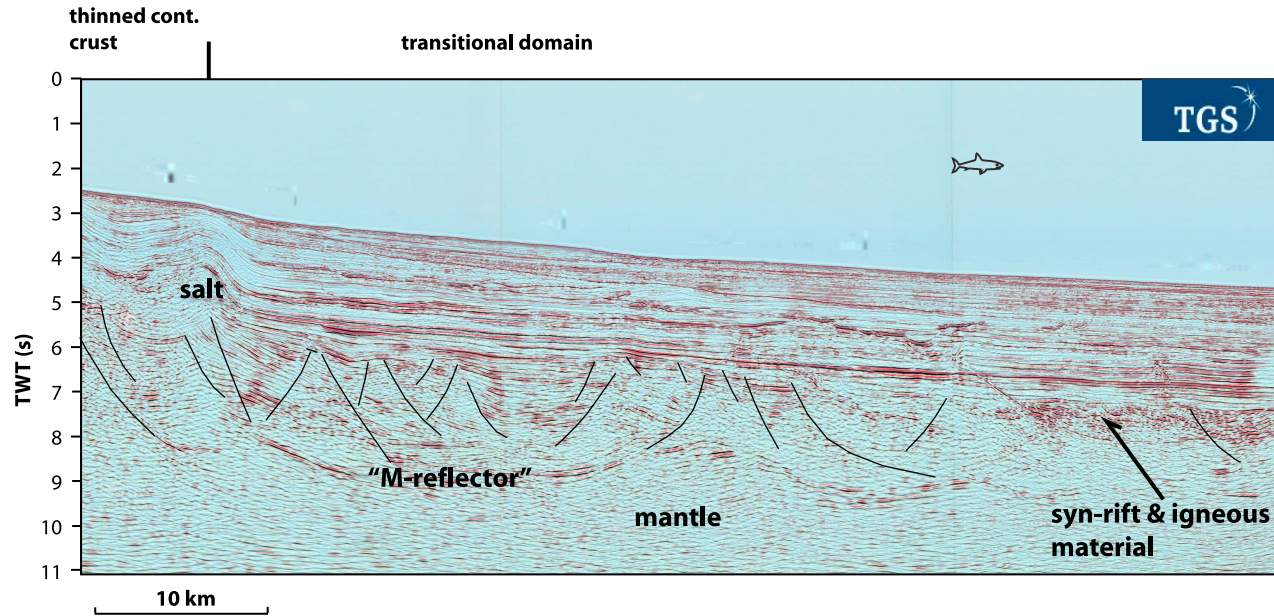


**Figure 3.** (a) Conjugate transects along Camamu-Gabon basins (location in Figure 2). Extracted along-margin Bouguer-corrected gravity anomaly and aeromagnetic anomaly [IAGA, 2007] are also shown. (b) Seismic example of the transitional domain along the Camamu Basin (location in Figure 2). (c) Seismic example of the transitional domain along the Camamu Basin (location in Figure 2). COB, continent-ocean boundary; asterisk indicates “line of fit” used for plate reconstructions (see discussion in text); ThD, thinned crystalline crust domain; TrD, transitional domain.

(b)



(c)

**Figure 3.** (continued)

(from east to west) from more than ~30 km to ~14 km over a distance of about 220 km, and it appears that crustal thinning is controlled by synthetic and antithetic listric faults (Figure 5). Since an anomalous high-velocity/density lower crust has been described along the northern Angola (Lower Congo Basin) [Contriucci *et al.*, 2004] and southern Gabon margins [Wannesson *et al.*, 1991; Blaich *et al.*, 2010], the possibility exists that such lower crust is also present along the Kwanza Basin. However, with the available data and due to the non-unique interpretation of gravity anomalies, it is impossible to resolve this issue. Furthermore, salt diapirs are clearly

depicted along the transect, where typical halokinetic structures are observed along the entire transect, extending from the onshore inner Kwanza Basin all the way to the deep water offshore Kwanza Basin (Figure 5). Inversion structures are evident on the eastern limit of the transect and are suggested to be related to ridge push forces, plate reorganization and mantle-driven uplift of the African superswell [Hudec and Jackson, 2002]. Evidence for an undeformed presalt "sag" basin is not overwhelming along the constructed transect (Figure 5), however, along the northern Angola margin (Lower Congo Basin) the presence of normal faults in the deep

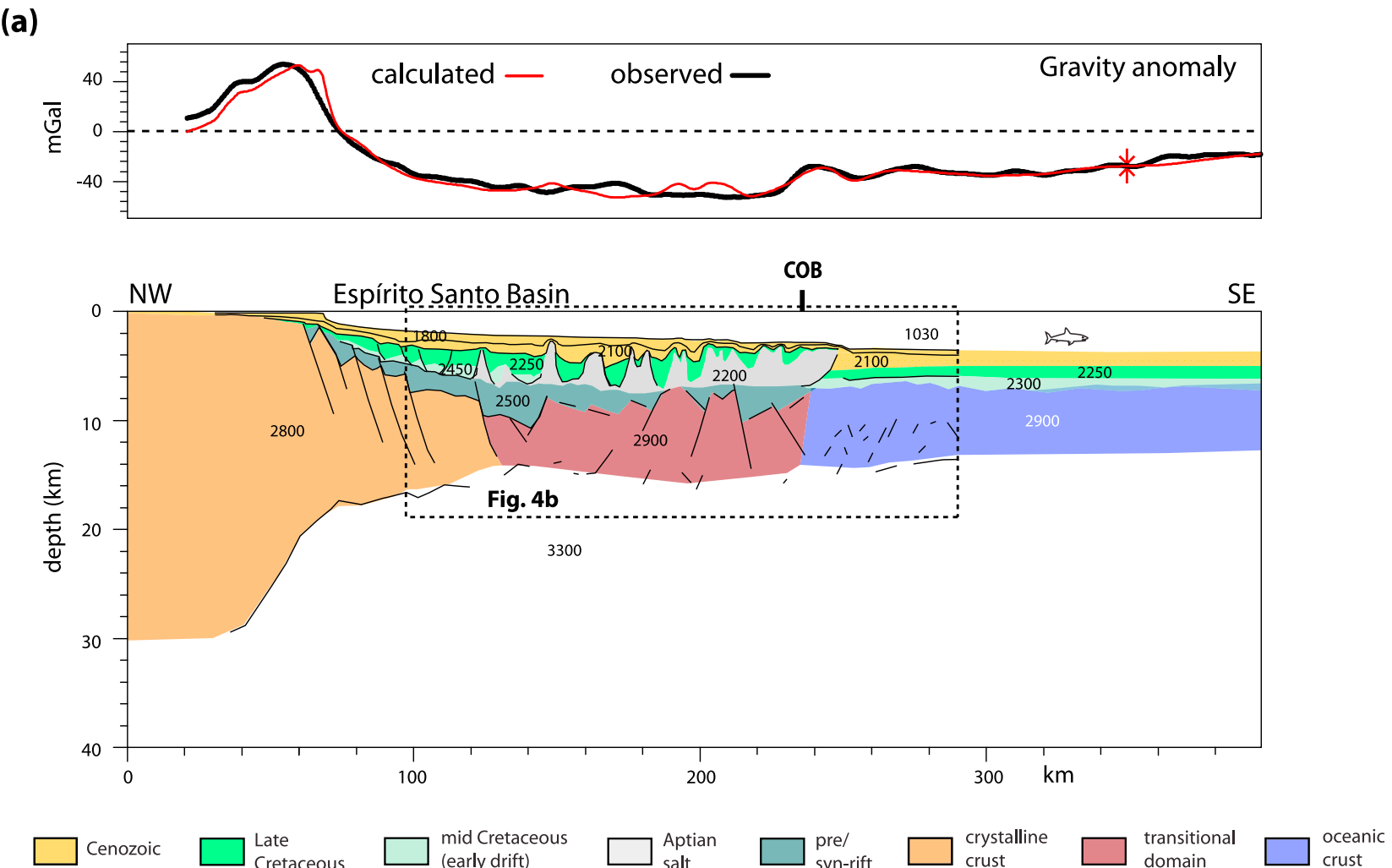


**Figure 4.** (a) Gravity modeled transect along the Espírito Santo Basin (location in Figure 2) utilizing the satellite radar altimeter free air gravity anomaly field ([Sandwell and Smith, 1997]; version 16.1). (b) Seismic example of the transitional domain along the Espírito Santo Basin (location in Figure 2). Indicated densities in  $\text{kg/m}^3$ . COB, continent-ocean boundary.

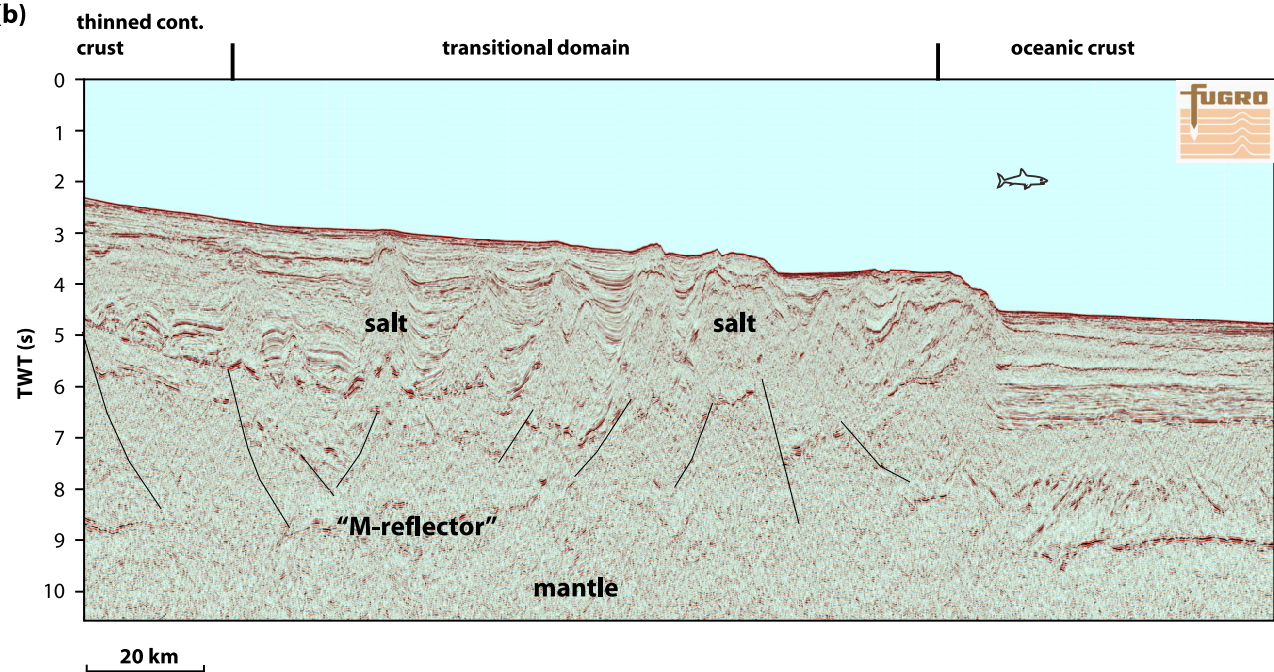


**Figure 4.** (continued)

part of the presalt basins was questioned [Contrucci *et al.*, 2004; Moulin *et al.*, 2005].

### 3.3. Continent-Ocean Transitional Domain

[18] The earlier defined COB location along the northeastern Brazilian margin, coinciding with a prominent Bouguer-corrected gravity high [Karner and Driscoll, 1999; Blaich *et al.*, 2008], is found to be closely related to the transition from the thinned continental domain to the transitional domain rather than to the COB location (Figure 3a) [Blaich *et al.*, 2010]. Furthermore, a prominent listric normal fault appears to be associated with this boundary (Figures 3a–3c). Typically, the transitional domain along the northeastern Brazilian margin indicates densities between 2800 and 2900 kg/m<sup>3</sup> and is characterized by rotated fault blocks and wedge-shaped synrift sedimentary sequences (Figures 3a–3c) [Blaich *et al.*, 2010]. Due to the limited extension of the industrial seismic reflection profiles toward normal oceanic crust, the oceanward limit of the transitional domain is poorly constrained. However, high-amplitude reflections observed within the wedge-shaped synrift sedimentary sequences at the oceanward edge of the MCS profiles have been interpreted as igneous material interbedded within sediments and as indicative of proximity to normal oceanic crust (Figures 3a–3c) [Blaich *et al.*, 2010]. A high-amplitude and undulated reflector (“M reflector,” [Blaich *et al.*, 2010]) is observed and underlies the rotated fault blocks at the transitional domain (Figures 3a and 3c), and the performed gravity modeling indicates that this prominent reflector probably corresponds to the Moho discontinuity that appears to be extremely shallow (Figure 3a).

[19] Along the conjugate margin off Gabon, a set of industrial and published deep seismic reflection profiles extend into the presumed normal oceanic crust. In this set-

ting, the boundary between thinned continental crust and transitional domain is defined by the oceanward edge of the anomalous lower crust, indicated by landward dipping reflections, and is characterized by shallowing of the Moho discontinuity (Figure 3a). The COB along this margin is placed approximately at the seaward limit of the salt basin, where the crust is clearly oceanic in seismic reflection character [e.g., Mohriak *et al.*, 1995; Torsvik *et al.*, 2009]. The oceanic crust observed along the Gabon margin is highly reflective, rough and characterized by relatively flat Moho (Figure 3a). In addition, the COB location along both Brazil and Gabon conjugate margins is characterized by flattening of the Bouguer-corrected gravity anomalies (Figure 3a). The interpreted COB along the Gabon margin is mirrored along the northeastern Brazilian margin and is defined as the “line of fit” used for potential field plate reconstructions (Figure 2).

[20] The transitional domain along the Espírito Santo Basin is also characterized by rotated fault blocks and wedge-shaped synrift sedimentary sequences, and a prominent listric normal fault appears to be related to the transition from the thinned continental domain to the transitional domain (Figures 4a and 4b). The crust at the transitional domain has been interpreted as igneous crust by Mohriak *et al.* [2008], however, the absence of seaward-dipping reflections (SDRs) and of major extrusive basalt flows from the available MCS profiles precludes the presence of igneous crust at the transitional domain. The oceanward limit of the transitional domain, the COB, is placed approximately at the seaward limit of the salt basin, where an allochthonous salt tongue advancing toward the oceanic crust is observed [Mohriak *et al.*, 2008]. The oceanic crust is characterized by a transparent upper layer, a highly reflective lower layer containing sets of seaward- and landward-dipping reflections

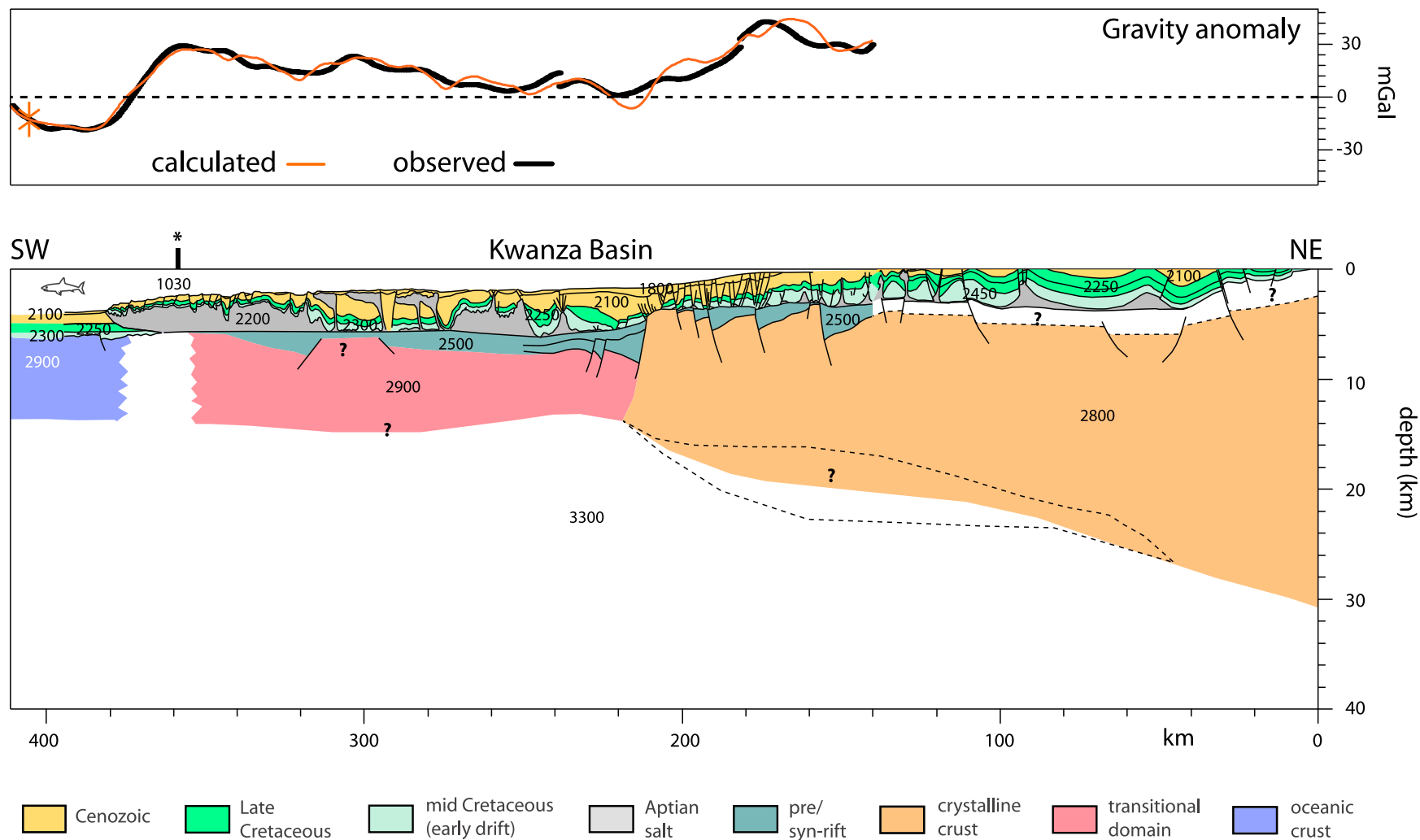


**Figure 5.** Gravity modeled transect along the Kwanza Basin (location in Figure 2) utilizing the satellite radar altimeter free air gravity anomaly field ([Sandwell and Smith, 1997]; version 16.1). Indicated densities in  $\text{kg/m}^3$ . Asterisk indicates “line of fit” used for plate reconstructions (see discussion in text).

and a high seismic amplitude, relatively flat Moho reflector (Figure 4b). Furthermore, the oceanic crust is covered by mostly subhorizontal layered sedimentary successions [Mohriak *et al.*, 2008]. Along the conjugate Kwanza Basin, the transitional domain is poorly imaged on the available MCS profiles and this obscures the potential identification of possible similar structures as in the Espírito Santo and Camamu basins, i.e., rotated fault blocks and wedge-shaped synrift sedimentary sequences (Figures 3 and 4). A transitional domain, however, located between the continental crust and normal oceanic crust has been recognized farther north [Contrucci *et al.*, 2004]. Similar to the Espírito Santo Basin, a prominent listric normal fault appears to be related to the transition from the thinned continental domain to the transitional domain along the conjugate Kwanza Basin (Figure 5). Furthermore, gravity modeling indicates densities of  $2900 \text{ kg/m}^3$  for the crust at the transitional domain along both Espírito Santo–Kwanza conjugate basins (Figures 4a and 5). The oceanward limit of the transitional domain, the COB location along the Kwanza Basin, is also placed approximately at the seaward limit of the salt basin where a massive allochthonous salt tongue is observed at the proximities of the COB (Figures 4a–4b and 5). The oceanic crust is covered by sedimentary successions with mostly subhorizontally layered sediments. Similar to the Camamu–South Gabon conjugate basins (Figure 3a), the conjugate transects along the Espírito Santo–Kwanza basins (Figure 6) indicate narrow/wide conjugate margin configuration. Farther oceanward from the COB, the conjugate transects are characterized by very similar allochthonous salt tongues that are advancing toward the oceanic crust [Fainstein and Krueger, 2005]. In addition, the COB is associated with a positive magnetic and gravimetric anomaly (Figures 4a, 5, and 6).

[21] A resume of the prominent features observed on plate reconstructions and on the modeled transects along the central segment is presented in Figure 7. The thinned continental crust domain along the Camamu–Gabon and Espírito Santo–Kwanza conjugate basins is formed by asymmetric lithospheric extension, where the African margin is characterized by a wide and gentle crustal taper that is conjugate to a narrow and sharp crustal taper along the Brazilian margin (Figures 3a, 6, and 7). Farther south, however, along the Santos–Namibe conjugate basins, the asymmetry is characterized by a wide/narrow margin configuration. This asymmetry was interpreted by Mohriak [2001] to be associated with a failed spreading center (Abimael Ridge) that advanced from the northern Pelotas Basin toward the southern Santos Basin but did not propagate effectively northward of the Florianópolis Fracture Zone, resulting in an eastward ridge jump that placed the rupture zone toward the African side. The lithospheric extension along the Camamu–Gabon and Espírito Santo–Kwanza conjugate basins resulted in the formation of an asymmetric thinned continental crust domain and an approximately symmetric transitional domain (Figure 7). In addition, the transitional domain along the Espírito Santo–Kwanza conjugate basins is considerably wider than the transitional domain along the Camamu–Gabon conjugate basins (Figure 7). North of the Salvador–N’Komi transfer zones, it seems to be an overlap of the COB, meaning that the prominent conjugate Salvador–N’Komi transfer zones appear to be first-order structural elements, governing the margin segmentation and evolution and may have acted as an intra-

plate decoupling zone [Teisserenc and Villemain, 1989; Wannesson *et al.*, 1991; Blaich *et al.*, 2010].

## 4. South Segment

### 4.1. Margin Setting

[22] Potential field plate reconstructions at Chron M0 ( $\sim 125 \text{ Ma}$ ; Figure 8) were performed using rotation poles of Moulin *et al.* [2010]. The continental shelf along the South American margin of the south segment, widens considerably southward, reaching a width of over 600 km along the Argentine margin (Figure 8a). On the other hand, the continental shelf along the African margin of the south segment does not vary much in width. In this setting, the southeastern Brazil–Namibia conjugate margin is characterized by a wide continental shelf along both parts, indicating a wide/wide margin configuration (Figure 8a). Farther south, the Argentine–South Africa conjugate margin is characterized by a very wide/wide margin configuration.

[23] The gridded aeromagnetic anomaly field map (Figure 8b) reflects an overall NE–SW trending magnetic pattern, and is characterized by well-defined magnetic anomalies that can be separated into zones of distinct internal magnetic character. Close to the Rio Grande Fracture Zone, however, where the Rio Grande Plateau and Walvis Ridge are located and interpreted as the trails of the Tristan da Cunha plume, a complex magnetic pattern is observed. There, the anomalies are more chaotic and do not show the same linear character as farther south, implying that magnetic anomalies in this area are not unambiguously recognized and thus disputed (Figure 8b). The prominent positive, linear “G magnetic anomaly” [Rabinowitz and LaBrecque, 1979] was interpreted as a magnetic “edge effect” caused by the different magnetic properties of continental and oceanic crust. The “G magnetic anomaly,” in this way, was defined as the COB and its location was set at the landward end of the broad positive anomaly (Figure 8b) [Rabinowitz and LaBrecque, 1979]. Alternative explanations for the “G magnetic anomaly” have been offered as the cause of this anomaly is controversial. For example, magnetic modeling across the Argentine [Hinz *et al.*, 1999], Namibia [Bauer *et al.*, 2000] and South Africa margins [Blaich *et al.*, 2009] has indicated thick layers of extrusive basalts, identified as SDRs, as the causal source of the “G magnetic anomaly.” Thus, the “G magnetic anomaly” coincides roughly with the landward edge of the SDRs [Hinz *et al.*, 1999; Blaich *et al.*, 2009]. As the major part of volcanic extrusives terminates largely southward of the Colorado transfer system [Franke *et al.*, 2007], the “G magnetic anomaly” is weak or absent southward of the Colorado–Hope transfer system. These observations suggest that the “G magnetic anomaly” is associated with the wedge of seaward dipping reflections and extrusive basaltic complexes, and does not necessarily correspond to the COB location.

[24] The oldest magnetic seafloor-spreading anomaly recognized along the south segment is correlated to M4 [Rabinowitz and LaBrecque, 1979]. The magnetic anomalies along the south segment have been recently reinterpreted based on additional industrial magnetic data [Moulin *et al.*, 2010]. Consequently, the large amplitude magnetic anomaly, including parts of “G magnetic anomaly” was grouped into a new anomaly called Large Marginal Anomaly (LMA, Figure 8b). The LMA along the South America margin is narrow and not

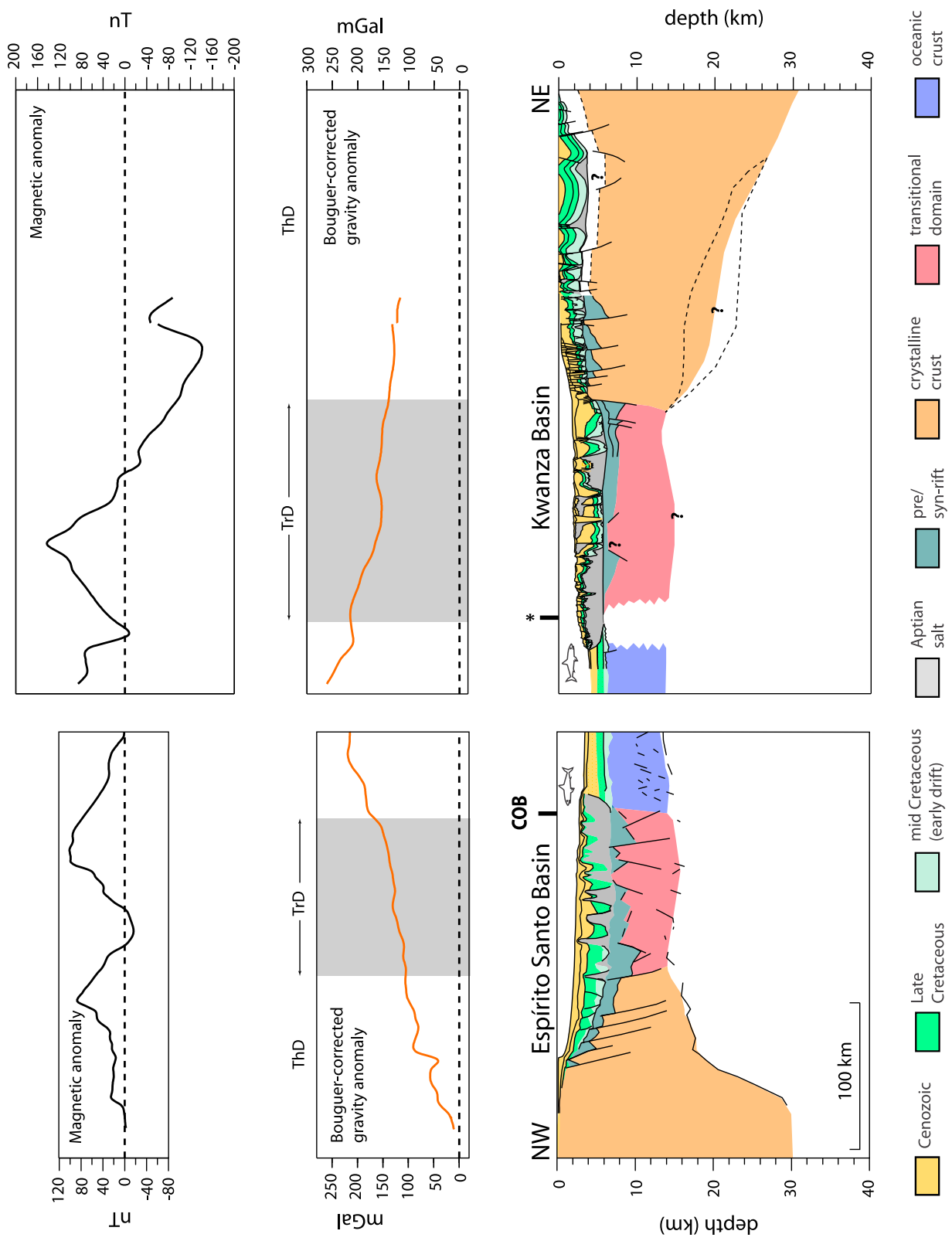
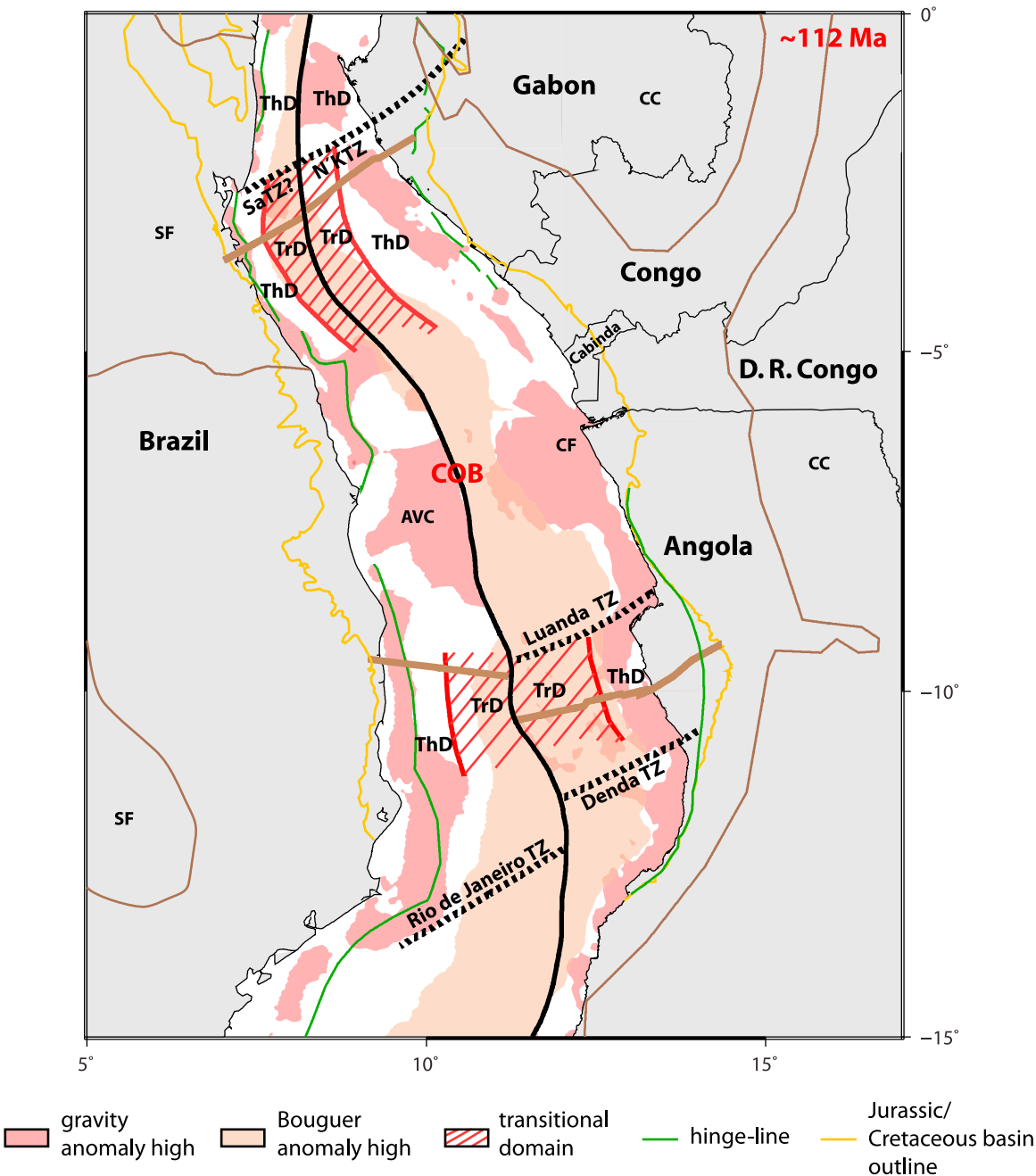
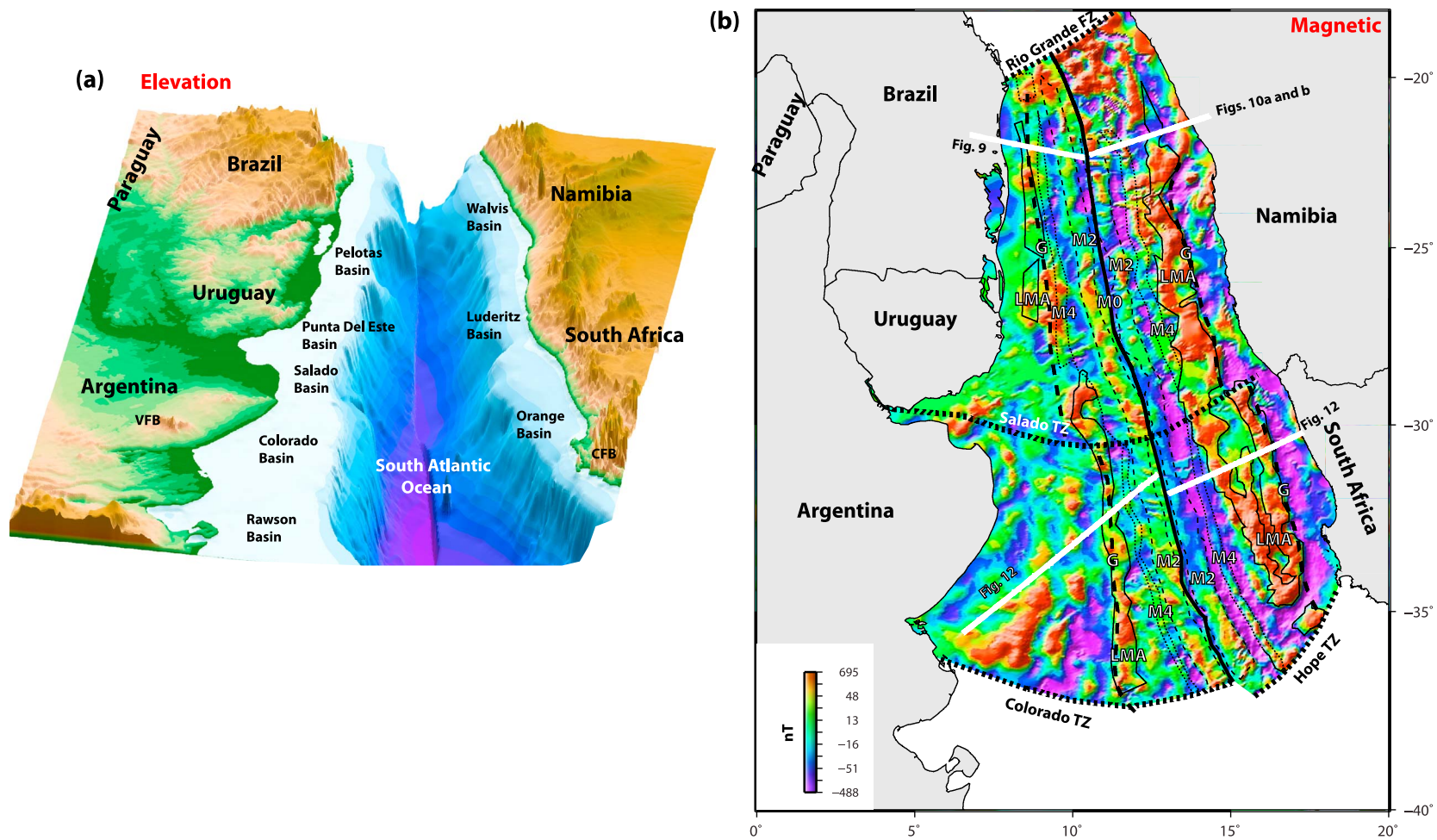


Figure 6



**Figure 7.** Resume of prominent features observed on plate reconstructions at forced breakup time (~112 Ma) (Figures 2c and 2d); the continent-ocean boundary (COB) location along the conjugate margin off northeastern Brazil-Gabon is based on Blaich et al. [2010]. Farther south, along the conjugate margin off southeastern Brazil-Angola the COB location is modified from Mohriak et al. [2008] and is consistent with observations made in this study. Hinge lines are derived from Karner and Driscoll [1999] and Mohriak et al. [2008] for the Brazilian margin and Hudec and Jackson [2002, 2004] and Mounguengui and Guiraud [2009] for the Africa margin. Jurassic/Cretaceous basin outlines are derived from Moulin et al. [2010, and references therein]. ThD, thinned crystalline crust domain; TrD, transitional domain; AVC, Abrolhos volcanic complex; CF, Congo Fan; SaTZ, Salvador Transfer Zone; N'KTZ, N'Komi Transfer Zone; CC, Congo Craton; SF, São Francisco Craton; TZ, transfer zone.

**Figure 6.** Conjugate transects along Espírito Santo–Kwanza basins (location in Figure 2). Extracted along-transect Bouguer-corrected gravity anomaly and aeromagnetic anomaly [IAGA, 2007] are also shown. COB, continent-ocean boundary; asterisk indicates “line of fit” used for plate reconstructions (see discussion in text); ThD, thinned crystalline crust domain; TrD, transitional domain.



**Figure 8.** Plate reconstructions at Chron M0 (~125 Ma) utilizing the rotation poles of Moulin *et al.* [2010]. (a) A  $1 \times 1'$  elevation grid [British Oceanographic Data Centre, 2003]. Offshore sedimentary basins are indicated. (b) A  $3 \times 3'$  gridded aeromagnetic anomaly field [IAGA, 2007]. (c) A  $1 \times 1'$  satellite radar free air gravity anomaly field ([Sandwell and Smith, 1997]; version 16.1). (d) Low-pass-filtered ( $>200$  km) Bouguer-corrected gravity anomaly field (utilizing a density of  $2670 \text{ kg/m}^3$  as infill to the bathymetric relief). The locations of conjugate transects are indicated. M sequences magnetic anomalies after Moulin *et al.* [2010]; LMA, Large Marginal Anomaly [Moulin *et al.*, 2010]. G, “G magnetic anomaly” after Rabinowitz and LaBrecque [1979]; TZ, transfer zone; FZ, fracture zone.

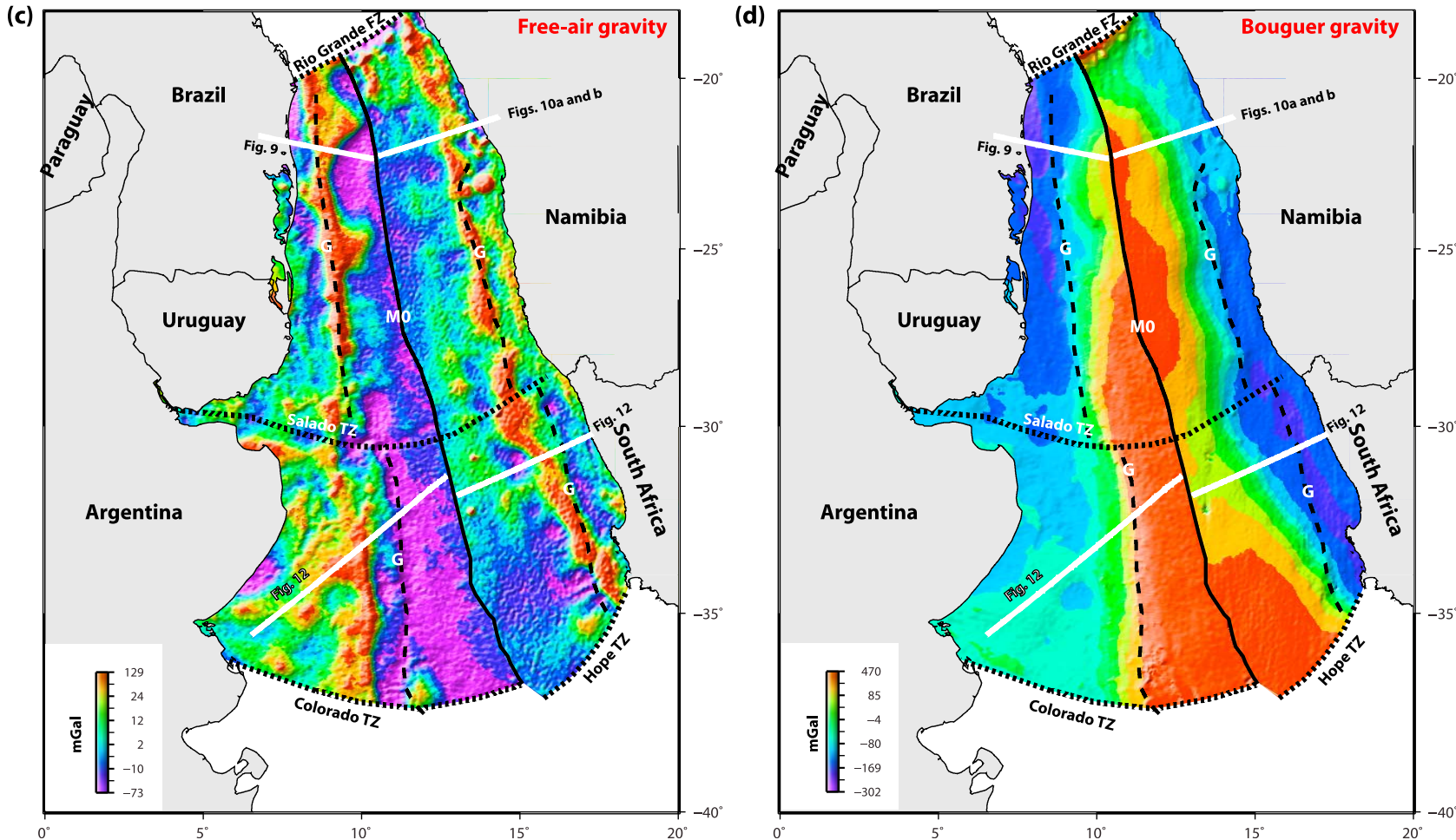


Figure 8. (continued)

as prominent and wide as in the conjugate African margin, where it is characterized by a double branch along the Orange Basin [Moulin *et al.*, 2010]. In this setting, the reconstructed conjugate magnetic anomaly map indicates overall symmetry at the Pelotas-Walvis conjugate basins, whereas, asymmetry is observed and is characterized by a narrow/wide margin configuration farther south. Along the NE Atlantic margin, a similar magnetic asymmetry has been explained by an asymmetric seafloor spreading [e.g., Larsen and Saunders, 1998] or by stretched and intruded continental crust, where the asymmetry is caused by the initial continental stretching rather than the subsequent seafloor spreading [e.g., White and Smith, 2009].

[25] The gravity grid along the conjugate margins of the south segment (Figure 8c) also reveals a continuous, prominent and elongated gravity anomaly high close to the shelf edge that trends subparallel to the coastline. The “edge effect” positive gravity anomalies along the Namibia margin have been interpreted to be caused by the juxtaposition of continental and oceanic crust [Rabinowitz and LaBrecque, 1979; Bauer *et al.*, 2000]. Furthermore, the interpreted “G magnetic anomaly” along the conjugate margins off southeastern Brazil-Namibia is spatially related to the “edge effect” gravity anomaly high (Figure 8c). Farther south, however, the “G magnetic anomaly” along the Argentine-South Africa conjugate margin deviates considerably from the “edge effect” gravity anomaly high. In this setting, seismic reflection profiles complemented by gravity modeling [Blaich *et al.*, 2009] and wide-angle seismic data [Schnabel *et al.*, 2008], clearly indicate that the “edge effect” positive gravity anomalies along the Argentine margin are associated with near-seafloor density contrasts and the equivalent depth difference of base crust compensation (as indicated in other continental margins worldwide [e.g., Talwani and Eldholm, 1972; Tsikalas *et al.*, 2005]) and not by the juxtaposition of continental and oceanic crust. Moreover, synrift rotated fault blocks and typical continental crust velocities are observed oceanward of the “edge effect” anomaly high [Franke *et al.*, 2006; Schnabel *et al.*, 2008]. On the other hand, the “edge effect” positive gravity anomaly along the conjugate South Africa margin requires a high-density body in the lower crust to produce the density contrast required by the gravity models [e.g., Blaich *et al.*, 2009; Hirsch *et al.*, 2009]. In this setting, the “edge effect” positive gravity anomaly along the conjugate South Africa margin is considered to be caused by heavily intruded continental crust and/or underplating, and again not necessarily by the juxtaposition of continental and oceanic crust. A more diffuse and less prominent elongated gravity high is observed farther oceanward of the “edge effect” anomaly high along the African margin (Figure 8c). This feature has been interpreted as an “edge effect” produced by the juxtaposition of transitional igneous crust and normal oceanic crust, correlating to the transitional igneous crust–normal oceanic crust boundary [Bauer *et al.*, 2000]. A similar feature is not observed along the conjugate South America margin (Figure 8c). The low-pass-filtered, Bouguer-corrected gravity field map (Figure 8d) reveals a prominent negative-positive gradient character that, along the Argentine margin, is spatially associated to the “G magnetic anomaly.” The “G magnetic anomaly,” however, deviates from the prominent negative-positive gradient farther north. Along the conjugate margin off South Africa, the

“G magnetic anomaly” deviates considerably from the negative-positive gradient on the Bouguer-corrected gravity field (Figure 8d). Finally, the high values of the Bouguer-corrected gravity field pinch out and are replaced by low values close to the Rio Grande Fracture Zone, suggesting thicker crust.

#### 4.2. Crustal Architecture

[26] The representative crustal transect obtained through 2-D gravity modeling in the current study (Figure 9) outlines the crustal structure of the Pelotas Basin and extends ~640 km in a W-E direction. Although evidence for synrift sedimentation is not overwhelming in the Pelotas Basin [Abreu, 1998; Talwani and Abreu, 2000], antithetic normal faults forming half-graben systems are observed and could be filled by prerift and/or synrift sedimentary rocks (Figure 9). These structures, however, are believed to be predominantly infilled by basalt flows [Talwani and Abreu, 2000]. Oceanward, a characteristic wedge of seaward dipping reflections (SDRs) is observed (Figure 9) and believed to have been emplaced during Early Cretaceous, during breakup [Abreu, 1998]. A very thick package of sedimentary strata overlies the basalt flows and SDRs (Figure 9). Although the Moho discontinuity has been poorly constrained by old vintage seismic reflection/refraction profiles along the Pelotas Basin [Fontana, 1996; Mohriak, 2003], the analysis performed in this study indicates a gentle shallowing of the Moho discontinuity from the platform to the shelf break, and a rapid climbing toward oceanic crust. Moreover, an acceptable 2-D gravity model fit is only accomplished by a high-density crystalline crust ( $3000 \text{ kg/m}^3$ ) and a high-density lower crustal body ( $3100 \text{ kg/m}^3$ ) located below the basalt flows and SDRs (Figure 9). The high-density crust located directly below the SDRs may indicate heavily intruded continental crust [e.g., Cornwell *et al.*, 2006; Schnabel *et al.*, 2008] and it can be interpreted as a region of feeder dikes related to the emplacement of the SDRs. Furthermore, the high-density lower crust is believed to be associated, analogously with other continental margins worldwide, with underplating and/or voluminous igneous rocks intruded into the lower crust [e.g., White *et al.*, 2008; White and Smith, 2009]. Gravity modeling further indicates continental crust densities ( $2800 \text{ kg/m}^3$ ) below the inner basalt flows, where the crust is characterized by synthetic and antithetic normal faults (Figure 9).

[27] Along the conjugate margin off Namibia, the representative crustal transect obtained from 2-D gravity modeling in the current study (Figure 10a) outlines the crustal structure of the Walvis Basin. The constructed transect extends ~617 km in an E-W direction. Geophysical constraints are robust along the transect and composed of MCS reflection profiles (e.g., Figure 3b) [Gladchenko *et al.*, 1998; Bauer *et al.*, 2000] and wide-angle seismic refraction studies [Bauer *et al.*, 2000]. Furthermore, gravity modeling provides additional constraints to the seismic interpretation, increasing the understanding of the crustal architecture (Figure 10a). Synthetic and antithetic normal faults forming half-graben systems are observed seaward and landward of the shelf edge (Figures 10a and 10b). Gladchenko *et al.* [1998] proposed that the grabens are infilled mostly with Paleozoic prerift sediments, forming a very deep and wide prerift sedimentary basin. Gravity modeling, constrained by wide-angle refraction data [Bauer *et al.*, 2000], however, suggests that the size of the prerift basin was overestimated (Figure 10a). Furthermore, similar to the conjugate

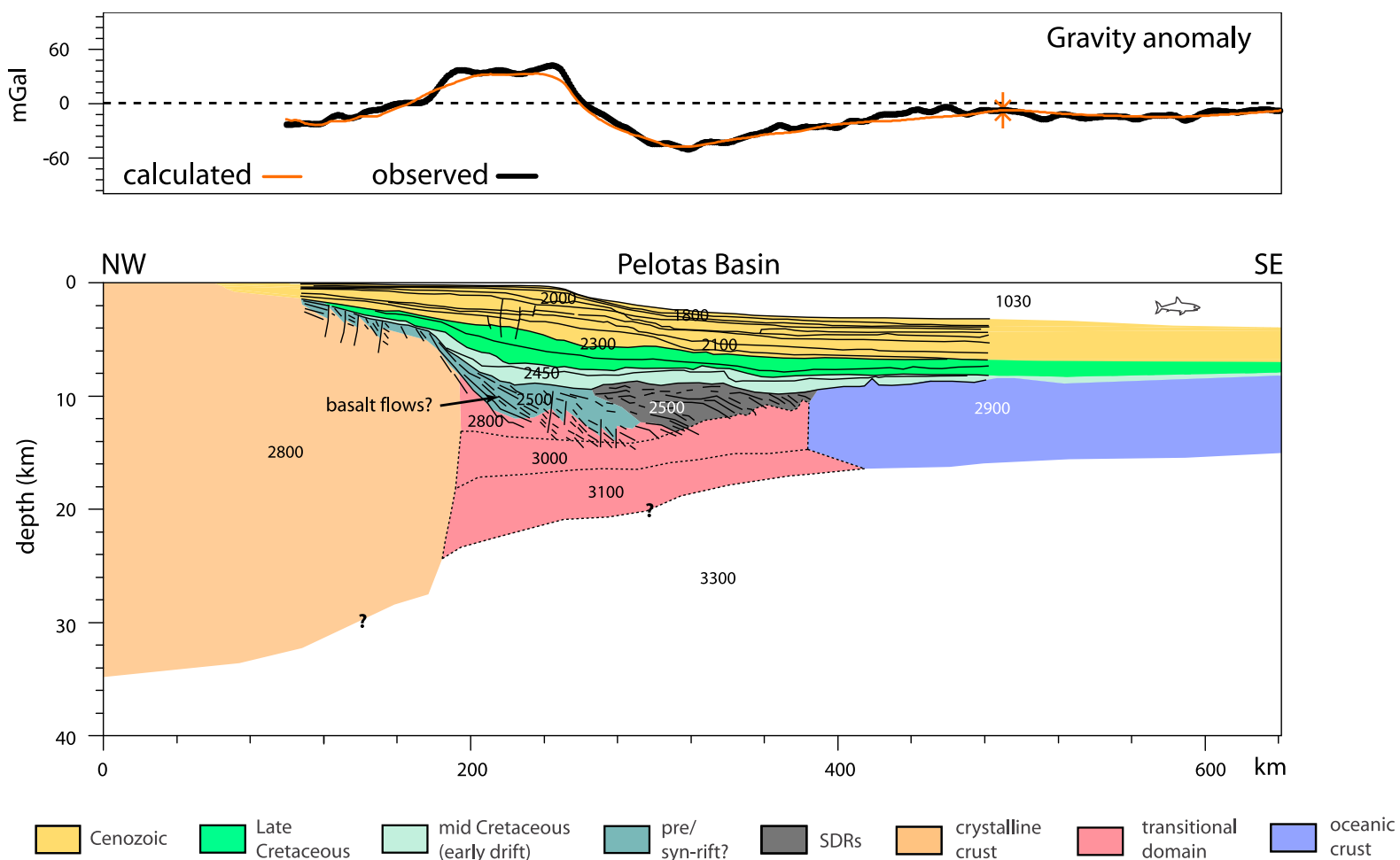


**Figure 9.** Gravity modeled transect along the Pelotas Basin (location in Figure 8) utilizing the satellite radar altimeter free air gravity anomaly field ([Sandwell and Smith, 1997]; version 16.1). Indicated densities in  $\text{kg/m}^3$ . SDRs, seaward dipping reflections.

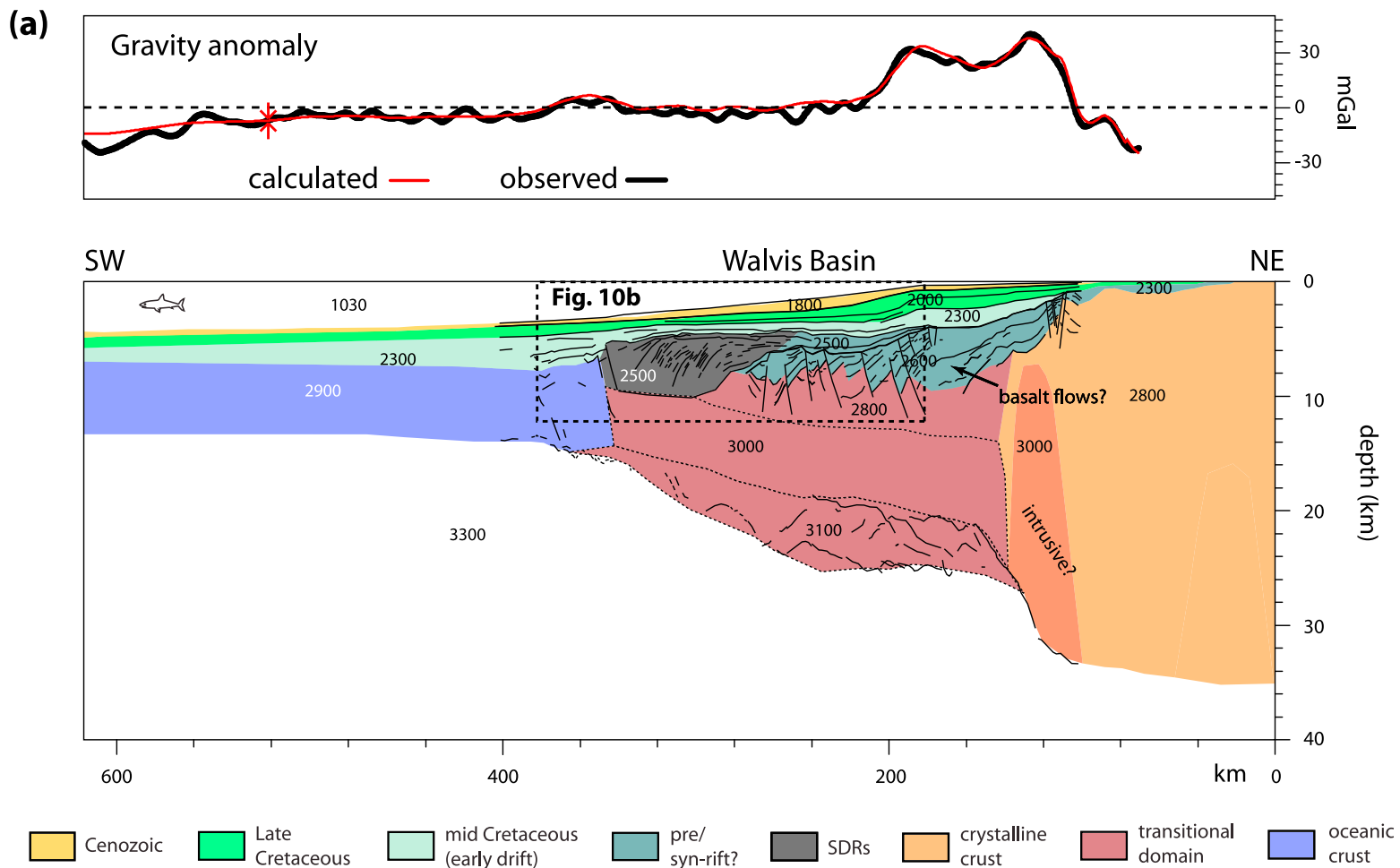


**Figure 10.** (a) Gravity modeled transect along the Walvis Basin (location in Figure 8) utilizing the satellite radar altimeter free air gravity anomaly field ([Sandwell and Smith, 1997]; version 16.1). (b) Seismic example of the transitional domain along the Walvis (location in Figure 8). Indicated densities in  $\text{kg/m}^3$ . SDRs, seaward dipping reflections.

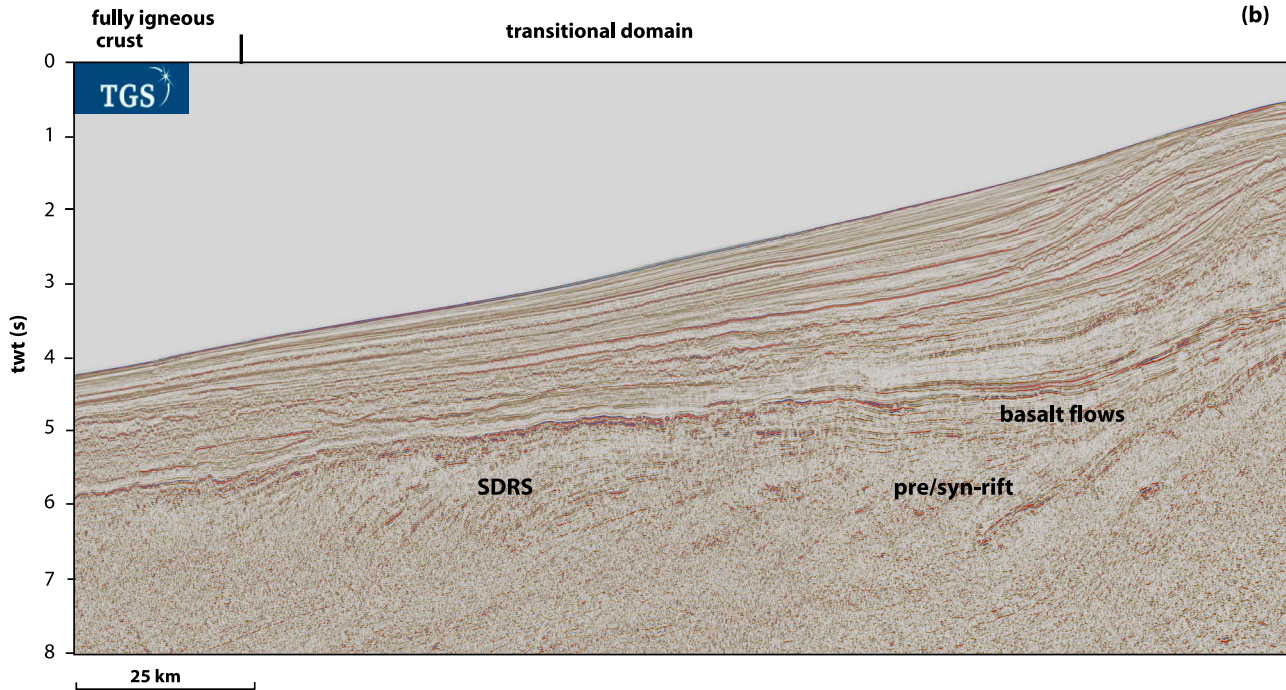


**Figure 10.** (continued)

Pelotas Basin, the half-graben systems along the Walvis Basin could also be filled with synrift sedimentary sequences and basalt flows (Figures 10a–10b and 11). This assumption is further supported by the fact that *Bauer et al.* [2000] have identified inner basalt flows (inner SDRs) that filled similar basins in the vicinity of the modeled transect. Gravity modeling further indicates continental crust densities ( $2800 \text{ kg/m}^3$ ) directly below the inner basalt flows, where the crust is characterized by synthetic and antithetic normal faults (Figures 10a–10b). Oceanward, a characteristic wedge of SDRs is observed (Figure 10b). Below the SDRs high seismic velocities ( $>7 \text{ km/s}$ ) [*Bauer et al.*, 2000] and high densities ( $3000 \text{ kg/m}^3$ ) are observed and interpreted as a region of feeder dikes related to the emplacement of the SDRs. An intracrustal band of high-amplitude seismic reflections that are subparallel to the gently shallowing Moho reflections seems to separate crustal levels with different reflectivity character [*Gladchenko et al.*, 1998]. Furthermore, the presence of high velocities ( $\sim 7.6 \text{ km/s}$ ) below the intracrustal band of seismic reflections was proposed to indicate underplating [*Bauer et al.*, 2000], however, this feature may also indicate voluminous igneous rocks intruded into the lower crust [e.g., *White and Smith*, 2009]. These observations are supported by our gravity modeling, where a high-density lower crustal body ( $3100 \text{ kg/m}^3$ ) is required (Figure 10a). Landward of the shelf edge, a single Moho reflector dips steeply landward (Figure 10a). In order to accomplish an acceptable 2-D gravity model fit, a high-density ( $3000 \text{ kg/m}^3$ ) body within the crust is required landward of the shelf edge. This body may be associated to the Cape Cross intrusive complex described by *Bauer et al.* [2000]. The conjugate transects along the Pelotas-Walvis basins (Figure 11) indicate approximately symmetric conjugate margin configuration that is characterized by a gentle crustal taper and by symmetric SDR provinces [e.g., *Talwani and Abreu*, 2000].

[28] At the southern part of south segment, the representative conjugate crustal transects obtained through 2-D gravity modeling (Figure 12) outline the crustal structure of the Argentine-South Africa conjugate margins. Explicit modeling details of the transects in Figure 12 are presented by *Blaich et al.* [2009], while in this study we discuss particular issues on the two transects that elucidate the margin evolution of the southern part of the south segment. Along the Argentine margin, wide-angle seismic refraction data [*Franke et al.*, 2006] combined with gravity modeling [*Franke et al.*, 2006; *Blaich et al.*, 2009] indicate a high-velocity/high-density lower crust on the western part of the transect (Figure 12). Such a high-velocity/high-density lower crustal body may be inherited from Paleozoic accretion of terranes against SW Gondwana [e.g., *Ramos*, 1996, 2004]. Unlike the enigmatic lower crustal body observed along the Gabon margin that affected mainly the Cretaceous rifting (Figure 3a), the high-velocity/high-density lower crustal body along the Argentine margin does not seem to influence the Cretaceous rifting in the same way as it is located mainly below Jurassic rifted basins (Figure 12). A similar lower crustal body is not observed along the conjugate South Africa margin.

[29] Seismic interpretation and gravity modeling indicate marginal rift basins characterized by half-graben structures along both Argentine and South Africa conjugate margins. These structures are locally compensated by shallowing of the Moho discontinuity along the South Africa margin (Figure 12). Farther oceanward, deeper and extensive central rift basins are interpreted along both conjugate margins and characterized by thinning of the continental crust. The sedimentary infill of the central rift basin is believed to comprise synrift sediments and basalt flows [*Séanne and Anka*, 2005; *Franke et al.*, 2007; *Blaich et al.*, 2009; *Hirsch et al.*, 2009]. Even though SDRs are not easily

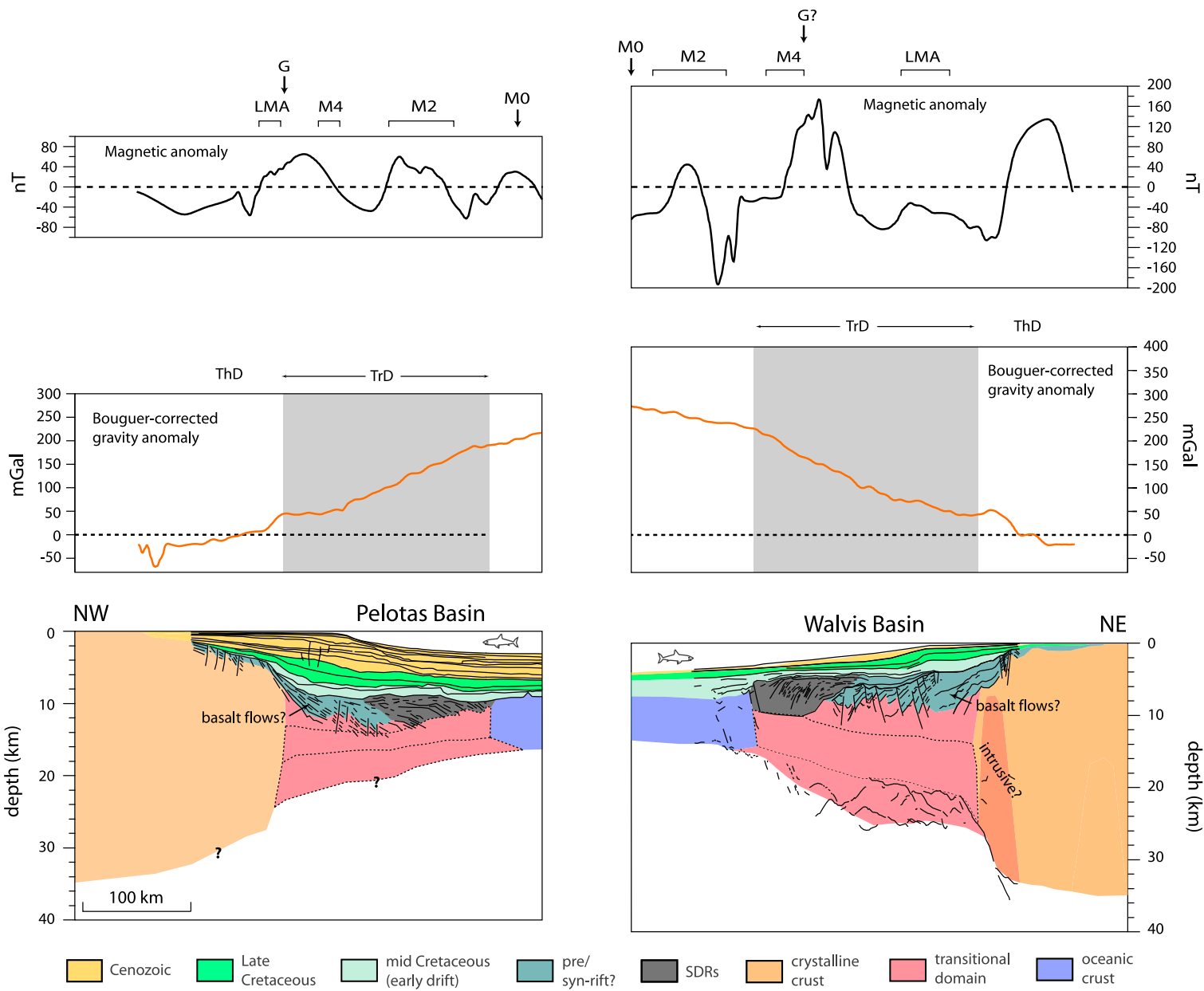


Figure 11

recognized on the seismic profile along the South Africa margin, such reflections have been earlier proposed [Séranne and Anka, 2005]. Furthermore, results from the gravity modeling and the prominent and positive magnetic anomalies across these basins tend to support the existence of extrusives (Figure 12). Underlying the extrusive lavas, these conjugate margins exhibit high-velocity/high-density lower crustal bodies which are associated with underplating [Franke et al., 2006; Hirsch et al., 2009; Blaich et al., 2009], however, the lower crustal body may be also interpreted as voluminous igneous rocks intruded into the lower crust [e.g., White and Smith, 2009]. Last, the observed prominent negative-positive gradient zone of the Bouguer-corrected gravity anomaly along the South Africa margin is less steep than along the Argentine margin, suggesting a gentle shallowing of the Moho discontinuity along the South Africa margin that is conjugate to an abrupt shallowing of the Moho discontinuity along the Argentine margin (Figure 12). These observations are further confirmed by wide-angle seismic refraction, MCS data and gravity modeling [Franke et al., 2006; Blaich et al., 2009; Hirsch et al., 2009].

#### 4.3. Continent-Ocean Transitional Domain

[30] A transitional domain is interpreted along the south segment and characterized by basalt flows and seaward dipping reflections (SDR) located above a high-density crust and a high-density lower crustal body (Figures 11 and 12). The extrusive basalts on the continent-ocean transitional domain form a series of SDR wedges. In Figure 13, we show a compilation of interpretations of the upper crustal structure, combined with the magnetic anomalies along the south segment conjugate margins. Therefore, Figure 13 depicts the morphology of the extrusive basalts and their relation to the magnetic anomalies. The description of the volcanic features along the south segment follows the volcanostratigraphy nomenclature of Planke et al. [2000]. Along the Pelotas Basin, seaward dipping reflectors are observed landward of the shelf edge and are associated with a prominent positive magnetic anomaly, including the LMA and “G magnetic anomaly” (Figure 13a). The striking similarity of these structures to the inner SDRs observed along the conjugate Walvis Basin [Bauer et al., 2000], suggests that inner SDRs may also be present along the Pelotas Basin (Figure 13). The Paleozoic prerift basin interpreted by Gladzenko et al. [1998] along the conjugate Walvis Basin is also associated with the LMA and with an unidentified magnetic anomaly high farther north. These observations suggest that the Paleozoic prerift basin may be filled with basalt flows and can also be interpreted as inner SDRs (Figure 13b). Along the Argentine margin farther south, there are clear evidences of inner SDRs (Figure 13a) [e.g., Franke et al., 2010] that are also associated with a prominent positive magnetic anomaly, including the LMA and “G magnetic anomaly.” Along the conjugate margin off South Africa, inner SDRs and inner basalt flows have also been

proposed [e.g., Bauer et al., 2000; Blaich et al., 2009; Hirsch et al., 2009] and appear to be associated with the landward part of the very wide LMA (Figure 13b). Therefore, the landward boundary of the transitional domain is characterized by the landward termination of the inner SDRs/inner basalt flows which, in turn, are associated with the prominent positive magnetic anomaly (LMA) [Moulin et al., 2010] and with the “G magnetic anomaly” [Rabinowitz and LaBrecque, 1979]. The fully oceanic (i.e., fully igneous) crust, characterizing the oceanward boundary of the transitional domain is placed near the seaward termination of the arcuate outer SDRs, which is also associated with prominent positive magnetic anomalies (Figure 13). This implies that the transitional domain–fully oceanic crust boundary is related to the oceanward termination of the synrift volcanic wedges [e.g., Skogseid and Eldholm, 1987; Gladzenko et al., 1998; White and Smith, 2009].

[31] A resume of the prominent features observed on plate reconstructions and on the modeled transects along the south segment is presented in Figure 14. North of the Salado Transfer Zone, the continental crust–transitional domain boundary along the south segment conjugate basins is closely associated with a prominent positive magnetic anomaly, including the LMA and “G magnetic anomaly” and with the prominent and elongated “edge effect” gravity anomaly high (Figure 14). Moreover, the “edge effect” positive gravity anomaly appears to be caused by heavily intruded continental crust and/or underplating, and not by the juxtaposition of continental and oceanic crust(s) (Figures 9 and 10a). Farther oceanward, the transitional domain–fully oceanic crust boundary is characterized by the seaward termination of the arcuate outer SDRs that are located between magnetic anomaly M2 and M0 along the Pelotas Basin (Figures 13 and 14) where the oceanic crust is characterized by transparent or chaotic seismic facies with diffractions [Abreu, 1998]. Along the Walvis Basin this boundary is associated with magnetic anomaly M4. However, due to the close proximity to the Rio Grande Rise-Walvis Ridge, magnetic interpretations are not unambiguous. The transitional domain–fully oceanic crust boundary along the Walvis Basin is characterized by a relatively flat Moho reflector (Figures 10a, 13, and 14) and by a gravity high interpreted as an “edge effect” produced by the juxtaposition of transitional domain crust and normal oceanic crust (Figures 8c and 10a). Farther south, along the conjugate margins of Argentine-South Africa, the landward boundary of the transitional domain is also closely associated with a prominent positive magnetic anomaly, including the LMA and “G magnetic anomaly.” However, the same boundary deviates considerably from the prominent and elongated “edge effect” gravity anomaly high (Figure 14). Unlike the southeastern Brasil-Namibia margin, the transitional domain along the Argentine-South Africa conjugate margin is asymmetric, being considerably wider along the South Africa margin (Figure 14). Furthermore, a magmatic asymmetry is also evident and is characterized by a broader

**Figure 11.** Conjugate transects along Pelotas-Walvis basins (location in Figure 8). Extracted along-transect Bouguer-corrected gravity anomaly and aeromagnetic anomaly [IAGA, 2007] are also shown. ThD, thinned crystalline crust domain; TrD, transitional domain; M sequences magnetic anomalies after Moulin et al. [2010]; LMA, Large Marginal Anomaly [Moulin et al., 2010]; G, “G magnetic anomaly” after Rabinowitz and LaBrecque [1979]; SDRs, seaward dipping reflections.

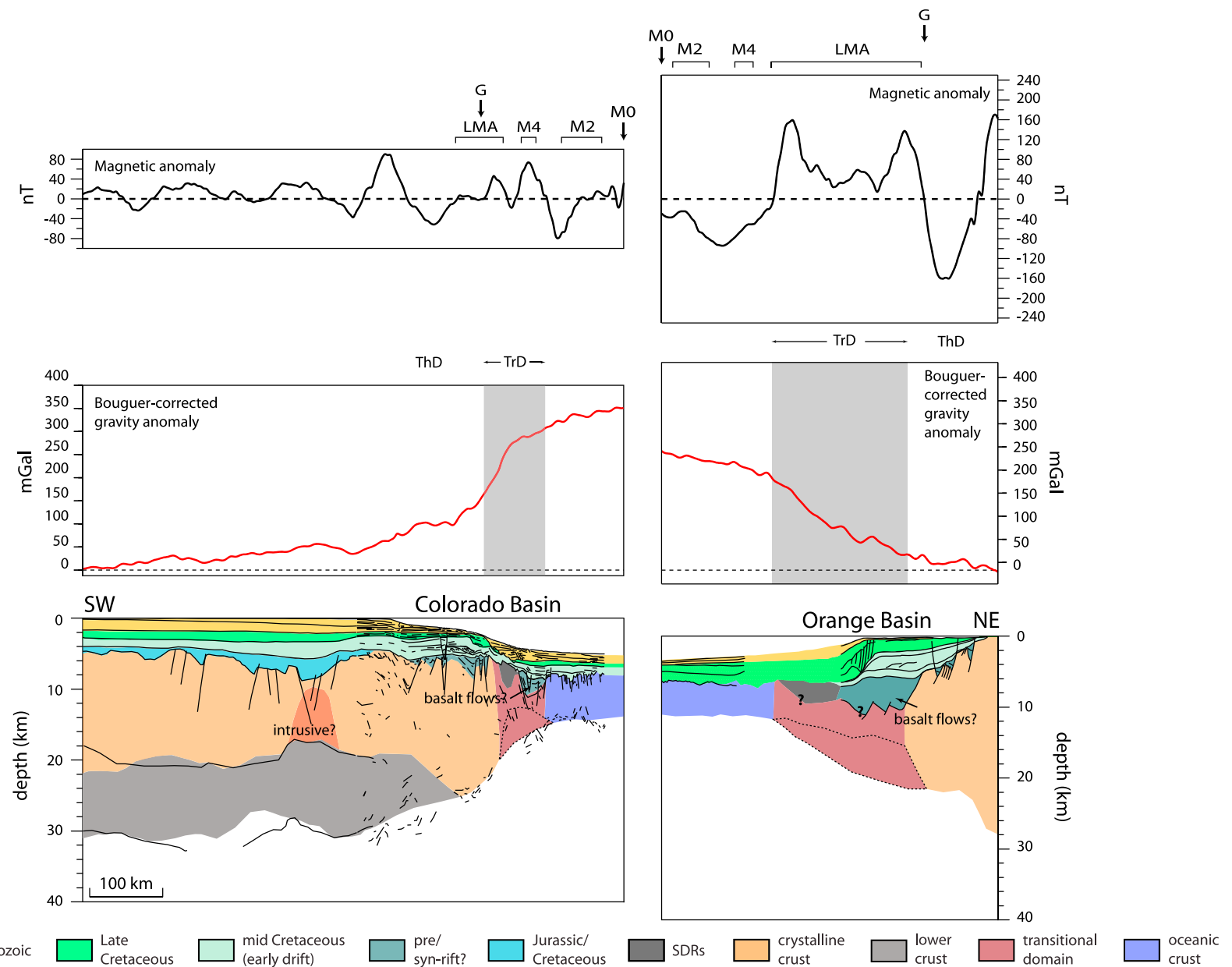


Figure 12

zone of positive magnetic anomalies along the South Africa margin (Figures 8c and 14), implying a wider zone influenced by extrusive volcanic material. The fully oceanic (i.e., fully igneous) crust, characterizing the oceanward boundary of the transitional domain is placed near the seaward termination of the basalt flows (Figure 13), where the Moho reflector along the Argentine margin is relatively flat (Figure 12). Furthermore, this boundary along both Argentine-South Africa conjugate margins is closely associated with magnetic anomaly M4 in the northern area, close to the Salado Transfer Zone. Farther south, however, the oceanward boundary of the transitional domain is associated with the oceanward termination of the LMA (Figures 13 and 14).

## 5. Continental Breakup

[32] Lithospheric extension from early rifting to breakup is a complex process as interaction of tectonic and magmatic processes takes place and the result is a wide variety of margin styles. Two such end-member margins have been subjected to intense debate, the “magma-dominated” and the “magma-poor” margins. In this context, possibly anomalous crust located within the continent-ocean transitional domain has been recognized along several margin segments in South Atlantic and described variously as ‘proto-oceanic crust,’ ‘attenuated continental crust’, and ‘transitional crust’ [e.g., Meyers et al., 1996a, 1996b; Rosendahl and Groschel-Becker, 1999; Wilson et al., 2003; Moulin et al., 2005; Rosendahl et al., 2005]. However, in most of the passive margins worldwide the nature and the precise evolution of the crust at the transitional domain from early rifting to breakup of the continental lithosphere is still unclear and several alternative models have been proposed [Whitmarsh et al., 1996; Wilson et al., 2003; Rosendahl et al., 2005; Kusznir and Karner, 2007; Afilhado et al., 2008; Reston, 2009a].

[33] The continent-ocean transitional domain along “magma-dominated” margins is characterized by high seismic velocities in the lower crust, which are associated with voluminous igneous rocks intruded into the lower crust [White et al., 2008]. The voluminous intrusives resulted from enhanced decompressional melting by mantle upwelling and from accretion processes of igneous material during breakup [e.g., White and McKenzie, 1989; Bauer et al., 2000; Mjelde et al., 2002, 2009]. These high seismic velocity bodies correlate particularly with breakup features such as the large volume of subaerial flood basalts which flow across the continental hinterlands during continental breakup forming the extrusive counterpart of the intruded crust [Planke and Eldholm, 1994; Gladzenko et al., 1998; Eldholm et al., 2000; Skogseid et al., 2000; Talwani and Abreu, 2000; White and Smith, 2009]. On the other hand, the “magma-poor” margins show evidence of polyphase rift evolution which is associated with a complex time-dependent thermal structure of the lithosphere [Lavier and Manatschal, 2006; Péron-Pinvidic et al., 2007; Péron-Pinvidic and Manatschal,

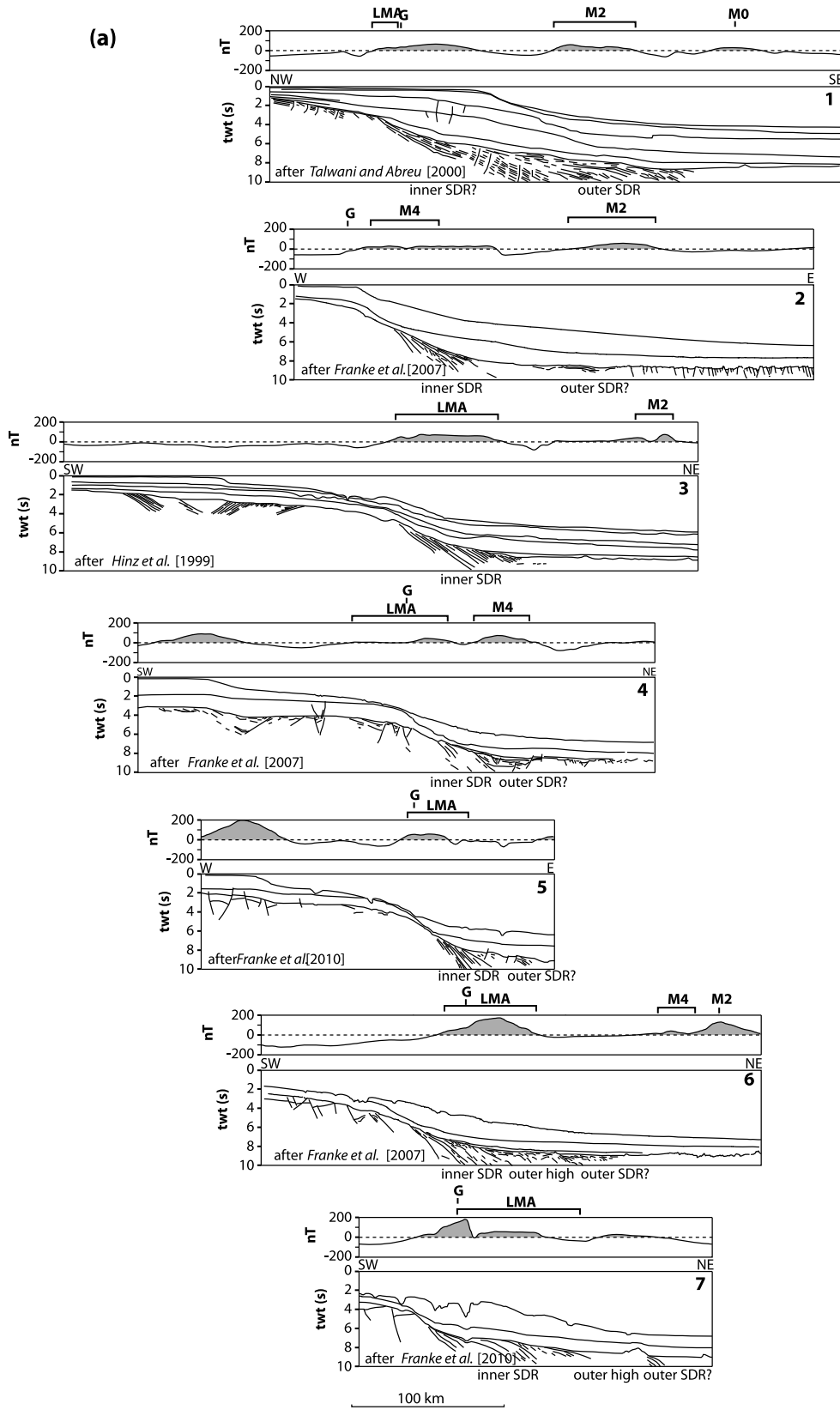
2009]. These margins show evidence of hyperextended crust, where the continent-ocean transitional domain is defined as a broad zone characterized by mantle serpentinization and exhumation of continental mantle [e.g., Whitmarsh et al., 2001; Lavier and Manatschal, 2006; Péron-Pinvidic et al., 2007; Reston and Pérez-Gussinyé, 2007; Reston, 2009a]. In addition, extensive volcanic activity, such as large volume of subaerial flood basalts and prominent magnetic anomalies, typically associated with breakup in “magma-dominated” margins, is absent [Afilhado et al., 2008]. In this chapter, we discuss and compare the lithospheric extension and breakup of the “magma-poor” central segment and the “magma-dominated” south segment.

### 5.1. Central Segment (Magma Poor)

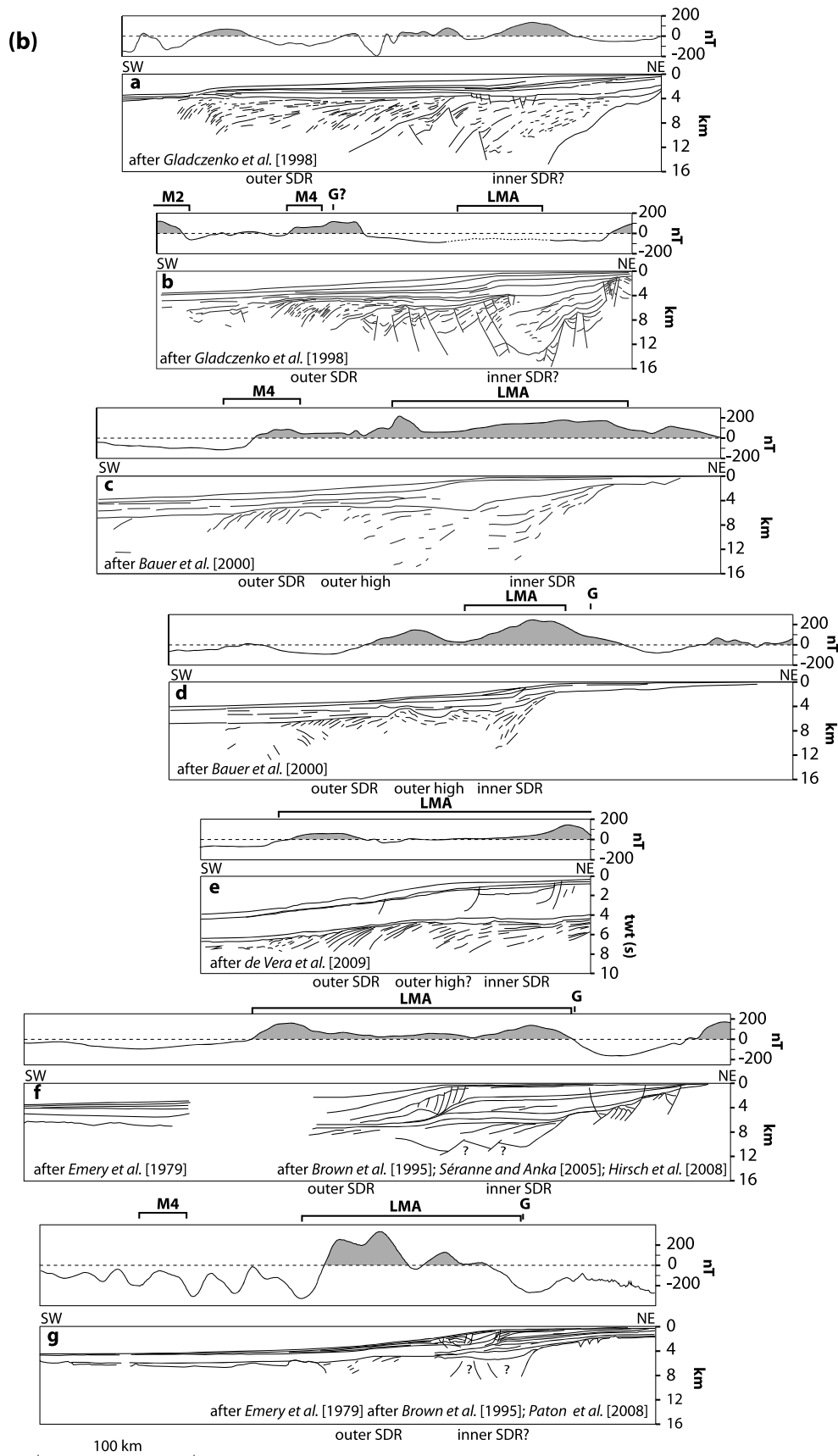
#### 5.1.1. Nature of Crust at Transitional Domain

[34] The crust at the continent-ocean transitional domain along the conjugate margins of the central segment has previously been defined as “proto-oceanic crust” (POC) [Mohriak and Rosendahl, 2003; Wilson et al., 2003; Rosendahl et al., 2005], “igneous crust” [Mohriak et al., 2008], exhumed lower/middle crust [Aslanian et al., 2009] and exhumed and serpentinized subcontinental mantle [Unternehr et al., 2010]. Our analysis of seismic reflection data integrated with gravity modeling, however, casts doubt on the previous interpretations as we believe that the transitional domain observed along the conjugate margins of the central segment is not necessarily oceanic or lower crust or serpentinized mantle in nature (Figures 3a–3c and 6). The transitional domain along the offshore Camamu and Espírito Santo basins is characterized by rotated fault blocks and wedge-shaped synrift sedimentary sequences, and occupies a zone of ~60 km and ~100 km width along the Camamu Basin and Espírito Santo Basin, respectively (Figures 3a and 6). Within the transitional domain, a high-amplitude and undulated “M reflector” is observed along the northeastern Brazilian margin, and defined as the boundary between an extremely thinned, possibly magmatically intruded continental crust and possible serpentinized lithospheric mantle (Figures 3a and 3c). Along the Espírito Santo Basin and along the conjugate basins off Gabon and Angola, the evaporitic deposits considerably mask the seismic signal at the transitional domain, obscuring the potential identification of possible similar structures as in the northeastern Brazilian margin, i.e., rotated fault blocks, wedge-shaped synrift sedimentary sequences and undulated “M reflector” (Figures 3a and 6). Furthermore, even though a possible increase in magmatic products adjacent to the normal oceanic crust may be present along the northeastern Brazilian margin [Blaich et al., 2010], large volume of breakup related magmatism such as seaward-dipping reflections are not recognized along the studied provinces of the central segment (Figures 3a–3c and 6). On the other hand, well-defined seaward dipping reflections were recognized along the Santos and Campos Basin [e.g., Mohriak, 2003; Mohriak

**Figure 12.** Conjugate transects along Argentine-South Africa margins (location in Figure 8). Extracted along-transect Bouguer-corrected gravity anomaly and aeromagnetic anomaly [IAGA, 2007] are also shown. ThD, thinned crystalline crust domain; TrD, transitional domain; M sequences magnetic anomalies after Moulin et al. [2010]; LMA, Large Marginal Anomaly [Moulin et al., 2010]; G, “G magnetic anomaly” after Rabinowitz and LaBrecque [1979]; SDRs, seaward dipping reflections.



**Figure 13.** Compilation of line-drawing interpretations of the upper crustal structure combined with extracted along-profile magnetic anomalies along the south segment conjugate margins (location in Figure 14a). (a) South America margin. (b) West Africa margin. M sequences magnetic anomalies after Moulin et al. [2010]; LMA, Large Marginal Anomaly [Moulin et al., 2010]; G, “G magnetic anomaly” after Rabinowitz and LaBrecque [1979]; SDRs, seaward dipping reflections.

**Figure 13.** (continued)

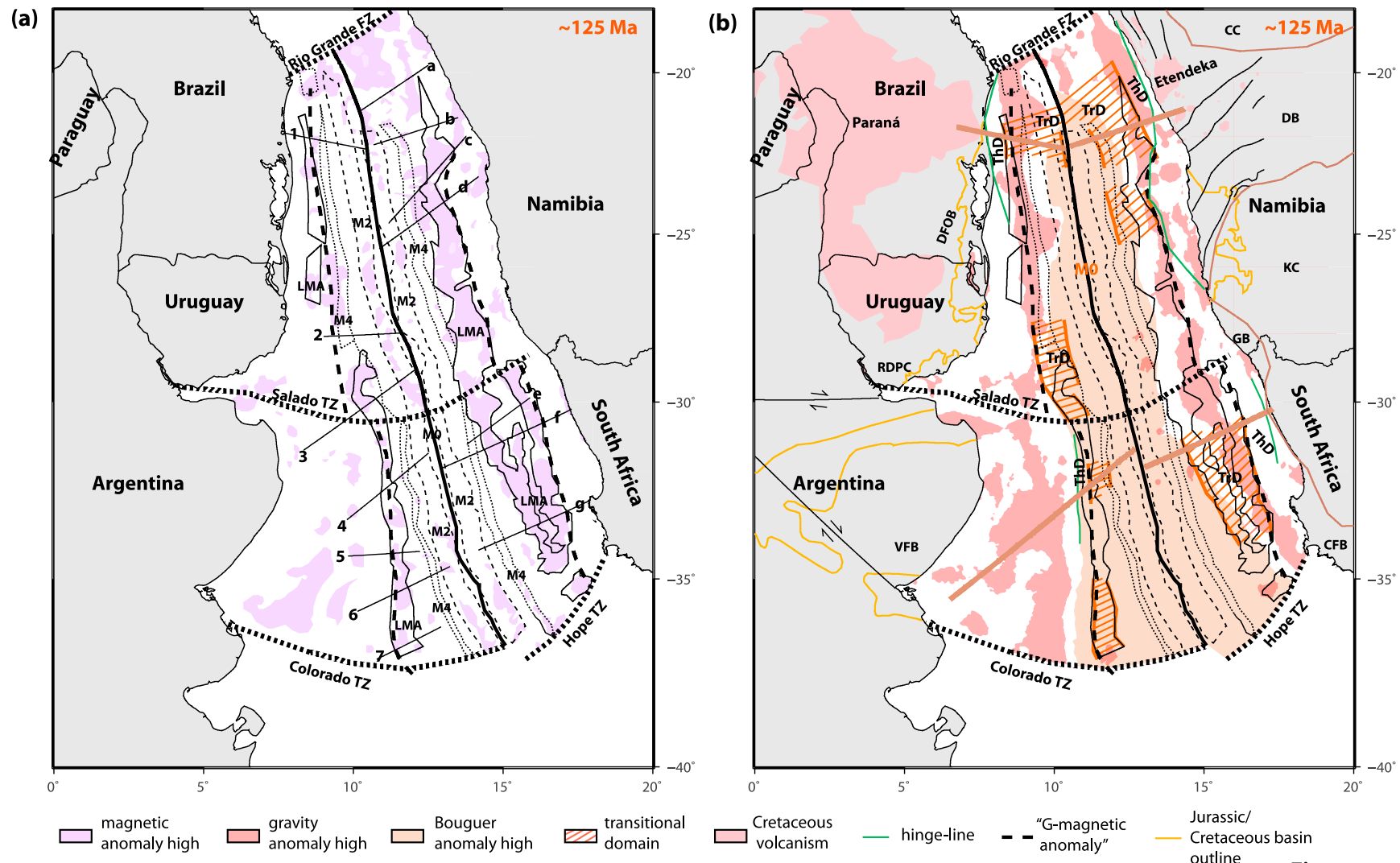


**Fig. 14**

**Figure 14**

*et al.*, 2008], implying along-margin changes in the distribution and volume of breakup-related magmatism.

[35] The transitional domain along the central segment shows evidence of hyperextended continental crust (Figures 3a and 6). In this margin setting, local outcrop of serpentized peridotite ridges across the remaining thin veil of crust may not be unusual [Sibuet, 1987]. If this is the case, serpentized upper lithospheric mantle has become unroofed and emplaced at the basement surface [e.g., Whitmarsh *et al.*, 2001; Wilson *et al.*, 2003; Lavier and Manatschal, 2006; Reston and Pérez-Gussinyé, 2007; Reston, 2009a]. Furthermore, as serpentized mantle may have a wide range of density values and due to the nonunique interpretation of gravity anomalies, it is difficult or even impossible to exclude such possibility. However, unlike the central and northern segment of the “magma-poor” end-member West Iberia margin, the present study of the conjugate margins along the central segment, does not reveal evidence of an exhumation phase (Figures 3a–3c and 6). The Moho discontinuity shallows considerably at the thinned continental crust–transitional domain boundary, yet it does not cut through the crystalline crust at the transitional domain (Figure 3c). On the contrary, the Moho discontinuity flattens out and is clearly located beneath the rotated fault blocks at the transitional domain (Figures 3a–3c and 6).

[36] The high-amplitude and undulated “M reflector” observed at depth of 7–9 s (twt) along the northeastern Brazilian margin (Figures 3b and 3c) shows remarkable resemblances to the prominent and undulated “S reflector” observed along the Galicia Bank continental margin [e.g., de Charpal *et al.*, 1978; Sibuet, 1987; Hoffmann and Reston, 1992; Reston *et al.*, 1996; Reston, 1996; Whitmarsh *et al.*, 1996; Reston and Pérez-Gussinyé, 2007; Reston, 2009a]. At this margin, seismic velocities indicate that parts of the “S reflector” correspond to the boundary between highly thinned, fractured continental crust and the underlying zone of partially serpentized mantle [Zelt *et al.*, 2003]. The “S reflector” is therefore interpreted as the crust–mantle boundary at the time of margin formation [Boillot *et al.*, 1987], characterizing a major detachment fault that was active during rifting and on which the overlying fault blocks ride [Hoffmann and Reston, 1992; Sibuet, 1992; Reston *et al.*, 2007]. Similarly, the analyses performed in this study suggest that the observed undulated “M reflector” characterizes a major detachment surface that cuts through the crust at its western end and on which the overlying fault blocks ride (Figure 3a). Furthermore, as serpentized mantle may have a wide range of density values, and due to the nonunique interpretation of gravity anomalies, a model that accounts for serpentized mantle beneath the “M reflector” is quite likely.

[37] Other possible explanations for the crust at the transitional domain that are applicable for the investigated conjugate margins in this study can be resumed as slow spreading (atypical) oceanic crust [e.g., Srivastava and Keen, 1995; Srivastava and Roest, 1999]; thinned and magmatically intruded continental crust [e.g., Whitmarsh and Miles, 1995; Russell and Whitmarsh, 2003]; and/or exhumed lower continental crust material [e.g., Rosenbaum *et al.*, 2005; Aslanian *et al.*, 2009]. Several studies have shown that oceanic crust formed at the early stages of breakup opening may apparently exhibit evidence of brittle deformation. In particular, if seafloor spreading is slow (half-spreading rates of 3–10 mm/yr) and ridge-axis propagation played an important role, rotated fault blocks may be observed on the oceanic crust [Srivastava and Keen, 1995; Srivastava and Roest, 1999]. In the absence of identifiable magnetic anomalies, best estimates of initial half-spreading rate of ~20 mm/yr have been proposed for the plate separation at the northeastern Brazilian margin [Greenroyd *et al.*, 2008; Müller *et al.*, 2008; Torsvik *et al.*, 2009], suggesting that the thin crust at the transitional domain is unlikely to be the result of ultra slow spreading. Extension of overthickened continental crust is commonly characterized by an early core-complex stage of extension and by movement along low-angle normal detachment faults, which exhume high-grade metamorphic lower crustal rocks [Lister and Davis, 1989; Buck, 1991; Hopper and Buck, 1996; Rosenbaum *et al.*, 2005]. The core-complex stage of extension is followed by a later stage of crustal-scale rigid block faulting [Rosenbaum *et al.*, 2005]. The model of core-complex extension can potentially explain the nature and character of the crust at the transitional domain, and the higher densities for this domain required by gravity modeling may be attributed to variable grade of metamorphism and/or variable amount of mafic intrusives in the exhumed lower crust. However, as stated earlier there is no evidence of an exhumation phase along the study area (Figures 3a–3c). In addition, as “M reflector” characterizes a major detachment surface, the eventually exhumed lower crust or exhumed mantle cannot be situated above this detachment [Blaich *et al.*, 2010]. This implies that the rotated fault blocks at the transitional domain cannot be composed of exhumed material. Apparently, the observed seismic reflection signature and the gravity modeling results, indicate that the crust at the transitional domain can be neither interpreted as normal oceanic crust, nor as exhumed lower crust/mantle. Therefore, the results obtained in this study favor a model in which the rotated fault blocks located at the transitional domain along the conjugate margins of the central segment are continental in nature and are overlying a high-amplitude

**Figure 14.** (a) Resume of prominent features observed on plate reconstructions (Figure 8b). Location of seismic reflection profiles shown in Figure 13 is also indicated. (b) Resume of prominent features observed on plate reconstructions (Figures 8c and 8d). Cretaceous volcanism and main structural constraints are after Gladzenko *et al.* [1998] and Moulin *et al.* [2010]. Jurassic/Cretaceous basins are derived from Abreu [1998] and Moulin *et al.* [2010]. Hinge lines are derived from Moulin *et al.* [2010] and references therein and observations made in the current study. M sequences magnetic anomalies after Moulin *et al.* [2010]; LMA, Large Marginal Anomaly [Moulin *et al.*, 2010]. ThD, thinned crystalline crust domain; TrD, transitional domain; “G magnetic anomaly” after Rabinowitz and LaBrecque [1979]; CC, Congo Craton; DB, Damara Belt; GB, Gariep Belt; KC, Kalahari Craton; CFB, Cape Fold Belt; DFOB, Dom Feliciano Orogenic Belt; RDPC, Río de La Plata Craton; VFB, Ventana Fold Belt; TZ, transfer zone; FZ, fracture zone.

and undulated “M reflector” (e.g., Figure 3a–3c), and were syntectonic sedimentary sequences (synrift, “sag” and late synrift) deposits are observed (TrD; Figure 15b).

### 5.1.2. Total Rift Evolution

[38] Lithospheric extension processes that rift and thin continental margins, resulting in symmetric or asymmetric lithospheric crustal structure, can be accounted by a variety of the pure shear and simple shear end-member models [McKenzie, 1978; Wernicke, 1981; Buck *et al.*, 1988]. For instance, upper crust decoupling from the lower crust and mantle by strain localization into detachment zones allows the dislocation of deformation [Lavier and Manatschal, 2006; Regenauer-Lieb *et al.*, 2006; Weinberg *et al.*, 2007]. In such setting and, when extension is slow, the lithosphere cools as it extends, thereby continuously renewing its frictional plastic layer and promoting asymmetric behavior and widening of the rift zone [Kusznir and Park, 1987; Bassi *et al.*, 1993; Huismans and Beaumont, 2002]. Asymmetric behavior is evident along the central segment, where the West African margin is characterized by a wide area where major crustal thinning occurs and a corresponding gradual Moho shallowing. On the other hand, the Brazilian margin is characterized by abrupt Moho shallowing and by a narrow zone of crustal thinning (Figures 3a, 6, and 7). This striking asymmetry is also evident in the Bouguer-corrected gravity anomaly field, where a wider area of negative-positive gradients is observed along the Gabon margin and indicates a wider area of crustal thinning (Figure 2d). These observations suggest a narrow and sharp crustal taper along the Brazilian margin that is conjugate to a wide and gentle crustal taper along the West Africa margin (Figures 3a and 6).

[39] The transition from a broadly distributed and symmetric extension to asymmetric and localized rifting along the Iberia/Newfoundland magma-poor margins is believed to be controlled by the existence of a strong gabbroic lower crust [Lavier and Manatschal, 2006]. Similarly, the asymmetric behavior as observed on the conjugate margins along the central segment may be controlled by the existence of an inherited strong lower crust along the West African margin, as well as by detachment faulting (Figures 3a and 6). The existence of an enigmatic high-velocity/high-density lower crustal body along the West Africa margin of the central segment is well documented [Wannesson *et al.*, 1991; Meyers *et al.*, 1996b; Rosendahl and Groschel-Becker, 1999; Contrucci *et al.*, 2004; Moulin *et al.*, 2005; Blaich *et al.*, 2010]. However, the origin and nature of this anomalous lower crustal body is debated and may be interpreted variously as high-grade metamorphic crustal rocks, a mixture of mafic and ultramafic crustal rocks or serpentinized mantle [Contrucci *et al.*, 2004]. The peculiar and characteristic landward-dipping structures observed within the lower crustal body (Figure 3a) [Rosendahl *et al.*, 1991; Rosendahl and Groschel-Becker, 1999], however, may be correlated with Pan-African age structures mapped on land [Rosendahl *et al.*, 1991]. Furthermore, the high-velocity/high-density lower crustal body has clearly affected the rift evolution of the central segment, however, the assumption that breakup related volcanism along the central segment was not voluminous, implies that the anomalous lower crustal body is most likely unrelated to breakup. Therefore the lower crustal body may be rather associated with crustal accretion processes, reflecting structure inheritance of crustal

domains and features related to older tectonic episodes and, possible, orogenies.

[40] The analysis performed in this study indicates that the margin segment located south of the Salvador-N’Komi transfer zones has a narrow-wide conjugate margin configuration (Figures 3a, 6, and 7), and that lithospheric extension resulted in the formation of an asymmetric thinned continental crust domain and an approximately symmetric transitional domain (Figure 7). This implies that the tectono-sedimentary evolution of the central segment is complex and may reflect a polyphase rifting evolution mode, which is associated with a complex time-dependent thermal structure of the lithosphere [e.g., Lavier and Manatschal, 2006; Péron-Pinvidic *et al.*, 2007; Huismans and Beaumont, 2008; Aslanian *et al.*, 2009; Péron-Pinvidic and Manatschal, 2009]. In the early stage of rifting, stretching of the crust is distributed across a wide region and characterized by the development of normal listric faulting and differential subsidence of half-grabens (Figure 15a) [Lavier and Manatschal, 2006; Huismans and Beaumont, 2008]. Unlike the stretching phase of Lavier and Manatschal [2006], however, our performed analysis is not able to document an initial symmetric extension phase. In the subsequent thinning phase, crustal extension becomes focused oceanward [Huismans and Beaumont, 2008], and the distributed normal listric faults are overprinted by localized detachment faulting (Figure 15a). The weak middle crust is able to flow over the strong lower crust, allowing for the delocalization of deformation [e.g., Lavier and Manatschal, 2006], and consequently lower crustal rocks are brought to shallower levels (Figure 15a) [e.g., Hendriks and Andriessen, 2002; Tsikalas *et al.*, 2005]. This model predicts the occurrence of crustal-scale shear zones that are able to thin the crust to less than 10 km, without the presence of distributed normal faulting in the upper crust [Lavier and Manatschal, 2006]. At the same time, even minor shallowing of the Moho may lead to decompressional melts that are accreted on to the lower crust thereby increasing its density [e.g., Tsikalas *et al.*, 2005]. Consequently thermal subsidence will enhance the accumulation of relatively thick and tectonically undeformed “sag” basins (Figures 15a and 15b) [e.g., Huismans and Beaumont, 2008].

[41] The thinned continental crust domain (ThD) and parts of the transitional domain (TrD part a) suggested in our study (Figure 15a) would document the outcome of the thinning phase, where the asymmetry between the conjugate margins is evident and probably controlled by a strong lower crust (Figures 3 and 15a). Since the distribution and style of subsidence observed on both conjugate margins suggest depth-dependent stretching/thinning, where the deposition of tectonically underformed “sag” basins are observed, detachments that separate the brittle and ductile deformation domains in the crust are proposed for both conjugate margins (Figure 15a).

[42] The hypothetical subsequent exhumation phase, which would predict exhumation of middle and lower crust followed by mantle exhumation [Lavier and Manatschal, 2006], is not evident along the central segment conjugate margins. This may be attributed to the fact that, even though the central segment margins show magma-poor affinity [Contrucci *et al.*, 2004; Moulin *et al.*, 2005; Sawyer *et al.*, 2007], they also experienced magmatism during thinning and breakup, implying that the central segment is not a

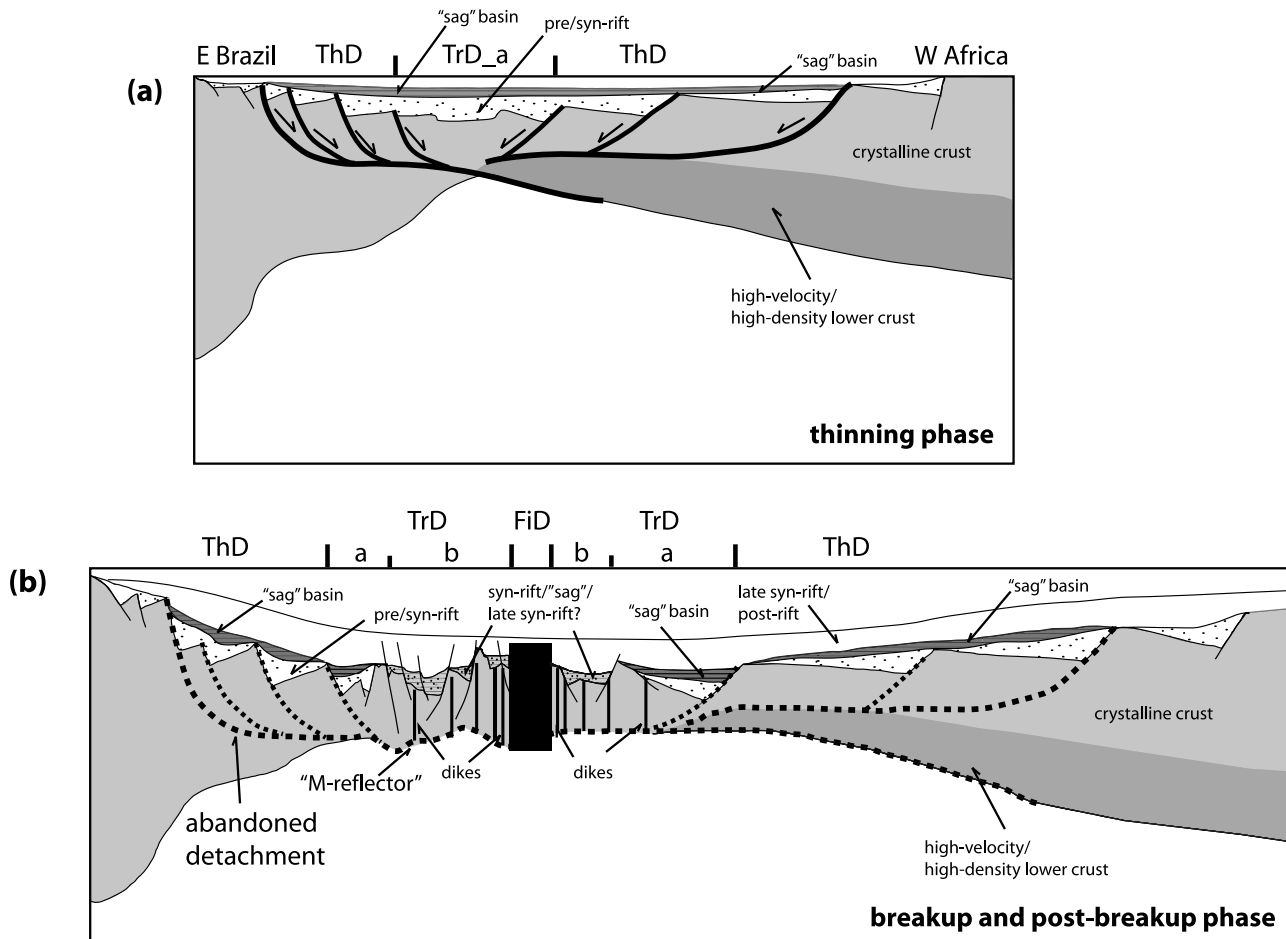


**Figure 15.** Conceptual model showing the tectonosedimentary and magmatic polyphase evolution of the conjugate “magma-poor” central segment. (a) Thinning phase, characterized by detachment faulting and depth-dependent stretching, which resulted in the deposition of thick and tectonically undeformed “sag” basins. (b) Breakup phase, the increase of volcanic activity followed by the abandon of the main detachment faults may have “interrupted” the extensional system implying a failed exhumation phase that is replaced instead by a symmetric transitional domain and finally continental breakup and emplacement of fully igneous crust (see discussion in text). ThD, thinned crystalline crust domain; TrD, transitional domain; FiD; fully igneous crust.

“magma-poor” end-member [Blaich *et al.*, 2010]. The increase of volcanic products at the transitional domain is indicated by higher densities required by gravity modeling for the crust at the transitional domain (Figures 5 and 6), and evidence of sediments interbedded with volcanic material located adjacent to the normal oceanic crust along the northeastern Brazilian margin (Figures 3b and 3c) [Blaich *et al.*, 2010]. Therefore, at the final stage of extension, magmatism increased oceanward affecting mainly the crust at the transitional domain, thereby increasing its proper densities. Consequently, the magmatically intruded crust may isostatically subside relative to the unintruded crust as a consequence of the increased mean density, promoting thermal subsidence (TrD part b; Figure 15a). Furthermore, the magma supply has been shown to allow the release of stress by dyking which, in turn, may effectively cut off the detachment faults [Ebinger and Casey, 2001]. Consequently, the increase of volcanic activity followed by the abandon of detachment faulting may have “interrupted” the extensional

system implying a failed exhumation phase that is replaced instead by continental breakup and emplacement of fully igneous crust (Figure 15b). Moreover, the abandon of detachment faulting followed by extension at the onset of breakup may deform the weak and intruded crust at the transitional domain (TrD part b) differently than the unintruded crust (Figure 15b). In this setting, excess thinning of the mantle underneath the rift flanks may be balanced by excess thinning of the upper crust in the final breakup stage [e.g., Reston, 2009b].

## 5.2. South Segment (Magma Dominated)

### 5.2.1. Nature of Crust at Transitional Domain

[43] The continent-ocean transitional domain along the south segment, between the Rio Grande Fracture Zone and the conjugate Colorado-Hope transfer system, is characterized by large volume of flood basalts that form a series of seaward dipping reflections (SDRs) [e.g., Gladzenko *et al.*, 1998; Hinz *et al.*, 1999; Franke *et al.*, 2007, 2010] and high

seismic velocities in the lower crust [e.g., *Bauer et al.*, 2000; *Franke et al.*, 2006; *Schnabel et al.*, 2008; *Hirsch et al.*, 2009]. Furthermore, the SDRs along both conjugate margins exhibit a characteristic convex upward shape (Figure 13), as a consequence of contemporaneous crustal stretching and subsidence with their emplacement [e.g., *Mutter et al.*, 1982]. In the northern province of the south segment, between Rio Grande Fracture Zone and the Salado Transfer Zone, the melt volume along both conjugate margins decreases southward, implying that the defined continent-ocean transitional domain along both conjugate margins are very wide close to the Tristan da Cunha plume and decreases southward (Figures 13a and 14) [e.g., *Blaich et al.*, 2009; *Hirsch et al.*, 2009]. The SDRs emplaced along this conjugate province are symmetrical [e.g., *Talwani and Abreu*, 2000], implying that the continent-ocean transitional domain is also symmetrical (Figures 11 and 14). In addition, fault blocks are inferred to be present in the upper crust within the continent-ocean transitional domain along both conjugate margins (Figure 11) [*Gladczenko et al.*, 1998; *Talwani and Abreu*, 2000]. The landward boundary of the continent-ocean transitional domain along this province is closely associated with a prominent positive magnetic anomaly and with the prominent and elongated “edge effect” gravity anomaly high (Figure 14).

[44] The central province of the south segment, between the Salado Transfer Zone and the conjugate Colorado-Hope transfer system is characterized by a continent-ocean transitional domain that on the Argentine margin appears to be narrow and relatively constant, slightly decreasing its width northward. In addition, the distribution of SDRs, varies extensively and systematically along the Argentine margin (Figure 13a), where the largest volumes of melts are emplaced close to the transfer zones and are decreasing internally within the individual margin segments, with a general northward diminishing trend toward the Salado Transfer Zone [*Franke et al.*, 2007, 2010]. Moreover, *Blaich et al.* [2009] confirmed that the emplacement of extrusive basalt flows along the Argentine margin is associated with magmatic high-density lower crustal which, in turn, indicates a general decrease in thickness and volume of magmatic products northward.

[45] The continent-ocean transitional domain along the conjugate South Africa margin is narrow close to the conjugate Colorado-Hope transfer system and broadens considerably northward, following the prominent and positive magnetic anomaly trend (Figure 14). The observed along-strike asymmetry on the central province of the south segment is expressed by the northward increase in thickness and volume of the extrusive/intrusive magmatic products on the South Africa margin. This consequently leads to the width increase of the interpreted continent-ocean transitional domain northward, which is conjugate to a continent-ocean transitional domain that is narrow and relatively constant, slightly decreasing its width northward (Figure 14). In addition, the double branch of the Large Marginal Anomaly (LMA) observed along the South Africa margin (Figure 8b) [*Moulin et al.*, 2010] is only present south of the Salado Transfer Zone. Finally, the landward boundary of the continent-ocean transitional domain along the central province deviates considerably from the prominent and elongate “edge effect” gravity anomaly high (Figure 14). The striking dissimilarity between the northern province and the central province of

the south segment suggests that the Salado Transfer Zone marks a distinct along-margin boundary in the distribution and volume of breakup-related magmatism.

[46] Plume-driven models are the traditional explanation for the formation of “magma-dominated” margins [e.g., *White and McKenzie*, 1989; *Eldholm and Grue*, 1994]. However, alternative models involving prebreakup extension [*van Wijk et al.*, 2001; *Gernigon et al.*, 2006], edge driven small-scale convection [*Mutter et al.*, 1988; *Boutilier and Keen*, 1999], thermal insulation by continents [*Anderson*, 1998], and compositional variations in the mantle [*Foulger and Anderson*, 2005] may also explain significant melt production. It is very likely that the Tristan da Cunha plume exerted an influence on the volcanic products distribution along the northern province of the south segment [e.g., *Gladczenko et al.*, 1998; *Bauer et al.*, 2000; *Trumbull et al.*, 2002]. Supporting the plume-driven model for this province are observations such as increase of breakup-related magmatism and thus widening of the continent-ocean transitional domain northward toward the Tristan da Cunha plume (Figure 14), and high-magnesium magma composition of the crust in this province [e.g., *Trumbull et al.*, 2007].

[47] On the central province, south of the Salado Transfer Zone (Figure 14) the influence of the Tristan da Cunha plume can be questioned. This is because the distance of the SDRs observed on the Argentine and its conjugate South Africa margin exceeds the ~2000 km diameter of influence of a “hotspot” as suggested by *White and McKenzie* [1989]. Moreover, the volume of breakup-related magmatism along the Argentine margin is diminishing toward the north [*Franke et al.*, 2007, 2010], followed by a southward decrease of magnesium composition in the crust along the conjugate margin off South Africa [*Trumbull et al.*, 2007]. Finally, the abrupt change in the volume of emplaced breakup-related magmatism from a “magma-poor” affinity south of the conjugate Colorado-Hope transfer system (southern province) to a “magma-dominated” margin northward [e.g., *Blaich et al.*, 2009; *Franke et al.*, 2010] leads us to consider alternative models that account for the gradual along-margin variations in the thermal regime of the lithosphere and sublithospheric mantle (plume-driven model). In this setting, the northward unzipping of the rift zones, where the transfer zones acted as lithospheric discontinuities at the onset of rifting, may have substantially influenced the along margin varying emplacement of breakup related magmatism [*Franke et al.*, 2010]. It was further suggested that the Argentine margin experienced a pulsed volcanic history, where an episodic emplacement of the individual SDRs is observed [*Franke et al.*, 2007]. In this way, the pulses of volcanism were controlled by interrupted rifting allowing the buildup of heat and were followed by massive outpouring of melt successively for each segment. Furthermore, small-scale convective instabilities during rifting are capable of explaining the origin of volcanic margins with moderate volumes of melts [*Simon et al.*, 2009]. Therefore, the central province of the south segment may not characterize a “magma-dominated” end-member margin.

### 5.2.2. Total Rift Evolution

[48] Reconstruction of conjugate passive margins frequently indicates a marked asymmetry where a lateral offset in the high-strain zones within the crust and/or upper mantle is observed [e.g., *Wernicke*, 1985; *Lister et al.*, 1991]. Furthermore, the asymmetry has been cited as evidence for detach-

ment faulting that accommodates large strain until breakup [e.g., Lister *et al.*, 1991; Driscoll and Karner, 1998; Karner and Driscoll, 1999]. The analysis performed in this study clearly indicates along-strike tectonomagmatic asymmetry along the central province of the south segment. In particular, the continent-ocean transitional domain of the South Africa margin is wide and underwent great amount of thinning and deformation, whereas the continent-ocean transitional domain along the Argentine conjugate margin is considerably narrower (Figure 12). Intracrustal detachment faulting is, therefore, invoked along the South Africa margin to explain the observed asymmetry (Figure 16a). The observed along-strike tectonomagmatic asymmetry along the central province of the south segment may be attributed to the long and complex history of lithospheric extension, initiated long before breakup of the Gondwana supercontinent. Thus, the early stage of formation of the south segment, i.e., the relief of the base of the lithosphere, may influence considerably the along-margin magmatic distribution where asthenospheric melts may preferentially move toward areas of accentuated crustal relief, or “thinspots” (Figure 16a) [e.g., Thompson and Gibson, 1991]. In addition, the existence of Paleozoic basins and the location of mobile belts along the Pan-African fold belt may have exerted a major influence on the tectonic development, and consequently on the magmatic distribution along the South Africa margin giving rise to the observed tectonomagmatic asymmetry [e.g., Gladzenko *et al.*, 1998].

[49] The continuous nature of the SDRs along the South Africa margin (Figure 13b), precludes the possibility of ridge jumps being invoked to explain the observed asymmetry [e.g., Hopper *et al.*, 2003]. Therefore, the tectonomagmatic asymmetry observed along the central province of the south segment (Figure 8b) can be inferred to be caused by the initial continental stretching and accompanying magmatism rather than by the subsequent seafloor spreading (Figure 16a) [e.g., White and Smith, 2009]. Therefore, the Tristan da Cunha plume on the central province may have influenced the volume of magmatism, but did not necessarily alter the process of rifted margin formation [Gladzenko *et al.*, 1998], further implying that the subsequent magmatism may have taken place within the inherited, asymmetrically stretched continental crust (Figure 16a) [e.g., White and Smith, 2009]. In this setting, apart from voluminous magmatism the extensional evolution of “magma-dominated” margins, such as the central province of the south segment, may have much in common with “magma-poor margins” (Figure 16a). Similarly to White and Smith [2009], we interpret the nature of crust at the continent-ocean transitional domain as a mixture of breakup-related intrusive and residual continental crust (Figure 16b). The consequent symmetrical seafloor spreading (Figure 14) may suggest that the steady supply of magma by dyking may release stress, allowing strain to occur at lower stresses than required for faulting [Ebinger and Casey, 2001]. In this way, extension of the crust by magmatic intrusion exceeds tectonic extension leading to continental breakup and emplacement of a symmetric fully igneous crust (Figure 16b) [Ebinger and Casey, 2001; Cornwell *et al.*, 2006].

## 6. Conclusions

[50] The integrated analysis of seismic reflection and refraction profiles, and potential field data, complemented

by crustal-scale gravity modeling and plate reconstructions are used to study the evolution of the central and south segments of the South Atlantic conjugate margins. The study elucidates structural elements and features that reflect the processes that lead to the rupture of the continental crust, as well as it refines and constrains the structural architecture and nature of the continent-ocean transitional domain. The later is defined as the part of the lithosphere which is located between the clearly identifiable stretched crystalline crust domain, and the first appearance of fully oceanic (i.e., fully igneous) crust formed by seafloor spreading.

[51] The performed analysis indicates that the “magma-poor” central segment (confined between Rio Grande Fracture Zone to the south and Ascension Fracture Zone to the north) is characterized by a hyperextended continent-ocean transitional domain that shows evidence of rotated fault blocks and wedge-shaped syntectonic sedimentary sequences (e.g., synrift, “sag” and late synrift) overlying a high-amplitude and undulated reflector (“M reflector”). The “M reflector” is interpreted as a major detachment surface active during rifting that defines the Moho discontinuity at the transitional domain. Our study favors a model in which the rotated fault blocks located at the transitional domain are continental in nature, overlying the high-amplitude and undulated “M reflector.” Furthermore, as serpentinized mantle may have a wide range of density values, a model that accounts for serpentinized mantle beneath the “M reflector” is quite likely.

[52] Asymmetric behavior is evident along the central segment and characterized by a sharp crustal taper along the Brazilian Camamu and Espírito Santo basins that is conjugate to a gentle crustal taper along the South Gabon and North Angola basins. Furthermore, lithospheric extension resulted in the formation of an asymmetrically extended and thinned continental crust domain and an approximately symmetric transitional domain. Similar to the Iberia/Newfoundland magma-poor margins, the asymmetric behavior as observed on the conjugate margins along the central segment may be controlled by the existence of an inherited strong lower crust along the West African margin, as well as by detachment faulting. A conceptual model is developed based on all detailed observations and results of our study. The conceptual model integrates, in a pragmatic way, regional-scale observations and several tectonic models at similar settings, providing a well-constrained polyphase model for the tectonomagmatic evolution of the central segment conjugate margins.

[53] In the early stage of rifting, stretching of the crust is distributed across a wide region and is characterized by the development of normal listric faulting and differential subsidence of half-grabens. In the subsequent thinning phase, crustal extension becomes focused oceanward and the distributed normal listric faults are overprinted by localized detachment faulting. It is inferred that the weak middle crust is able to flow over the strong lower crust along crustal-scale shear zones, allowing for the delocalization of deformation, and consequently thinning of the crust without the presence of distributed normal faulting in the upper crust. At the same time, even minor shallowing of the Moho may lead to decompressional melts that are accreted on to the lower crust thereby increasing its density. Consequently thermal subsidence will enhance the accumulation of relatively thick and tectonically undeformed “sag” basins. The

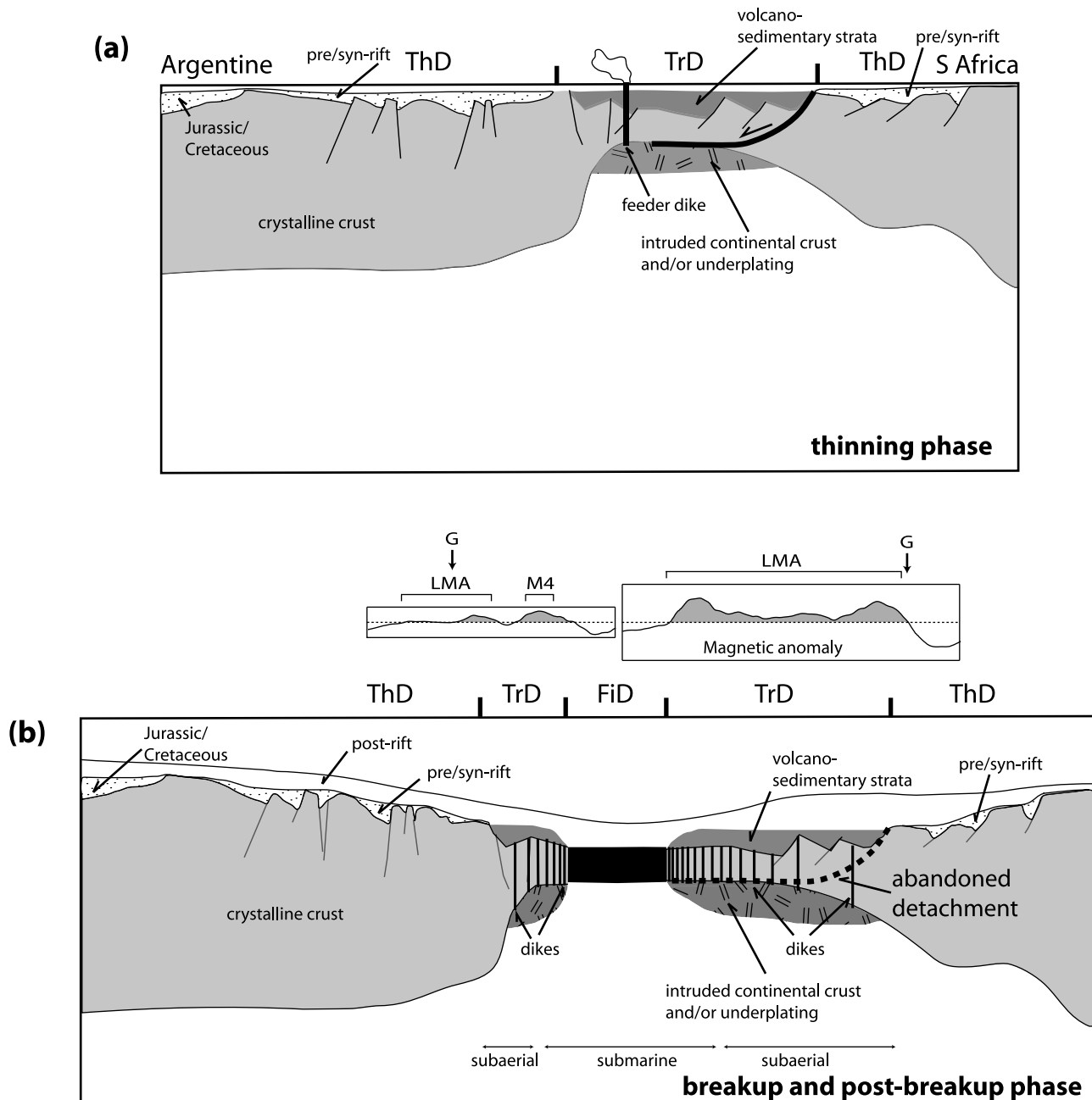


**Figure 16.** Conceptual model showing the tectonosedimentary and magmatic polyphase evolution of the conjugate “magma-dominated” south segment. (a) Thinning phase, characterized by detachment faulting and possible depth-dependent stretching. (b) Breakup phase, volcanic activity associated with voluminous igneous rocks intruded into the lower crust followed by abandon of the main detachment faults. The breakup phase is also associated with large volume of subaerial and submarine flood basalts (see discussion in text). ThD, thinned crystalline crust domain; TrD, transitional domain; FiD; fully igneous crust.

hypothetical subsequent exhumation phase, which would predict exhumation of middle and lower crust followed by mantle exhumation, is not evident along the central segment conjugate margins. This may be attributed to the fact that, even though the central segment margins show magma-poor affinity, they also experienced magmatism during thinning and breakup, implying that the central segment is not a “magma-poor” end-member. Consequently, the increase of volcanic

activity followed by the abandon of detachment faulting may have “interrupted” the extensional system implying a failed exhumation phase that was replaced instead by final continental breakup and emplacement of fully igneous crust.

[54] The continent-ocean transitional domain along the “magma-dominated” south segment is characterized by large volume of flood basalts that form a series of seaward dipping reflections (SDRs) and high-velocity/high-density

lower crust, which are associated with voluminous igneous activity during continental breakup. The northern province of the south segment, between Rio Grande Fracture Zone and the Salado Transfer Zone, is characterized by symmetrical SDRs and symmetrical continent-ocean transitional domain. Furthermore, the melt volume along both conjugate margins decreases southward. It is very likely that the Tristan da Cunha plume exerted an influence on the volcanic products distribution along the “magma-dominated” northern province of the south segment.

[55] The central province of the south segment, between the Salado Transfer Zone and the conjugate Colorado-Hope transfer system is characterized by along-strike tectonomagmatic asymmetry. In this setting, the continent-ocean transitional domain of the South Africa margin is wide and underwent great amount of thinning and deformation, whereas the continent-ocean transitional domain along the Argentine conjugate margin is considerably narrower. Moreover, the volume of breakup-related magmatism along the Argentine margin is diminishing toward the north and the largest volumes of melts are emplaced close to the transfer zones. The asymmetry observed along the central province of the south segment can be inferred to be caused by the initial continental stretching and accompanying magmatism rather than by the subsequent seafloor spreading. Thus, the early stage of formation of the south segment, i.e., the relief at the base of the lithosphere, may have influenced considerably the along-margin magmatic distribution where asthenospheric melts may preferentially have moved toward areas of accentuated crustal relief, or “thin-spots.” The Tristan da Cunha plume on the central province may have influenced the volume of magmatism, but did not necessarily alter the process of rifted margin formation, further implying that the subsequent magmatism may have taken place within the inherited, asymmetrically stretched continental crust. Thus, the central province of the south segment may not characterize a “magma-dominated” end-member margin. Furthermore, apart from voluminous magmatism the extensional evolution of “magma-dominated” margins, such as the central province of the south segment, may have much in common with “magma-poor margins.”

[56] **Acknowledgments.** We thank Statoil, TGS-NOPEC, Fugro Multi Client Services, and ION-GXT for providing the MCS profiles used in this study. Eni E&P is acknowledged for providing the time and resources (to Filippou Tsikalas) to fulfill the study. We also thank Asbjørn Johan Breivik and Webster Mohriak for fruitful discussions. The study is part of the University of Oslo Conjugate South Atlantic Margin Studies project funded by Statoil.

## References

- Abreu, V. S. (1998), Geologic evolution of conjugate volcanic passive margins: Pelotas Basin (Brazil) and Offshore Namibia (Africa): Implications for global sea-level changes, Ph.D. thesis, 355 pp., Rice Univ., Houston, Tex.
- Afiflado, A., L. Matias, H. Shiobara, A. Hirn, L. Mendes-Victor, and H. Shimamura (2008), From unthinned continent to ocean: The deep structure of the West Iberia passive continental margin at 38°N, *Tectonophysics*, **458**, 9–50, doi:10.1016/j.tecto.2008.03.002.
- Agarwal, B. N. P., L. K. Das, K. Chakravorty, and C. Sivaji (1995), Analysis of the Bouguer anomaly over central India: A regional perspective, *Mem. Geol. Soc. India*, **31**, 469–493.
- Anderson, D. L. (1998), The scales of mantle convection, *Tectonophysics*, **284**, 1–17, doi:10.1016/S0040-1951(97)00169-8.
- Aslanian, D., et al. (2009), Brazilian and African passive margins of the central segment of the South Atlantic Ocean: Kinematic constraints, *Tectonophysics*, **468**, 98–112, doi:10.1016/j.tecto.2008.12.016.
- Asmus, H. E., and F. C. Ponte (1973), The Brazilian marginal basins, in *The Oceans Basins and Margins*, vol. 1, *The South Atlantic*, edited by A. E. Nair and F. G. Stehli, pp. 87–132, Plenum, New York.
- Austin, J. A. J., and E. Uchupi (1982), Continental-oceanic crustal transition off southwest Africa, *AAPG Bull.*, **66**, 1328–1347.
- Bassi, G., C. E. Keen, and P. Potter (1993), Contrasting styles of rifting: Models and examples from the eastern Canadian margin, *Tectonics*, **12**, 639–655, doi:10.1029/93TC00197.
- Bauer, K., S. Neben, B. Schreckenberger, R. Emmermann, K. Hinz, N. Fechner, K. Gohl, A. Schulze, R. B. Trumbull, and K. Weber (2000), Deep structure of the Namibia continental margin as derived from integrated geophysical studies, *J. Geophys. Res.*, **105**, 25,829–25,853, doi:10.1029/2000JB900227.
- Blaich, O. A., F. Tsikalas, and J. I. Faleide (2008), Northeastern Brazilian margin: Regional tectonic evolution based on integrated analysis of seismic reflection and potential field data and modeling, *Tectonophysics*, **458**, 51–67, doi:10.1016/j.tecto.2008.02.011.
- Blaich, O. A., J. I. Faleide, F. Tsikalas, D. Franke, and E. León (2009), Crustal-scale architecture and segmentation of the Argentine margin and its conjugate off South Africa, *Geophys. J. Int.*, **178**, 85–105, doi:10.1111/j.1365-246X.2009.04171.x.
- Blaich, O. A., J. I. Faleide, F. Tsikalas, R. Lilletveit, D. Chirossi, P. Brockbank, and P. Cobbold (2010), Structural architecture and nature of the continent-ocean transitional domain at the Camamu and Almada Basins (northeastern Brazil) within a conjugate margin setting, in *Petroleum Geology: From Mature Basins to New Frontiers—Proceedings of the 7th Conference*, edited by B. A. Vining and S. C. Pickering, pp. 1–17, Geol. Soc., London, doi:10.1144/070000.
- Boillot, G., et al. (1987), *Proceedings of the Ocean Drilling Program, Initial Reports*, vol. 103, Ocean Drill. Program, College Station, Tex.
- Boutilier, R. R., and C. E. Keen (1999), Small-scale convection and divergent plate boundaries, *J. Geophys. Res.*, **104**, 7389–7403, doi:10.1029/1998JB900076.
- British Oceanographic Data Centre (2003), *Centenary Edition of the GEBCO Digital Atlas* [CD-ROM], Intergov. Oceanogr. Comm. and the Int. Hydrogr. Organ., Liverpool, UK.
- Brown, L. F., Jr., J. M. Benson, G. J. Brink, S. Doherty, A. Jollands, E. H. A. Jungslager, J. H. G. Keenen, A. Muntingh, and N. J. S. van Wyk (1995), Sequence stratigraphy in offshore South African divergent basins: An atlas on exploration of Cretaceous lowstand traps by Soekor (Pty) Ltd, *AAPG Stud. Geol.*, **41**, 1–184.
- Buck, W. R. (1991), Models of continental lithospheric extension, *J. Geophys. Res.*, **96**, 20,161–20,178, doi:10.1029/91JB01485.
- Buck, W. R., F. Martinez, M. Steckler, and J. Cochran (1988), Thermal consequences of lithospheric extension: Pure and simple, *Tectonics*, **7**, 213–234, doi:10.1029/TC007i002p00213.
- Castro, A. C. M., Jr. (1988), Structural evolution of the Sergipe-Alagoas Basin, Brazil, Ph.D. thesis, 183 pp., Rice Univ., Houston, Tex.
- Chang, H. K., R. O. Kowsmann, A. M. F. Figueiredo, and A. A. Bender (1992), Tectonics and stratigraphy of the East Brazil Rift System: An overview, *Tectonophysics*, **213**, 97–138, doi:10.1016/0040-1951(92)90253-3.
- Confrucci, I., L. Matias, M. Moulin, L. Géli, F. Klingelhofer, H. Nouzé, D. Aslanian, J-L. Olivet, J-P. Réhault, and J-C. Sibuet (2004), Deep structure of the West African continental margin (Congo, Zaire, Angola), between 5°S and 8°S, from reflection/refraction seismics and gravity data, *Geophys. J. Int.*, **158**, 529–553, doi:10.1111/j.1365-246X.2004.02303.x.
- Cornwell, D. G., D. McKenzie, R. W. England, P. K. H. Maguire, L. M. Asfaw, and B. Oluma (2006), Northern Main Ethiopian Rift crustal structure from new high-precision gravity data, in *The Afar Volcanic Province Within the East African Rift System*, edited by G. Yirgu et al., *Geol. Soc. Spec. Publ.*, **259**, 307–321, doi:10.1144/GSL.SP.2006.259.01.23.
- Das, L. K., B. N. P. Agarwal, and R. N. Bose (1996), Moho relief in central India from spectral analysis of gravity data, *Mem. Geol. Soc. India*, **36**, 225–234.
- Davison, I. (2007), Geology and tectonics of the South Atlantic Brazilian salt basins, in *Deformation of the Continental Crust: The Legacy of Mike Coward*, edited by A. C. Ries et al., *Geol. Soc. Spec. Publ.*, **272**, 345–359.
- de Charpal, O., P. Guennoc, L. Montadert, and D. G. Roberts (1978), Rifting and subsidence of the northern continental margin of the Bay of Biscay, *Nature*, **275**, 706–711.
- de Vera, J., P. Granado, and K. McClay (2010), Structural evolution of the Orange Basin gravity-driven system, offshore Namibia, *Mar. Pet. Geol.*, **27**, 223–237, doi:10.1016/j.marpgeo.2009.02.003.

- Driscoll, N. W., and G. D. Karner (1998), Lower crustal extension across the northern Carnarvon basin, Australia: Evidence for an eastward dipping detachment, *J. Geophys. Res.*, **103**, 4975–4991, doi:10.1029/97JB03295.
- Ebinger, C. J., and M. Casey (2001), Continental breakup in magmatic provinces: An Ethiopian example, *Geology*, **29**, 527–530, doi:10.1130/0091-7613(2001)029<0527:CBIMPA>2.0.CO;2.
- Eldholm, O., and K. Grue (1994), North Atlantic volcanic margins: Dimensions and production rates, *J. Geophys. Res.*, **99**, 2955–2968, doi:10.1029/93JB02879.
- Eldholm, O., J. Thiede, and E. Taylor (1989), Evolution of the Voring volcanic margin, *Proc. Ocean Drill. Program Sci. Results*, **104**, 1033–1065.
- Eldholm, O., T. P. Gladzenko, J. Skogseid, and S. Planke (2000), Atlantic volcanic margins: A comparative study, in *Dynamics of the Norwegian Margin*, edited by A. Nøttvedt et al., *Geol. Soc. Spec. Publ.*, **167**, 411–428, doi:10.1144/GSL.SP.2000.167.01.16.
- Emery, K. O., E. Uchupi, C. O. Bowin, J. Phillips, and E. S. W. Simpson (1979), Continental margin off Western Africa: Cape St. Francis (South Africa) to Walvis Ridge (South-West Africa), *AAPG Bull.*, **59**, 3–59.
- Fainstein, R., and A. Krueger (2005), Salt tectonics comparisons near the continent-ocean boundary escarpments, paper presented at Petroleum Systems of Divergent Continental Margin Basins: GCSSEPM 25th Annual Bob F. Perkins Research Conference, Gulf Coast Sect. SEPM Found., Houston, Tex.
- Fontana, R. L. (1996), SDR (Seaward-dipping reflectors) e a transição crustal na Bacia de Pelotas, paper presented at Anais do 39 Congresso Brasileiro de Geologia, pp. 425–430, Salvador, Bahia, Brazil.
- Foulger, G. R., and D. L. Anderson (2005), A cool model for the Iceland hotspot, *J. Volcanol. Geotherm. Res.*, **141**, 1–22, doi:10.1016/j.jvolgeores.2004.10.007.
- Franke, D., S. Neben, B. Schreckenberger, A. Schulze, M. Stiller, and C. M. Krawczyk (2006), Crustal structure across the Colorado Basin, offshore Argentina, *Geophys. J. Int.*, **165**, 850–864, doi:10.1111/j.1365-246X.2006.02907.x.
- Franke, D., S. Neben, S. Ladage, B. Schreckenberger, and K. Hinz (2007), Margin segmentation and volcano-tectonic architecture along the volcanic margin off Argentina/Uruguay, South Atlantic, *Mar. Geol.*, **244**, 46–67, doi:10.1016/j.margeo.2007.06.009.
- Franke, D., S. Ladage, M. Schnabel, B. Schreckenberger, C. Reichert, K. Hinz, M. Paterlini, J. de Abelleyra, and M. Siciliano (2010), Birth of a volcanic margin off Argentina, South Atlantic, *Geochim. Geophys. Geosyst.*, **11**, Q0AB04, doi:10.1029/2009GC002715.
- Gernigon, L., F. Lucazeau, F. Brigaud, J. C. Ringenbach, S. Planke, and B. Le Gall (2006), A moderate melting model for the Voring margin (Norway) based on structural observations and a thermo-kinematical modeling: Implication for the meaning of the lower crustal bodies, *Tectonophysics*, **412**, 255–278, doi:10.1016/j.tecto.2005.10.038.
- Gladzenko, T. P., J. Skogseid, and O. Eldholm (1998), Namibia volcanic margin, *Mar. Geophys. Res.*, **20**, 313–341, doi:10.1023/A:1004746101320.
- Greenroyd, C. J., C. Peirce, M. Rodger, A. B. Watts, and R. W. Hobbs (2008), Demerara Plateau—the structure and evolution of a transform passive margin, *Geophys. J. Int.*, **172**, 549–564, doi:10.1111/j.1365-246X.2007.03662.x.
- Hendriks, B. W. H., and P. A. M. Andriessen (2002), Pattern and timing of the post-Caledonian denudation of northern Scandinavia constrained by apatite fission-track thermochronology, in *Exhumation of the North Atlantic Margin: Timing, Mechanisms and Implications for Petroleum Exploration*, edited by A. G. Doré et al., *Geol. Soc. Spec. Publ.*, **196**, 117–137, doi:10.1144/GSL.SP.2002.196.01.08.
- Hinz, K., S. Neben, B. Schreckenberger, H. A. Roeser, M. Block, G. K. de Souza, and H. Meyer (1999), The Argentine continental Margin north of 48°S: Sedimentary successions, volcanic activity during breakup, *Mar. Pet. Geol.*, **16**, 1–25, doi:10.1016/S0264-8172(98)00060-9.
- Hirsch, K. K., K. Bauer, and M. Scheck-Wenderoth (2009), Deep structure of the western South African passive margin—Results of a combined approach of seismic, gravity and isostatic investigations, *Tectonophysics*, **470**, 57–70, doi:10.1016/j.tecto.2008.04.028.
- Hoffmann, H. J., and T. J. Reston (1992), The nature of the S reflector beneath the Galicia Bank rifted margin: Preliminary results from pre-stack depth migration, *Geology*, **20**, 1091–1094.
- Hopper, J. R., and W. R. Buck (1996), The effect of lower crustal flow on continental extension and passive margin formation, *J. Geophys. Res.*, **101**, 20,175–20,194, doi:10.1029/96JB01644.
- Hopper, J. R., T. Dahl-Jensen, W. S. Holbrook, H. C. Larsen, D. Lizarralde, J. Korenaga, G. M. Kent, and P. B. Kelemen (2003), Structure of the SE Greenland margin from seismic reflection and refraction data: Implications for nascent spreading center subsidence and asymmetric crustal accretion during North Atlantic opening, *J. Geophys. Res.*, **108(B5)**, 2269, doi:10.1029/2002JB001996.
- Hudec, M. R., and M. P. A. Jackson (2002), Structural segmentation, inversion, and salt tectonics on a passive margin: Evolution of the Inner Kwanza Basin, Angola, *Geol. Soc. Am. Bull.*, **114**, 1222–1244, doi:10.1130/0016-7606(2002)114<1222:SSIAST>2.0.CO;2.
- Hudec, M. R., and M. P. A. Jackson (2004), Regional restoration across the Kwanza Basin, Angola: Salt tectonics triggered by repeated uplift of a metastable passive margin, *AAPG Bull.*, **88**, 971–990, doi:10.1306/02050403061.
- Huismans, R. S., and C. Beaumont (2002), Asymmetric lithospheric extension: The role of frictional plastic strain softening inferred from numerical experiments, *Geology*, **30**, 211–214, doi:10.1130/0091-7613(2002)030<0211:ALETRO>2.0.CO;2.
- Huismans, R. S., and C. Beaumont (2008), Complex rifted continental margins explained by dynamical models of depth-dependent lithospheric extension, *Geology*, **36**, 163–166, doi:10.1130/G24231A.1.
- International Association of Geomagnetism and Aeronomy (IAGA) (2007), World Digital Magnetic Anomaly Map (WDMAM), Perugia, Italy.
- Jackson, M. P. A., C. Cramez, and J. M. Fonck (2000), Role of subaerial volcanic rocks and mantle plumes in creation of South Atlantic margins: Implications for salt tectonics and source rocks, *Mar. Petrol. Geol.*, **17**, 477–498, doi:10.1016/S0264-8172(00)00006-4.
- Karner, G. D., and N. W. Driscoll (1999), Tectonic and stratigraphic development of the West African and eastern Brazilian margins; insights from quantitative basin modeling, in *The Oil and Gas Habitats of the South Atlantic*, edited by N. R. Cameron et al., *Geol. Soc. Spec. Publ.*, **153**, 11–40.
- Karner, G. D., and L. A. P. Gambôa (2007), Timing and origin of the South Atlantic pre-salt sag basins and their capping evaporites, in *Evaporites Through Space and Time*, edited by B. C. Schreiber et al., *Geol. Soc. Spec. Publ.*, **285**, 15–35.
- Kusznir, N. J., and G. D. Karner (2007), Continental lithospheric and breakup in response to upwelling divergent mantle flow: Application to the Woodlark, Newfoundland and Iberia margins, in *Imaging, Mapping and Modelling Continental Lithosphere Extension and Breakup*, edited by G. D. Karner et al., *Geol. Soc. Spec. Publ.*, **282**, 389–419, doi:10.1144/SP282.16.
- Kusznir, N. J., and R. G. Park (1987), The extensional strength of the continental lithosphere: Its dependence on geothermal gradient, crustal composition and thickness, in *Continental Extensional Tectonics*, edited by M. P. Coward et al., *Geol. Soc. Spec. Publ.*, **28**, 35–42.
- Larsen, H. C., and A. D. Saunders (1998), Tectonism and volcanism at the southeast Greenland rifted margin: A record of plume impact and later continental rifting, *Proc. Ocean Drill. Program Sci. Results*, **152**, 503–533.
- Lavier, L. L., and G. Manatschal (2006), A mechanism to thin the continental lithosphere at magma-poor margins, *Nature*, **440**, 324–328, doi:10.1038/nature04608.
- Lawver, L. A., L. M. Gahagan, and I. W. D. Dalziel (1999), A tight fit—Early Mesozoic Gondwana: A plate reconstruction perspective, in *Origin and Evolution of Continents: Proceedings of the International Symposium “Origin and Evolution of Continents”*, edited by Y. Motoyoshi and K. Shiraiishi, *Mem. Natl. Inst. Polar Res.*, **53**, 214–229.
- Lefort, J. P., and B. N. P. Agarwal (2000), Gravity and geomorphological evidence for a large crustal bulge cutting across Brittany (France): A tectonic response to the closure of the Bay of Biscay, *Tectonophysics*, **323**, 149–162, doi:10.1016/S0040-1951(00)00103-7.
- Lister, G. S., and G. A. Davis (1989), The origin of metamorphic core complexes and detachment faults formed during Tertiary continental extension in the northern Colorado River region, US, *J. Struct. Geol.*, **11**, 65–94, doi:10.1016/0191-8141(89)90036-9.
- Lister, G. S., M. A. Etheridge, and P. A. Symonds (1991), Detachment models for the formation of passive continental margins, *Tectonics*, **10**, 1038–1064, doi:10.1029/90TC01007.
- Marton, L. G., G. C. Tari, and C. T. Lehmann (2000), Evolution of the Angolan Passive Margin, West Africa, with emphasis on post-salt structural styles, in *Atlantic Riffs and Continental Margins*, *Geophys. Monogr. Ser.*, vol. 115, edited by W. U. Mohriak and M. Talwani, pp. 129–150, AGU, Washington, D. C.
- Matos, R. M. D. (2000), Tectonic evolution of the equatorial South Atlantic, in *Atlantic Riffs and Continental Margins*, *Geophys. Monogr. Ser.*, vol. 115, edited by W. U. Mohriak and M. Talwani, pp. 331–354, AGU, Washington, D. C.
- McKenzie, D. P. (1978), Some remarks on the development of sedimentary basins, *Earth Planet. Sci. Lett.*, **40**, 25–32, doi:10.1016/0012-821X(78)90071-7.
- Menezes, P. E. de L., and P. da S. Milhomem (2008), Tectônica de sal nas bacias de Cumuruxatiba, do Almada e de Camamu, in *Sal: Geologia e Tectônica: Exemplos nas Bacias Brasileiras*, edited by W. U. Mohriak et al., pp. 252–273, Beca, São Paulo, Brazil.

- Meyers, J. B., B. R. Rosendahl, H. Groschel-Becker, J. A. Austin Jr., and P. A. Rona (1996a), Deep penetrating MCS imaging of the rift-to-drift transition, offshore Douala and North Gabon basins, West Africa, *Mar. Pet. Geol.*, **13**, 791–835, doi:10.1016/0264-8172(96)00030-X.
- Meyers, J. B., B. R. Rosendahl, and J. A. Austin Jr. (1996b), Deep-penetrating MCS images of the South Gabon Basin: Implications for rift tectonics and post-breakup salt remobilization, *Basin Res.*, **8**, 65–84, doi:10.1111/j.1365-2117.1996.tb00115.x.
- Mjelde, R., A. J. Breivik, H. Elstad, A. E. Ryseth, J. R. Skilbrei, J. G. Opsal, H. Shimamura, Y. Murai, and Y. Nishimura (2002), Geological development of the Sorvestsnaget Basin, SW Barents Sea, from ocean bottom seismic, surface seismic and potential field data, *Nor. Geol. Tidsskr.*, **82**, 183–202.
- Mjelde, R., T. Raum, B. Myhren, H. Shimamura, and Y. Murai (2005), Continent-ocean transition on the Vøring Plateau, NE Atlantic, derived from densely sampled ocean bottom seismometer data, *J. Geophys. Res.*, **110**, B05101, doi:10.1029/2004JB003026.
- Mjelde, R., T. J. I. Faleide, A. J. Breivik, and T. Raum (2009), Low crustal composition and crustal lineaments on the Vøring Margin, NE Atlantic: A review, *Tectonophysics*, **472**, 183–193, doi:10.1016/j.tecto.2008.04.018.
- Mohriak, W. U. (2001), Salt tectonics, volcanic centers, fracture zones and their relationship with the origin and evolution of the South Atlantic Ocean: Geophysical evidence in the Brazilian and West African margins, paper presented at 7th International Congress of the Brazilian Geophysical Society, Salvador, Brazil, 28–31 Oct.
- Mohriak, W. U. (2003), Bacias Sedimentares da Margem Continental Brasileira, in *Geologia, Tectônica e Recursos Minerais do Brasil*, edited by L. A. Buzzi et al., pp. 87–165, Serv. Geol. Brasil, Brasilia, Brazil.
- Mohriak, W. U. (2004), Recursos energéticos associados à ativação tectônica Mesozóico-Cenozóica da América do Sul, in *Geologia do Continente Sul-Americano: Evolução da Obra de Fernando Flávio Marques de Almeida*, edited by V. M. Neto et al., pp. 293–318, Beca, São Paulo, Brazil.
- Mohriak, W. U., and B. R. Rosendahl (2003), Transform zones in the South Atlantic rifted continental margins, in *Intraplate Strike-Slip Deformation Belts*, edited by F. Storti et al., *Geol. Soc. Spec. Publ.*, **210**, 211–228.
- Mohriak, W. U., J. H. L. Rabelo, R. D. Matos, and M. C. Barros (1995), Deep seismic reflection profiling of sedimentary basins offshore Brazil: Geological objectives and preliminary results in the Sergipe Basin, *J. Geodyn.*, **20**, 515–539, doi:10.1016/0264-3707(95)00024-4.
- Mohriak, W. U., M. Bassetto, and I. S. Vieira (1998), Crustal architecture and tectonic evolution of the Sergipe-Alagoas and Jacuípe basins, offshore northeastern Brazil, *Tectonophysics*, **288**, 199–220, doi:10.1016/S0040-1951(97)00294-1.
- Mohriak, W. U., M. Nemčok, and G. Enciso (2008), South Atlantic divergent margin evolution: Rift-border uplift and salt tectonics in basins of SE Brazil, in *West Gondwana: Pre-Cenozoic Correlations Across the South Atlantic Region*, edited by R. J. Pankhurst et al., *Geol. Soc. Spec. Publ.*, **294**, 365–398, doi:10.1144/SP294.19.
- Moulin, M., D. Aslanian, J. L. Olivet, I. Contrucci, L. Matias, L. Géli, F. Klingelhoefer, H. Nouzé, J. P. Réhault, and P. Unternehr (2005), Geological constraints on the evolution of the Angolan margin based on reflection and refraction seismic data (ZaiAngo project), *Geophys. J. Int.*, **162**, 793–810, doi:10.1111/j.1365-246X.2005.02668.x.
- Moulin, M., D. Aslanian, and P. Unternehr (2010), A new starting point for the South and Equatorial Atlantic Ocean, *Earth Sci. Rev.*, **98**, 1–37, doi:10.1016/j.earscirev.2009.08.001.
- Mounguengui, M. M., and M. Guiraud (2009), Neocomian to early Aptian syn-rift evolution of the normal to oblique-rifted North Gabon Margin (Interior and N'Komi Basins), *Mar. Pet. Geol.*, **26**, 1000–1017, doi:10.1016/j.marpetgeo.2008.11.001.
- Müller, R. D., M. Sdrolias, C. Gaina, and W. R. Roest (2008), Age, spreading rates, and spreading asymmetry of the world's ocean crust, *Geochem. Geophys. Geosyst.*, **9**, Q04006, doi:10.1029/2007GC001743.
- Mutter, J. C., M. Talwani, and P. L. Stoffa (1982), Origin of seaward dipping reflectors in oceanic crust off the Norwegian margin by “subaerial seafloor spreading,” *Geology*, **10**, 353–357, doi:10.1130/0091-7613(1982)10<353:OOSRIO>2.0.CO;2.
- Mutter, J. C., W. R. Buck, and C. M. Zehnder (1988), Convective partial melting: 1. A model for the formation of thick basaltic sequences during the initiation of spreading, *J. Geophys. Res.*, **93**, 1031–1048, doi:10.1029/JB093iB02p01031.
- Nürnberg, D., and R. D. Müller (1991), The tectonic evolution of the South Atlantic from Late Jurassic to present, *Tectonophysics*, **191**, 27–53, doi:10.1016/0040-1951(91)90231-G.
- Paton, D. A., D. van der Spuy, R. di Primio, and B. Horsfield (2008), Tectonically induced adjustment of passive-margin accommodation space; influence on the hydrocarbon potential of the Orange Basin, South Africa, *AAPG Bull.*, **91**, 589–609, doi:10.1306/12280707023.
- Péron-Pinvidic, G., and G. Manatschal (2009), The final rifting evolution at deep magma-poor passive margins from Iberia-Newfoundland: A new point of view, *Int. J. Earth Sci.*, **98**, 1581–1597, doi:10.1007/s00531-008-0337-9.
- Péron-Pinvidic, G., G. Manatschal, T. A. Minshull, and D. S. Sawyer (2007), Tectono-sedimentary evolution of the deep Iberia-Newfoundland margins: Evidence for a complex breakup history, *Tectonics*, **26**, TC2011, doi:10.1029/2006TC001970.
- Planke, S., and O. Eldholm (1994), Seismic response and construction of seaward dipping wedges of flood basalts: Vøring volcanic margin, *J. Geophys. Res.*, **99**, 9263–9278, doi:10.1029/94JB00468.
- Planke, S., P. A. Symonds, E. Alvestad, and J. Skogseid (2000), Seismic volcanostratigraphy of large-volume basaltic extrusive complexes on rifted margins, *J. Geophys. Res.*, **105**, 19,335–19,351, doi:10.1029/1999JB900005.
- Rabinowitz, P. D., and J. L. LaBrecque (1979), The mesozoic South Atlantic Ocean and evolution of its continental margins, *J. Geophys. Res.*, **84**, 5973–6002, doi:10.1029/JB084iB11p05973.
- Ramos, V. A. (1996), Evolución tectónica de la Plataforma Continental, in *Geología y Recursos Naturales de la Plataforma Continental Argentina, relatorio XIIIº Congreso Geológico Argentino y IIIº Congreso de Exploración de Hidrocarburos*, edited by V. A. Ramos and M. A. Turic, Assoc. Geol. Argent., 385–404.
- Ramos, V. A. (2004), La plataforma Patagónica y sus relaciones con la plataforma Brasileira, in *Geología do Continente Sul-Americano: Evolução da Obra de Fernando Flávio Marques de Almeida*, edited by V. M. Neto et al., pp. 371–381, Beca, São Paulo, Brazil.
- Regenauer-Lieb, K., R. F. Weinberg, and G. Rosenbaum (2006), The effect of energy feedbacks on continental strength, *Nature*, **442**, 67–70, doi:10.1038/nature04868.
- Reston, T. J. (1996), The S reflector west of Galicia: The seismic signature of a detachment fault, *Geophys. J. Int.*, **127**, 230–244, doi:10.1111/j.1365-246X.1996.tb01547.x.
- Reston, T. J. (2009a), The structure, evolution and symmetry of the magma-poor rifted margins of the North and central Atlantic: A synthesis, *Tectonophysics*, **468**, 6–27, doi:10.1016/j.tecto.2008.09.002.
- Reston, T. J. (2009b), The extension discrepancy and synrift subsidence deficit at rifted margins, *Petrol. Geosci.*, **15**, 217–237, doi:10.1144/1354-079309-845.
- Reston, T. J., and M. Pérez-Gussinyé (2007), Lithospheric extension from rifting to continental breakup at magma-poor margins: Rheology, serpen-tinisation and symmetry, *Int. J. Earth Sci.*, **96**, 1033–1046, doi:10.1007/s00531-006-0161-z.
- Reston, T. J., C. M. Krawczyk, and D. Klaeschen (1996), The S reflector west of Galicia (Spain): Evidence from prestack depth migration for detachment faulting during continental breakup, *J. Geophys. Res.*, **101**, 8075–8091, doi:10.1029/95JB03466.
- Reston, T. J., T. Leythaeuser, G. Booth-Rea, D. Sawyer, D. Klaeschen, and C. Long (2007), Movement along a low-angle normal fault: The S reflector west of Spain, *Geochem. Geophys. Geosyst.*, **8**, Q06002, doi:10.1029/2006GC001437.
- Rosenbaum, G., K. Regenauer-Lieb, and R. F. Weinberg (2005), Continental extension: From core complexes to rigid block faulting, *Geology*, **33**, 609–612, doi:10.1130/G21477.1.
- Rosenbaum, G., R. F. Weinberg, and K. Regenauer-Lieb (2008), The geo-dynamics of lithospheric extension, *Tectonophysics*, **458**, 1–8, doi:10.1016/j.tecto.2008.07.016.
- Rosendahl, B. R., and H. Groschel-Becker (1999), Deep seismic structure of the continental margin in the Gulf of Guinea: A summary report, in *The Oil and Gas Habitats of the South Atlantic*, edited by N. R. Cameron et al., *Geol. Soc. Spec. Publ.*, **153**, 75–83, doi:10.1144/GSL.SP.1999.153.01.005.
- Rosendahl, B. R., H. Groschel-Becker, J. Meyers, and K. Kaczmarick (1991), Deep seismic reflection study of a passive margin, southeastern Gulf of Guinea, *Geology*, **19**, 291–295, doi:10.1130/0091-7613(1991)019<0291:DSRSOA>2.3.CO;2.
- Rosendahl, B. R., W. U. Mohriak, M. E. Odegard, J. P. Turner, and W. G. Dickson (2005), West African and Brazilian conjugate margins: Crustal types, architecture, and plate configurations, in *Petroleum Systems of Divergent Continental Margin Basins*, edited by P. Post et al., in *25th Gulf Coast Section, SEPM Research Conference*, CD-ROM.
- Russell, S. M., and R. B. Whitmarsh (2003), Magmatism at the west Iberia non-volcanic rifted continental margin: Evidence from analyses of magnetic anomalies, *Geophys. J. Int.*, **154**, 706–730, doi:10.1046/j.1365-246X.2003.01999.x.
- Sandwell, D. T., and W. H. F. Smith (1997), Marine gravity anomaly from Geosat and ERS 1 satellite altimetry, *J. Geophys. Res.*, **102**, 10,039–10,054, doi:10.1029/96JB03223.

- Sawyer, D. S., M. F. Coffin, T. J. Reston, J. M. Stock, and J. R. Hopper (2007), COBBOOM: The Continental Breakup and Birth of Oceans Mission, *Sci. Drill.*, 5, 13–25, doi:10.2204/iodp.sd.5.02.2007.
- Schnabel, M., D. Franke, M. Engels, K. Hinz, S. Neben, V. Damm, S. Grassmann, H. Pelliza, and P. R. Dos Santos (2008), The structure of the lower crust at the Argentine continental margin, South Atlantic at 44°S, *Tectonophysics*, 454, 14–22, doi:10.1016/j.tecto.2008.01.019.
- Séranne, M., and Z. Anka (2005), South Atlantic continental margins of Africa: A comparison of the tectonic vs climate interplay on the evolution of equatorial west Africa and SW Africa margins, *J. Afr. Earth Sci.*, 43, 283–300, doi:10.1016/j.jafrearsci.2005.07.010.
- Sibuet, J. C. (1987), Contribution à l'étude des mécanismes de formation des marges continentales passives, Doctorat d'Etat thesis, Univ. de Bretagne Occidentale, Brest, France, p. 351.
- Sibuet, J. C. (1992), New constraints on the formation of the nonvolcanic continental Galicia-Flemish Cap conjugate margins, *J. Geol. Soc. London*, 149, 829–840.
- Simon, K., R. S. Huismans, and C. Beaumont (2009), Dynamical modeling of lithospheric extension and small-scale convection: Implications for magmatism during the formation of volcanic rifted margins, *Geophys. J. Int.*, 176, 327–350, doi:10.1111/j.1365-246X.2008.03891.x.
- Skogseid, J., and O. Eldholm (1987), Early Cenozoic crust at the Norwegian continental margin and the conjugate Jan Mayen Ridge, *J. Geophys. Res.*, 92, 11,471–11,491, doi:10.1029/JB092iB11p11471.
- Skogseid, J., S. Planke, J. I. Faleide, T. Pedersen, O. Eldholm, and F. Neverdal (2000), NE Atlantic continental rifting and volcanic margin formation, in *Dynamics of the Norwegian Margin*, edited by A. Nøttvedt et al., *Geol. Soc. Spec. Publ.*, 167, 295–326.
- Smith, W. H. F. (1993), On the accuracy of digital bathymetric data, *J. Geophys. Res.*, 98, 9591–9603, doi:10.1029/93JB00716.
- Souza-Lima, W. (2008), Seqüências evaporíticas da bacia de Sergipe-Alagoas, in *Sal: Geologia e Tectônica: Exemplos nas Bacias Brasileiras*, edited by W. U. Mohriak et al., pp. 232–251, Beca, São Paulo, Brazil.
- Srivastava, S., and C. E. Keen (1995), A deep seismic reflection profile across the extinct Mid-Labrador Sea spreading center, *Tectonics*, 14, 372–389, doi:10.1029/94TC02453.
- Srivastava, S., and W. R. Roest (1999), Extent of oceanic crust in the Labrador Sea, *Mar. Pet. Geol.*, 16, 65–84, doi:10.1016/S0264-8172(98)00041-5.
- Talwani, M., and V. Abreu (2000), Inferences regarding initiation of oceanic crust formation from the US east coast margin and conjugate south Atlantic margins, in *Atlantic Rifts and Continental Margins*, *Geophys. Monogr. Ser.*, vol. 115, edited by W. Mohriak and M. Talwani, pp. 211–233, AGU, Washington, D. C.
- Talwani, M., and O. Eldholm (1972), Continental margin off Norway: A geophysical study, *Geol. Soc. Am. Bull.*, 83, 3575–3606, doi:10.1130/0016-7606(1972)83[3575:CMONAG]2.0.CO;2.
- Teisserenc, P., and J. Villemain (1989), Sedimentary basin of Gabon—geology and oil systems, in *Divergent Passive Margin Basins*, edited by J. D. Edwards and P. A. Santogrossi, *AAPG Mem.*, 48, 117–199.
- Thompson, R. N., and S. A. Gibson (1991), Subcontinental mantle plumes, hotspots and pre-existing thinspots, *J. Geol. Soc.*, 148, 973–977, doi:10.1144/gsjgs.148.6.0973.
- Torsvik, T. H., S. Rousse, C. Labails, and M. A. Smethurst (2009), A new scheme for the opening of the South Atlantic Ocean and the dissection of an Aptian salt basin, *Geophys. J. Int.*, 177, 1315–1333, doi:10.1111/j.1365-246X.2009.04137.x.
- Trumbull, R. B., S. V. Sobolev, and K. Bauer (2002), Petrophysical modeling of high seismic velocity crust at the Namibian volcanic margin, in *Volcanic Rifted Margins*, edited by M. A. Menzies et al., *Spec. Pap. Geol. Soc. Am.*, 221–230, doi:10.1130/0-8137-2362-0.221.
- Trumbull, R. B., D. L. Reid, C. de Beer, D. van Acken, and R. L. Romer (2007), Magmatism and continental breakup at the west margin of southern Africa: A geochemical comparison of dolerite dikes from northwestern Namibia and the Western Cape, *S. Afr. J. Geol.*, 110, 477–502, doi:10.2113/gssajg.110.2-3.477.
- Tsikalas, F., O. Eldholm, and J. I. Faleide (2005), Crustal structure of the Lofoten-Vesterålen continental margin, off Norway, *Tectonophysics*, 404, 151–174, doi:10.1016/j.tecto.2005.04.002.
- Unternehr, P., G. Péron-Pinvidic, G. Manatschal, and E. Sutra (2010), Hyperextended crust in the South Atlantic: In search of a model, *Petrol. Geosci.*, 16, 207–215, doi:10.1144/1354-079309-904.
- van Wijk, J. W., R. S. Huismans, M. ter Voorde, and S. A. P. L. Cloetingh (2001), Melt generation at volcanic continental margins: No need for a mantle plume?, *Geophys. Res. Lett.*, 28, 3995–3998, doi:10.1029/2000GL012848.
- Wannesson, J., J. C. Icart, and J. Ravat (1991), Structure and evolution of adjoining segments of the west African margin determined from deep seismic profiling, in *Continental Lithosphere: Deep Seismic Reflections, Geodyn. Ser.*, vol. 22, edited by R. Meissner et al., pp. 275–289, AGU, Washington, D. C.
- Watts, A. B. (2001), Gravity anomalies, flexure and crustal structure at the Mozambique rifted margin, *Mar. Pet. Geol.*, 18, 445–455, doi:10.1016/S0264-8172(00)00079-9.
- Watts, A. B., and J. D. Fairhead (1999), A process-oriented approach to modeling the gravity signature of continental margins, *Lead. Edge*, 18, 258–263, doi:10.1190/1.1438270.
- Watts, A. B., and J. Stewart (1998), Gravity anomalies and segmentation of the continental margin offshore West Africa, *Earth Planet. Sci. Lett.*, 156, 239–252, doi:10.1016/S0012-821X(98)00018-1.
- Weinberg, R. F., K. Regenauer-Lieb, and G. Rosenbaum (2007), Mantle detachments and the break-up of cold continental crust, *Geology*, 35, 1035–1038, doi:10.1130/G23918A.1.
- Wernicke, B. (1981), Low-angle normal faults in the Basin and Range province: Nappe tectonics in an extending orogen, *Nature*, 291, 645–648, doi:10.1038/291645a0.
- Wernicke, B. (1985), Uniform-sense normal simple shear of the continental lithosphere, *Can. J. Earth Sci.*, 22, 108–125, doi:10.1139/e85-009.
- Wessel, P., and A. B. Watts (1988), On the accuracy of marine gravity measurements, *J. Geophys. Res.*, 93, 393–413, doi:10.1029/JB093iB01p00393.
- White, R. S., and D. McKenzie (1989), Magmatism at rift zones: The generation of volcanic continental margins and flood basalts, *J. Geophys. Res.*, 94, 7685–7729, doi:10.1029/JB094iB06p07685.
- White, R. S., and L. K. Smith (2009), Crustal structure of the Hatton and the conjugate east Greenland rifted volcanic continental margins, NE Atlantic, *J. Geophys. Res.*, 114, B02305, doi:10.1029/2008JB005856.
- White, R. S., L. K. Smith, A. W. Roberts, F. Christie, N. J. Kusznir, and iSIMM Team (2008), Lower-crustal intrusion on the North Atlantic continental margin, *Nature*, 452, 460–464, doi:10.1038/nature06687.
- Whitmarsh, R. B., and P. R. Miles (1995), Models of the development of the west Iberia rifted continental margin at 40°30'N deduced from surface and deep-tow magnetic anomalies, *J. Geophys. Res.*, 100, 3789–3806, doi:10.1029/94JB02877.
- Whitmarsh, R. B., R. S. White, S. J. Horsefield, J. C. Sibuet, M. Recq, and V. Louvel (1996), The ocean-continent boundary off the western continental margin of Iberia: Crustal structure west of Galicia Bank, *J. Geophys. Res.*, 101, 28,291–28,314, doi:10.1029/96JB02579.
- Whitmarsh, R. B., G. Manatschal, and T. A. Minshull (2001), Evolution of magma-poor continental margins from rifting to seafloor spreading, *Nature*, 413, 150–154, doi:10.1038/35093085.
- Wilson, P. G., J. P. Turner, and G. K. Westbrook (2003), Structural architecture of the ocean-continent boundary at an oblique transform margin through deep-imaging seismic interpretation and gravity modelling; Equatorial Guinea, West Africa, *Tectonophysics*, 374, 19–40, doi:10.1016/S0040-1951(03)00326-3.
- Zelt, C. A., K. Kalachand, J. V. Naumenko, and D. S. Sawyer (2003), Assessment of crustal velocity models using seismic refraction, *Geophys. J. Int.*, 153, 609–626.

O. A. Blaich, Fugro Multi Client Services, Hoffsveien 1C P.O Box 490 Skøyen, NO-0213 Oslo, Norway. (o.blaich@fugro.no)

J. I. Faleide, Department of Geosciences, University of Oslo, P.O. Box 1047 Blindern, NO-0316 Oslo, Norway. (j.i.faleide@geo.uio.no)

F. Tsikalas, Eni E&P, GEOLAB, Via Maritano 26, I-20097 San Donato Milanese, Milan, Italy. (filippos.tsikalas@eni.it)